Speciation of Tetravalent Plutonium in Contact with Humic Substances and Kaolinite under Environmental Conditions

Thesis submitted for
attaining the degree of

"Doktor der Naturwissenschaften"
doctor rerum naturalium

at the
Department of Chemistry, Pharmacy, and Geosciences
of the
Johannes Gutenberg-University Mainz

Nidhu lal Banik
Born in Noakhali, Bangladesh

Mainz, 2006

To My Family

Contents

Zusammenfassung

Plutonium trägt über einen Zeitraum von bis zu mehreren hunderttausend Jahren maßgeblich zur Radiotoxizität von abgebrannten Kernbrennstoffen bei. Für die Endlagerung von nuklearem Abfall ist es daher wichtig, die Speziation von Plutonium im Aquifer zu bestimmen und Erkenntnisse über das Mobilisierungs und Immobilisierungsverhalten von Pu in natürlichen Aquifersystemen zu erlangen. In wässrigen Lösungen kann Plutonium in bis zu vier Oxydationszuständen nebeneinander existieren, und jeder von ihnen zeigt ein unterschiedliches chemisches und physikalisches Verhalten. Vierwertiges Plutonium ist unter natürlichen Bedingungen am häufigsten anzutreffen. In der vorliegenden Arbeit sind deshalb ausführliche Speziationsuntersuchungen des vierwertigen Plutoniums im Kontakt mit Huminstoffen (HS) und Kaolinit als Modell-Tonmineral durchgeführt worden.

Plutonium kommt in der Umwelt nur im Ultraspurenbereich vor. Deshalb ist die Speziation von Pu im Ultrasuprenberich erforderlich. Kapillar-Elektrophorese (CE) verbunden mit der Resonanzionisations-Massenspektrometrie (RIMS) findet hierzu als neue Speziationsmethode Anwendung. Mit CE-RIMS ist es möglich, die Nachweisgrenze für Plutonium um 2 bis 3 Größenordnungen im Vergleich zur herkömmlichen CE-ICP-MS zu verbessern. Um das Verhalten von Pu (IV) in wässrigen Systemen zu verstehen, wurden Redox-, Komplexierungs-, und Sorptionsverhalten des Plutoniums studiert. Das Redox -Verhalten des Plutoniums im Kontakt mit Huminsäure (HA) und Fulvinsäure (FA) wurde untersucht. Eine relativ schnelle Reduktion von Pu (VI) im Kontakt mit HS wurde beobachtet. Es wird innerhalb weniger Wochen fast vollständig zu Pu(IV) und Pu(III) reduziert. Die Zeitabhängigkeit der Komplexierung von Pu(IV) mit Aldrich HA wurde untersucht. Dabei wurde unter Anwendung der Ultrafiltration und unter Berücksiditigung des Beladungskapazität (loading capacity, LC) eine Komplexbildungskonstante ($\log ß_{LC}$) zwischen 6,4 – 8,4 bestimmt.

Das Sorptionsverhalten von vierwertigem Pu an Kaolinit wurde in Abhängigkeit vom pH-Wert in Batch-Experimenten unter aeroben und anaeroben Bedingungen untersucht. Die Sorptionskante wurde bei pH = 1 gefunden; die maximale Sorption fand bei pH=8,5 statt. In Anwesenheit von CO_2 über einem pH-Wert von 8,5 nimmt die Sorption von Pu (IV) wieder ab, vermutlich durch Bildung von löslichen Carbonatkomplexen. Zum Vergleich wurde ebenfalls das Sorptionsverhalten von Th(IV) an Kaolinit untersucht, und es wurden übereinstimmende Ergebnisse gefunden. Die Sorption von Pu(IV) wurde mittels XANES und EXAFS bei pH-Werten von 1, 4 und 9 untersucht; die Oxidationstufe blieb dabei erhalten. In Abhängigkeit vom pH-Wert werden bei Kontakt mit frischer Lösung nur 1-10% des adsorbierten Pu wieder desorbiert. Weiterhin wurde das Sorptionsverhalten von Huminstoffen an Kaolinit bei variierenden Konzentrationen untersucht. Dies diente als Vorstudie zum Studium des wesentlich komplexeren ternären Systems. Huminsäure wird besser (mehr) an Kaolinit sorbiert als Fulvinsäure.

Die Studien zum ternären System (Pu-Kaolinit-HS) wurden in Abhängigkeit vom pH-Wert, von der Konzentration an HS und der Reihenfolge der Zugabe der Reaktanden durchgeführt. Die Anwesenheit von HS hat großen Einfluss auf die Sorption von Pu(IV) an Kaolinit über den gesamten pH-Bereich. Auch hier führten vergleichende Versuche mit Th(IV) zu übereinstimmenden Ergebnissen.

Abstract

Plutonium represents the major contribution to the radiotoxicity of spent nuclear fuel over storage times of up to several hundred thousand years. The speciation of plutonium in aquifer systems is important in order to assess the risks of high-level nuclear waste disposal and to acquire a deep knowledge of the mobilization and immobilization behavior of plutonium.

In aqueous solutions, plutonium can coexist in four oxidation states and each one of them has different chemical and physical behavior. Tetravalent plutonium is the most abundant under natural conditions. Therefore, detailed speciation studies of tetravalent plutonium in contact with humic substances (HS) and kaolinite as a model clay mineral have been performed in this work.

Plutonium is present in the environment at an ultratrace level. Therefore, speciation of Pu at the ultratrace level is mandatory. Capillary electrophoresis (CE) coupled to resonance ionization mass spectrometry (RIMS) was used as a new speciation method. CE-RIMS enables to improve the detection limit for plutonium species by 2 to 3 orders of magnitude compared to the previously developed CE-ICP-MS.

For understanding the behavior of Pu(IV) in aqueous systems, redox reactions, complexation, and sorption behavior of plutonium were studied. The redox behavior of plutonium in contact with humic acid (HA) and fulvic acid (FA) was investigated. A relatively fast reduction of Pu(VI) in contact with HS was observed. It was mainly reduced to Pu(IV) and Pu(III) within a couple of weeks. The time dependence of the Pu(IV) complexation with Aldrich HA was investigated and a complex constant ($\log ß_{LC}$) between 6.4 - 8.4 of Pu(IV) was determined by means of ultrafiltration taking into account the loading capacity (LC).

The sorption of tetravalent plutonium onto kaolinite was investigated as a function of pH in batch experiments under aerobic and anaerobic conditions. The sorption edge was found at about pH = 1 and a maximum sorption at around pH = 8.5. In the presence of CO_2 at pH > 8.5, the sorption of plutonium was decreased probably due to the formation of soluble carbonate complexes. For comparison, the sorption of Th(IV) onto kaolinite was also investigated and consistent results were found. The Pu(IV) sorption onto kaolinite was studied by XANES and EXAFS at pH 1, 4, 9 and the sorbed species on kaolinite surface was Pu(IV). Depending on the pH, only 1 - 10 % of the sorbed plutonium is desorbed from kaolinite and released into a fresh solution at the same pH value. Furthermore, the sorption of HS onto kaolinite was studied as a function of pH at varying concentrations of HS, as a prerequisite to understand the more complex ternary system. The sorption of HA onto kaolinite was found to be higher than that of FA.

The investigation of the ternary systems (plutonium-kaolinite-humic substances) is performed as a function of pH, concentration of HS, and the sequences of adding the reactants. The presence of HS strongly influences the sorption of Pu(IV) onto kaolinite over the entire pH range. For comparison, the influence of HS on the sorption of Th(IV) onto kaolinite was also investigated and a good agreement with the results of Pu(IV) was obtained.

1.0 Introduction

Since the middle of last century, a large amount of long-lived radionucldies, mainly actinides, have been released by nuclear weapons tests, which have posed a great challenge to nuclear scientists. In 1934, artificial radioactivity was discovered by I. Curie and F. Joliot. The concept of artificial radioisotopes was multiplied manifold with the discovery of nuclear fission by O. Hahn and F. Strassmann in 1938 [Hahn 39]. Nuclear weapons and nuclear power generation were developed using nuclear fission.

At the moment, 444 power plants are in operation worldwide producing about 368 GW electric power, which annually generates about 8500 tons of spent fuel [Fuku 2003]. Up to now, a huge amount of spent fuel is produced, containing about 2,400 tons of plutonium and a considerable amount of minor actinides and fission products. The dominant contribution to the radiotoxicity over long storage times (up to one million years) is delivered by plutonium and other minor actinides [Kim 2000]. Their environmental behavior, especially their migration, depends mainly on their complexation-, redox- , and sorption chemistry, and is of special interest for the evaluation of the safety of nuclear waste repositories.

The principle of deep geological disposal for high level nuclear waste, spent fuel, and long-lived intermediate level waste is recognized internationally and reflected in the radioactive waste policies of many countries. Every country has its own concept for waste disposal systems in the underground site. Especially the study of mobilization and immobilization of plutonium in underground waste repository sites is essential in order to be able to predict its eventual dispersion in the environment.

In order to perform long-term safety assessments for high-level nuclear waste repositories, it is necessary to understand the migration and retardation of plutonium in the neighborhood of the nuclear waste disposal site. Under natural conditions, the migration and the retardation of plutonium in aquatic systems depends on physical and chemical processes. To understand the behavior of plutonium, the plutonium species (physical/chemical) which exist in the underground of the disposal site must be investigated. Chemical speciation involves the determination of the soluble plutonium species, their oxidation states, complexation with anions (organic or inorganic), and redox reactions. Physical speciation involves, among others, the plutonium colloid formation and the sorption of plutonium onto mineral surfaces.

In aqueous solutions, plutonium can coexist in four oxidation states, Pu^{3+}, Pu^{4+}, $Pu(V)O_2^{+}$, and $Pu(VI)O_2^{2+}$ [Alla 82, Chop 88]. Each one of them has a different chemical and physical

behavior in solution. Tetravalent plutonium is the most abundant species under natural conditions [Chop 2003] and has a strong tendency to exhibit hydrolysis. Furthermore, Pu(IV) can easily form polymeric species or colloids under certain conditions [Alla 82, Chop 2003, Knop 99, Guil 92]. An understanding of the behavior of plutonium under environmental conditions is required for the investigation of the physical and chemical processes: Redox reactions, complexation, colloid formations, and sorption of plutonium onto mineral surfaces.

Prior to the studies of the plutonium speciation in aqueous solution, Th(IV) and Np(IV), which are considered to be homologues of Pu(IV), have been investigated in the present work. The aim of this study is a comparison of Pu(IV) with Th(IV) and Np(IV). Thorium and neptunium are also important in a nuclear waste disposal site. The chemistry of Th(IV) and Np(IV) is quite similar (through not identical) to that of Pu(IV) including hydrolysis, colloid formation, complexation, and sorption characteristics.

Besides inorganic ligands, humic substances (HS), a mixture of organic macromolecules, are distributed ubiquitously in the ecosphere and play an important role in the interaction processes with actinide ions. HS are considered as essential natural organic matter [Jano 2003], which can influence drastically the sorption of actinides onto mineral surfaces and thus the migration and the transport of actinides. In this work, kaolinite is used as a model clay mineral. Kaolinite contains mainly hydroxylated sites of silicon (Si) and aluminum (Al) [Payn 2004].

The speciation of the plutonium oxidation states in solution is a challenging task. A few speciation methods have been developed until now for the speciation of plutonium oxidation states under environmental conditions but most of these speciation methods are not applicable at low plutonium concentrations (10^{-8} - 10^{-11} mol/L), which is of interest in the far field of a nuclear waste repository site. Consequently, the offline coupling of capillary electrophoresis (CE) to resonance ionization mass spectrometry (RIMS) for the speciation of the plutonium oxidations states in solution at ultra trace concentrations has been introduced [Bürg 2005a].

The chemical behavior of plutonium is strongly influenced by its oxidation states in solution. Due to variations in the chemical behavior of plutonium in different oxidation states, the chemistry is difficult to understand in natural ground water systems. Therefore, the redox speciation of Pu(VI) under natural conditions, in contact with Aldrich humic acid (AHA) and Gorleben fulvic acid (FA) is investigated by online coupling of capillary electrophoresis to inductively coupled plasma - mass spectrometry (CE-ICP-MS) and UV-Vis spectroscopy. In natural aqueous systems, the oxidation state of plutonium is mainly governed by pH and Eh in

solution. In general, an increasing pH-value favors higher oxidation states. The same holds for higher Eh´s. At moderate pH or oxygen containing ground water, Pu(III) is readily oxidized to Pu(IV) [Chop 97b]. Farr et al. show that Pu(III) is rapidly oxidized by water around neutral pH because of its negative potential [Farr 2000]. From the redox potential of plutonium at neutral pH value, it can be concluded that Pu(IV), Pu(V), and Pu(VI) are the relevant oxidation states in the natural environment. The oxidation state can also be changed by disproportionation with a single substance serving as oxidizing as well as reducing agent. Pu(IV) is assumed to disproportionate to Pu(III) and Pu(V). However, Cho et al. have shown that the so-called “disprotionation” is a two-step process [Cho 2006 a].

The complexation of actinides by humic substances has been a subject of extensive investigations in the past decades. Due to the polyfunctionality of humic substances (HS), their complexation with actinide ions is not simple to understand. Different models have been proposed to interpret the nature of the interaction of the metal ion and humic substances at the binding sites.

The complexation of the tri-, penta- and hexavalent actinide ions with humic substances has been reported in the literature [Marq 96, Kim 91b]. The complexation constants of tetravalent actinide ions with humic substances are scarcely reported in the literature. The main reason for the lack of complexation studies for tetravalent actinides is the hydrolysis, the lower solubility constant and colloid formation. No reliable complexation data are available for Pu(IV) and Np(IV) with humic substances. Solvent extraction technique has been applied to determine the binding constant of Th(IV) with soil humic acid [Nash 80, Chop 81]. In the case of Pu(IV), $Pu(OH)_4$ is expected to be the predominant species in the absence of humic acids at the pH value of ground water. In presence of humic substances, Pu(IV) could form mixed complexes like $Pu(OH)_3HA(I)$ as reported by Czerwinski et al. [Czer 97]. Moreover, Bondietti et al. [Bond 76] showed the apparent interaction between plutonium and humic substances. Pirlet [Pirl 2003a] has estimated the complexation constants of tetravalent Np species with Boom clay fulvic acid. In aqueous systems, plutonium in contact with humic substances is present mainly in the tri- and tetravalent state.

The sorption of actinide ions onto kaolinite and other mineral surfaces has been investigated in the last decades [Zava 2005, Yama 2004, Righ 91]. The results show that the sorption depends significantly on the oxidation state, pH, ionic strength, temperature, aerobic or anaerobic conditions, and the type of mineral surface. Sorption studies of plutonium and other tetravalent actinides onto mineral surfaces, e.g., goethite [Sanc 85], calcite [Zava 2005], or

other soils [Tana 2002], were carried out. The sorption of tri-, tetra-, and pentavalent actinides (Am, Th, Np) on silica was also investigated [Righ 91]. The sorption of tetravalent actinides, Th(IV) and Pu(IV), onto kaolinite has not yet been studied in detail. Therefore, the sorption behavior of tetravalent Pu and Th onto kaolinite has been investigated in this work. Strong sorption of tetravalent actinides onto kaolinite is expected due to their strong tendency to hydrolyze [Neck 2001a].

Some data on the sorption behavior of humic acid (HA) onto kaolinite are reported in the literature [Sama 2000]. Contrary, the investigation of the sorption behavior of fulvic acid (FA) onto minerals, like kaolinite, has not been reported at all. The understanding of the interactions of humic acid and fulvic acid with kaolinite in natural aquifers is of concern for the assessment of nuclear waste repositories. Consequently, the sorption behavior of Gorleben FA in contact with kaolinite is also studied and compared with the results of the HA sorption onto kaolinite.

In this work, the following binary systems have been investigated: plutonium-humic substance, plutonium-kaolinite, thorium-kaolinite, and humic substance-kaolinite. The ternary system Pu(IV)-HS-kaolinite is not well understood; interactions and mechanisms are not accurately predictable. Therefore, the ternary system plutonium-kaolinite-humic substance is studied here in order to understand and predict the speciation and migration behavior of plutonium in a geogenic aquatic system in the vicinity of a radioactive waste repository or a contaminated site.

2.0 Theoretical Part

2.1 Actinide Chemistry

2.1.1 History

In 1945 the actinide theory was postulated by Seaborg “we would like to advance the attractive hypothesis that this rare-earth like series begins with actinium in the same sence that the “lanthanide” series begins with lanthanum. On this basis it might be termed the “Actinide” series and the first 5f electron might appear in thorium”[Seab 45]. This theory could explain the chemical similarity between the heavier actinides and the lanthanides that was not possible before. Thus, the actinide series of fourteen 5f elements is homologous to the lanthanide series of fourteen elements in which the 4f electron shell is filled.

Table 1: Valence shell electron configuration of all actinide elements [Katz 86]

Actinide		Configuration
Ac	actinium	$6d^1\ 7s^2$
Th	thorium	$6d^2\ 7s^2$
Pa	protactinium	$5f^2\ 6d^1\ 7s^2$
U	uranium	$5f^3\ 6d^1\ 7s^2$
Np	neptunium	$5f^4\ 6d^1\ 7s^2$
Pu	plutonium	$5f^6\ 7s^2$
Am	americium	$5f^7\ 7s^2$
Cm	curium	$5f^7\ 6d^1\ 7s^2$
Bk	berkelium	$5f^9\ 7s^2$
Cf	californium	$5f^{10}\ 7s^2$
Es	einsteinium	$5f^{11}\ 7s^2$
Fm	fermium	$5f^{12}\ 7s^2$
Md	mendelevium	$5f^{13}\ 7s^2$
No	nobelium	$5f^{14}\ 7s^2$
Lr	lawrencium	$5f^{14}\ 6d^1\ 7s^2$

The actinides are the elements with atomic numbers 89 (actinium) through 103 (lawrencium) (Table 1). The first four actinide elements, actinium (89), thorium (90), protactinium (91) and uranium (92) are naturally occurring elements and have been known for a considerable time. The dates of their discovery are 1789 for uranium, 1829 for thorium, 1899 for actinium and 1913 for protactinium. Neptunium (93) was discovered in 1940 and plutonium (94) was discovered shortly afterwards in the same year. Many isotopes of the remaining elements were produced using different reaction. Over the following two decades the heavier actinides were discovered: americium (95) and curium (96) in 1944, berkelium (97) in 1949,

californium (98) in 1950, einsteinium (99) and fermium (100) in 1952, mendelevium (101) in 1955, nobelium (102) in 1957 and lawrencium (103) in 1961.

In general, the lanthanide and actinide elements show vary similar chemical and physical behavior because both have 4f and 5f orbital electron shell. In the actinide series, the 5f orbital is very similar in energy level to the 6d orbital. The actinide series is divided into two subgroups owing to their electronic configuration, the lighter actinides (from Ac to Am) and the heavier actinides (from Cm to Lw). At the begining of the actinide series, electrons can easily switch between the 5f and 6d orbitals. This is because the 5f electrons (in contrast to the 4f electrons) are strongly delocalised due to relativistic effects. The chemical consequence is a non lanthanide like behavior of elements 90-94.

Table 2: Different isotopes of the lighter actinides and their production [Tabl 96]

Nuclides	**Half- life [Y]**	**Type of decay**	**Energy [Mev]**	**Production**
^{237}Np	2.14×10^{6}	α	4.789 4.774	$^{238}U\ (n,2n)\ ^{237}U \xrightarrow{\beta^-} {}^{237}Np$
^{238}Pu	87.7	α	5.499 5.456	$^{239}Pu\ (n,2n)\ ^{238}Pu$
^{239}Pu	2.41×10^{4}	α	5.157 5.144	$^{238}U\ (n,\gamma)\ ^{239}U \xrightarrow{\beta^-} {}^{239}Np \xrightarrow{\beta^-} {}^{239}Pu$
^{240}Pu	6563	α	5.168 5.123	$^{239}Pu\ (n,\gamma)\ ^{240}Pu$
^{241}Pu	14.35	β^-	0.021	$^{240}Pu\ (n,\gamma)\ ^{241}Pu$
^{242}Pu	3.73×10^{5}	α	4.902 4.858	$^{241}Pu\ (n,\gamma)\ ^{242}Pu$
^{241}Am	432.2	α	5.486 5.443	$^{241}Pu \xrightarrow{\beta^-} {}^{241}Am$
^{244}Cm	18.1	α	5.805 5.762	$^{243}Am\ (n,\gamma)\ ^{244}Am \xrightarrow{\beta^-} {}^{244}Cm$

Two of the actinides, thorium and uranium, are found in relatively high abundance in the environment and can be detected by standard chemical techniques. The other actinides have a very low natural abundance and must be analyzed using sensitive detection techniques.

Two isotopes of the actinides, ^{235}U and ^{239}Pu, are used extensively in nuclear power reactors and for nuclear weapons. Tons of ^{239}Pu have been produced by neutron capture of ^{238}U in

nuclear power plants. ^{239}Pu poses a great challenge for storage because it is highly toxic due to its intense alpha particle emission and its half-life of 24,100 years.

Because the technology for fabricating nuclear weapons is now widespread and many nations would be capable of manufacturing these weapons if they had access to large amounts of ^{235}U or ^{239}Pu, the quantities of these isotopes that are available also pose a security challenge for the next generation in the world. Other important isotopes of the actinide elements are ^{238}Pu, which is used in heart pacemakers and space instrumentation, ^{241}Am which is used in smoke detectors, and ^{252}Cf which is used in analytical techniques that involve production of isotopes of other elements by neutron-capture. The isotopes ^{237}Np, ^{238}Pu, ^{239}Pu, ^{240}Pu, ^{241}Pu, ^{242}Pu, ^{241}Am, ^{244}Cm, etc. are the most important ones with respect to the nuclear waste and the environment. Table 2 shows some of the light actinide isotopes and their production.

2.1.2 Actinide solution chemistry

The lighter actinides (Ac-Am) show transition metal like behavior and exhibit a broad range of oxidation states (up to oxidation state VII) and thus a complex chemical behavior. The heavier actinides have analogous lanthanide character, and the main oxidation state is the +3 state [Clar 2000].

Table 3: Oxidation states of the lighter actinide elements

Th	**Pa**	**U**	**Np**	**Pu**	**Am**	**Cm**
III	III	III	III	(III)	**(III)**	**(III)**
IV	IV	(IV)	(IV)	**(IV)**	IV	IV
	V	V	**(V)**	(V)	V	
		(VI)	(VI)	(VI)	VI	
			VII	VII		

(Bold indicates the most stable oxidation state; parentheses indicate environmentally important oxidation state).

The 5f electrons of the actinide elements are shielded to a larger extent from the nuclear charge of the atoms than the 4f electrons resulting in a smaller energy difference between the 5f, 6d, and 7s electrons than the 4f, 5d, and 7s electrons in the lanthanide series. Therefore, a wide range of oxidation states (Table 3) from III to VII is possible in the case of the actinide series [Katz 86].

2.1.3 Hydrolysis and solubility of Th(IV) and Np(IV)

The solution chemistry of tetravalent actinides, particularly their hydrolysis, is of major importance for nuclear waste repositories. Hydrolysis reactions can limit the concentration of free actinide ions in solution; can lead to precipitation or adsorption, and /or complexation by other ligands (CO_3^{2-}, Cl^-, SO_4^{2-}, NO_3^{2-}, etc). The tendency for hydrolysis reaction follows the effective charge of the actinide ions in the following order [Kim 86]:

$An^{4+} > AnO_2^{2+} > An^{3+} > AnO_2^{+}$

The tendency for hydrolysis is the strongest for tetravalent actinides in the following order: Th(IV) < U(IV) < Np(IV) < Pu(IV) (Table 4) [Neck 2001b]. The hydrolysis reaction of the tetravalent actinides, An^{4+} ions, can be expressed by,

$$xAn^{4+} + yH_2O \leftrightarrow An_x(OH)_y^{\,4x-y} + yH^+ \quad (1)$$

or

$$xAn^{4+} + yOH^- \leftrightarrow An_x(OH)_y^{\,4x-y} \quad (2)$$

The hydrolysis constant K'_{xy} (in a given medium) and K^0_{xy} (at infinite dilution) are given by

$$K_{xy}' = \frac{\left[An_x(OH)_y^{\,4x-y}\right]\left[H^+\right]^y}{\left[An^{4+}\right]^x} = \frac{K_{xy}^{\,0}(g_{An^{4+}})^x(a_w)^y}{(g_{An_x(OH)_y})(g_H)^y} \quad (3)$$

and the corresponding formation constants β'_{xy} and β^0_{xy} are given by

$$b_{xy}' = \frac{\left[An_x(OH)_y^{\,4x-y}\right]}{\left[An^{4+}\right]^x\left[OH^-\right]^y} = \frac{b^{\,0}{}_{xy}(g_{An^{4+}})^x(g_{OH^-})^y}{(g_{An_x(OH)_y})} \quad (4)$$

where [i] denotes the concentration of the species i, γ_i its activity coefficient and a_w the activity of water. The hydrolysis constant $\log K^0_{xy}$ is related to $\log\beta^0_{xy}$ by the ion product of water ($\log K_w = -14.00$) [Cho 2006].

Table 4: Hydrolysis constants of Th(IV), Np(IV), and Pu(IV) hydrolysis species at I = 0 and 25^0C [Neck 2001b]

Hydrolysis constants ($\log b_{xy}^0$)	**Th(IV)**	**Np(IV)**	**Pu(IV)**
$An(OH)^{3+}$	11.8±0.2	14.5±0.2	14.6±0.2
$An(OH)_2^{2+}$	22.0±0.6	28.3±0.3	28.6±0.3
$An(OH)_3^{+}$	31.0±1.0	39.2±1.0	39.7±0.4
$An(OH)_{4\,(aq)}$	38.5±1.0	47.7±1.1	48.1±0.9

Throrium has the largest tetravalent cation and the least susceptibility to hydrolyze. The hydrolysis of Th(IV) has extensively been studied for over 35 years [Ekbe 2000]. The hydrolytic behavior of Th(IV) is known to be extremely complex because of its extensive polymerization reaction, which occurs even in the low pH range. The stability constants of Th(IV) hydrolysis species have been measured by Ekberg et al. [Ekbe 2000]. In considering thorium carbonate complexation, five mononuclear species $Th(OH)_2(CO_3)$, $Th(OH)_3(CO_3)^-$, $Th(OH)_2(CO_3)_2^{2-}$, $Th(OH)(CO_3)_4^{4-}$and $Th(CO_3)_5^{6-}$ have been presented by Altmaier et al. [Altm 2005].

The effect of carobonate and bicarbonate on the solubility of Th(IV) was studied by Rai et al. and they found a considerable Th(IV) solubility indicating the presence of highly charged aqueous pentacarbonate complexes [Rai 95]. The strong tendency towards hydrolysis of Np(IV) in aqueous solution even at low pH and the low solubility of Np(IV) hydroxide were investigated by Neck et al. [Neck 2001b].

The mononuclear Np(IV) hydrolysis constants were predicted by Duplesis et al. [Dupl 77]. The most dominant species is $Np(OH)_2^{2+}$at low Np concentrations and a pH range 1.5-3. Neck et al. [Neck 2001a] have calculated the possible Np(IV) hydroxide species in aqueous solution (Figure 1).

Eriksen et al. have studied Np(IV)-carbonate complexes $Np(OH)_4CO_3^{2-}$, $Np(OH)_3CO_3^-$, and $Np(CO_3)_5^{6-}$ etc. These species are likely to be dominating only at high pH, Eh and may influence the total solubility determined by $Np(OH)_4(s)$ at high carbonate concentration [Erik 93].

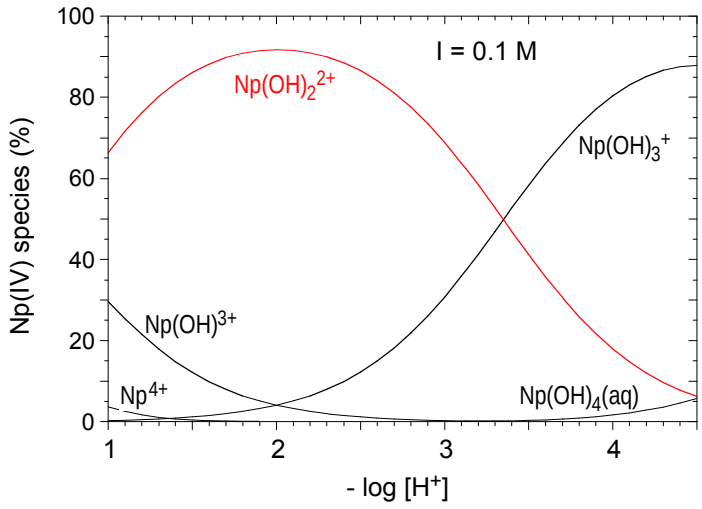

Figure 1: Species of Np(IV) as a function of pH in aqueous solution at I = 0.1 M $NaClO_4$ and 25^{0}C [Neck 2001a]

Eriksen et al. [Erik 93] have investigated the Np(IV)-carbonate complexes $Np(OH)_4CO_3^{2-}$, $Np(OH)_3CO_3^-$, and $Np(CO_3)_5^{6-}$ etc. The chemical formation of precipitated or aged An(IV) solid phases is called either amorphous hydroxides $An(OH)_4$(am) or amorphous partly microcrystalline hydrous oxides $AnO_2.xH_2O$(am). In general, they have no definite composition but consist of hydrated oxy hydroxide $AnO_{(2-n)}(OH)_{2n}$(am) with $0 < n < 2$, where n decreases with aging or temperature. The solubility products K'_{sp} (at given medium) and K^0_{sp} (at infinite dilution) of amorphous An(IV) precipitates, $An(OH)_4$(am) or hydrous oxides $AnO_2.xH_2O$(am), and crystalline dioxides AnO_2 refer to the dissolution equilibrium [Neck 2001b] (Figure 2).

$$An(OH)_4(s) \leftrightarrow An^{4+} + 4OH^- \quad (5)$$

and

$$AnO_2.xH_2O(s) + (2-x)H_2O \leftrightarrow An^{4+} + 4OH^- \quad (6)$$

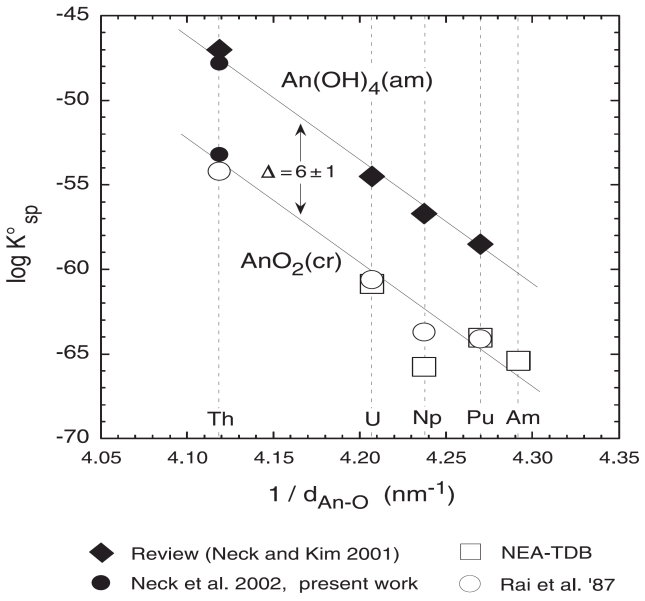

Figure 2: Solubility products of $An(OH)_4$(am) and AnO_2(cr) as a function of the distance $d_{An\text{-}O}$ (sum of crystal radii of An^{4+} and O^{2-} in the fluorite structure [Shan 76]. Filled symbols represent $logK^0_{sp}$ values derived from experimental solubility data, open symbols represent calculated values from thermodynamic data [Neck 2003].

The solubility products K'_{sp} (in a given medium) and K^0_{sp} (at infinite dilution) are expressed by

$$K_{sp}' = [An^{4+}] \cdot [OH^-]^4 \quad (7)$$

and

$$K_{sp}^{0} = K_{xy}'(g_{An})(g_{OH})^{4} \text{ [for An(OH)}_4\text{(am)]} \quad (8)$$

$$K_{sp}^{0} = K_{xy}'(g_{An})(g_{OH})^{4}(a_{w})^{(x-2)} \text{ [for AnO}_2\text{.xH}_2\text{O(s)]} \quad (9)$$

The preparation of water-free crystalline dioxide AnO_2(cr) requires heating above 700^0C. Solubility products for crystalline An(IV) dioxides are generally calculated from thermodynamic data [Neck 2003]. At low pH values, hydrous ThO_2 is quite soluble, but at pH values higher than 3-4 its solubility decreases significantly. In the literature, the solubility value of hydrous ThO_2 is found to decrease steeply from 10^{-3}-10^{-2} M to 10^{-9}-10^{-8} M between pH 3.6 and 4.7. In 1999, Neck & Kim [Neck 99] observed that the experimental solubility values for Th(IV) in the absence of carbonates in the pH range 6-13 were between 10^{-9}-10^{-8} M. Crystalline ThO_2 equilibrates very slowly with the aqueous phases at room temperature.

Table 5: Solubility products for tetravalent actinides Th(IV), Np(IV), and Pu(IV) at I = 0 and 25^0C [Neck 2001a]

Solubility products ($\log K_{sp}^{0}$)	**Th(IV)**	**Np(IV)**	**Pu(IV)**
$AnO_{2\,(cr)}$	-54.2±1.3	-63.7±01.8	-64.0±1.2
$An(OH)_4$(am) / $AnO_2.xH_2O$(am)	-47.0±0.8	-56.7±0.5	-58.5±0.7

Based on the hydrolysis constants of Np(IV), the solubility products of $NpO_2.xH_2O$ (am) ($\log K^{0}_{sp}$ = -56.7±0.5) are calculated from solubility data determined by Rai et al. in acidic medium [Rai 87]. The solubility products of the amorphous An(IV) hydroxides (Table 5) decreases by orders of magnitude in the series Th(IV) > U(IV) > Np(IV) > Pu(IV), which correlates with decreasing distance $d_{An\text{-}O}$ in the lattice [Shan 76].

2.1.4 Complexation, sorption, and colloids of Th(IV) and Np(IV)

Complexation

Ground water contains large amounts of inorganic complexing anions like HCO_3^-/CO^{2-}_3, Cl^-, SO_4^{2-}, PO_4^{3-}, etc. The complexation properties of inorganic anions with metals are in the followings order [Kim 86]:

$$CO_3^{2-} > SO_4^{2-} > PO_4^{3-} > Cl^- > \ldots$$

Important organic matters in natural water are humic acid (HA) and fulvic acid (FA) and also small chained organic acids like citric acid. These form strong complexes with tetravalent actinides like Th(IV), Np(IV), and Pu(IV). In the absence of humic materials, hydrolysis species dominate the Np(IV) speciation even at low pH values. However, in the presence of humic materials, Np(IV) is strongly complexed leading to an increase of the mobility of Np(IV) in the natural aquifer [Arti 2000]. Detailed studies on the interaction of tetravalent neptunium with humic substances (HS) are still missing. Therefore, Pirlet and Marquardt et al. have performed first studies on the interaction of neptunium with HS [Pirl 2003a, Marq 2001]. The reduction of Np(V) to Np(IV) in contact with humic substances has been investigated in the neutral pH range [Zeh 99b]. The complexation of Th(IV) with humic substances was investigated by Nash et al. [Nash 80].

Sorption

The sorption of thorium onto mineral surfaces such as silica, TiO_2, goethite, hematite, and alumina, has been studied and cited in the literature [Reil 2002]. A strong sorption of Th(IV) was found at a pH range of 2-3 which is also expected for the other tetravalent actinides. So far, the sorption of Np(IV) onto minerals has not yet well been studied because of its high redox sensitivity and colloid formation even at low pH values. This is also found for Pu(IV).

Colloids

In 1860, Thomas Graham defined “colloids” as substances, which do not diffuse through a semiparemeable membrane. Colloids can be defined in various ways, e.g., by size, by origin, by composition, etc. According to size, colloids are species between 1 and 1000 nm diameter that may be suspended or dispersed in liquids and maintained in suspension for indefinitely long periods due Brownian motion. The amount and nature of aquatic colloids depends on the geochemical nature of a given aquifer system. When actinide ions are introduced into ground water, two types of colloids can be formed: 1) Real (pure, eigen, true or intrinsic) colloids or 2) Pseudo (associative) colloids. Real colloids are generated by the aggregation of hydrolyzed or precipitated actinide ions. The tendency of actinides to generate real colloids is in the same tendency as for hydrolysis, $An^{4+} > AnO_2^{2+} > An^{3+} > AnO_2^{+}$ [Cho 2006, Kim 89, Kim 90]. Pseudo colloids are generated by the adsorption of trace amount of actinide ions on groundwater colloids. The chemical properties of these kinds of colloids might not be altered by the adsorbed actinide ion. Several methods have been introduced in the literature for the characterization of actinide colloids such as: centrifugation, ultrafiltration, electrophoresis, ion exchange, spectroscopic methods like, Laser induced break down detection (LIBD) and Laser

induced photoacoustic spectroscopy (LPAS) as well as Scanning and transmission microscopy (STM).

The formation of Th(IV) and Np(IV) colloids was investigated by laser breakdown detection (LIBD) in combination with ultrafiltration in the concentration range from 10^{-5}-10^{-2} M at pH 2-5 [Bite 2003, Neck 2001b]. With LIBD, Th(IV) and Pu(IV) colloids in the size range < 20 nm can be measured [Bite 2002, Neck 2001a]. The colloids $Th_nO_{2n-x}(OH)_y^{nz+}$ with a charge $0 < z < 1$ per Th unit may be written in the simplified form as '$Th(OH)_4$(coll)'. At low Th concentration, $ThOH^{3+}$ is known to be the predominant hydroxide species in the pH range 3.2-4.5. The dissolution of colloids leads to an increase of pH:

$$Th(OH)_4(coll) \rightarrow ThOH^{3+} + 3OH^- \quad (10)$$

On the contrary, the formation of colloids leads to an acidification of the solution:

$$ThOH^{3+} + 3H_2O \rightarrow Th(OH)_4(coll) + 3H^+ \quad (11)$$

2.2 Plutonium Chemistry

Plutonium was the second transuranium element of the actinide series that was discovered by Seaborg et al. [Seab 46]. In 1940, Seaborg, McMillan, Kennedy, and Wahl produced the isotope ^{238}Pu by deuteron bombardment of uranium at the 60-inch cyclotron in Berkeley, California and by neutron bombardment of ^{238}U in the chain.

$$U\ (n, \gamma) \xrightarrow[23\ min]{\beta-} {}^{239}Np \xrightarrow[2.3\ d]{\beta-} {}^{239}Pu \quad (12)$$

In both cases, the growth of α activity from the Np precursor was observed and their ranges in air indicated that ^{238}Pu has the higher α energy (and shorter half-life) as compared to that of ^{239}Pu.

Plutonium also exists in trace quantities in naturally occurring uranium ores. So far 18 different isotopes of plutonium with a half-life range from 1 minute to million years are known; the isotopes 236-243 are of highest biological concern. Almost all the isotopes are α emitters. Since World War (II), more than 2400 metric tons of plutonium has been produced in the world. From this amount, about 260 metric tons have been generated by military applications and the rest produced by nuclear reactors.

Isotopic ratios among different plutonium isotopes have been used to determine the origin of plutonium contamination found in samples. Figure 3 describes the production of plutonium isotopes through neutron irradiation of uranium.

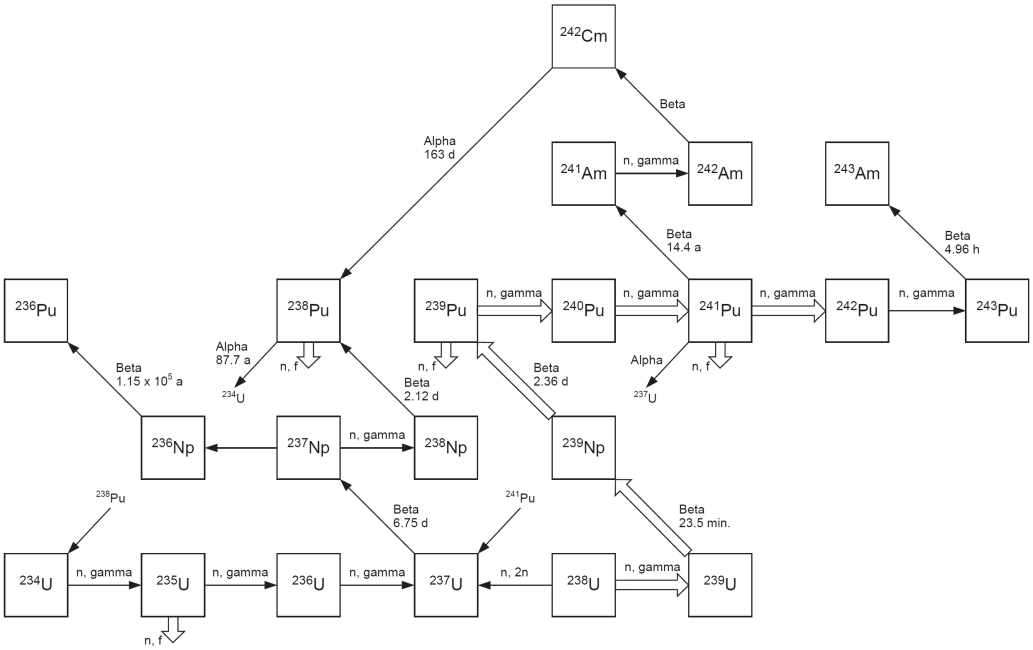

Figure 3: Principal modes of plutonium production through neutron irradiation of uranium [IAEA 98]

2.2.1 Physical and chemical properties

Plutonium is a silvery-white metal that exists as a solid under normal conditions. The plutonium metal readily dissolves in concentrated hydrochloric acid, hydroiodic acid, or perchloric acid. Pu metal exhibits six allotropic modifications having various crystalline structures and densities from 16.00 to 19.86 g/cm^3. The reaction of plutonium metal with air at room temperature is slow. The oxidation rate depends on various factors such as: i) temperature, ii) surface area (iii) oxygen concentration, (iv) concentration of moisture and other vapours in the air. Table 6 shows the ionic radius of the different plutonium oxidations states.

Table 6: Ionic radius of the plutonium oxidation states [Clev 79]

Plutonium	Oxidation state	Ionic radius [Å]
III	Pu^{3+}	0.99
IV	Pu^{4+}	0.90
V	PuO_2^{+}	0.87
VI	PuO_2^{2+}	0.81

2.2.2 Plutonium solution chemistry

The solution chemistry of plutonium is complicated in comparison to other actinides due to the multiplicity of oxidation states in the aqueous solution. The ground state electron configuration of plutonium is $5f^6\ 7s^2\ 6d^0$. The energy level of the 6d and 5f orbital are similar, so the electrons can easily move from the f orbital to the d orbital, leading to multiple oxidation states in solution. Each oxidation state shows a different characteristic color in aqueous solution (Figure 4). Pu(VII) only exists as the PuO_3^+ species at high pH values in the laboratory but is not found in nuclear operation processes or in the environment. In aqueous solution the four oxidation states Pu(III)-Pu(VI) can coexist in the same solution. Aqueous solutions of plutonium are frequently employed in reprocessing operations.

In concentrated acid solutions, e.g., perchloric acid, Pu(III) and Pu(IV) exists as hydrated (or aquo) ions. Water molecules are coordinated around the plutonium ion in numerous ways such as $Pu(H_2O)_n^{3+}$ and $Pu(H_2O)_n^{4+}$, where n can vary depending on the concentration of Pu ions and ionic strength of the solution.

Figure 4: Characteristic color of the oxidation states of plutonium due to their various electron transitions in the solution [Clar 2000, Rund 2000].

Hydrolysis and solubility constant of Pu(IV)

Tetravalent plutonium ion has a tendency to hydrolyze and to form polymeric species even at low pH range.

$$Pu^{4+} + 4H_2O \leftrightarrow Pu(OH)_4(aq) + 4H^+ \qquad (13)$$

Various hydrolysis species of Pu(IV) are formed as a function of the pH –value. $Pu(OH)^{+3}$, $Pu(OH)_2^{+2}$, $Pu(OH)_3^{+}$, $Pu(OH)_4^{0}$. Figure 61 shows the hydrolysis species of Pu(IV) as a function of pH. At Pu(IV) concentration greater than 10^{-7} M, $Pu(OH)_4$(s) precipitates as an amorphous hydroxide polymer in the solution that can be separated by ultrafilation. The extent of polymer formation depends on the Pu(IV) concentration, pH, the presence of other ions, and temperature. The hydrolysis constants reported in the literature for Pu(IV) are summarized in Table 4. The aqueous chemistry of Pu(IV) is usually controlled by the extremely low solubility of $Pu(OH)_4$ (am) or $PuO_2.xH_2O$ (am) and PuO_2 (cr) species in the solution.

The solubility products ($\log K^0_{sp}$) of $Pu(OH)_4$ (am) or $PuO_2.xH_2O$ (am) and PuO_2 (cr) species have been reported (Figure 5) as –58.5 and –64.1, receptively, in the literature [Neck 2001a]. The solubility product of $Pu(OH)_4$ (am) or $PuO_2.xH_2O$ (am) is defined as

$$K_{sp}^{'} = \left[Pu^{4+}\right] \cdot \left[OH^{-}\right]^4 \qquad (14)$$

with

$$K_{sp}^{0} = K_{xy}^{'}(g_{An})(g_{OH})^4 \text{ [for } Pu(OH)_4\text{(am)]} \qquad (15)$$

$$K_{sp}^{0} = K_{xy}^{'}(g_{An})(g_{OH})^4(a_w)^{(x-2)} \text{ [for } PuO_2.xH_2O\text{(s)]} \qquad (16)$$

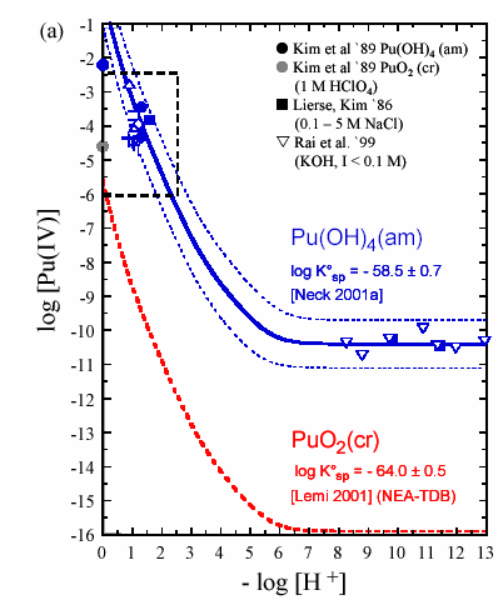

Figure 5: Solubility products of $Pu(OH)_4$(am) and PuO_2(cr) as a function of pH in aqueous solution [Neck 2001b]

If the concentration of polynuclear and colloidal species of Pu(IV) is small compared to that of mononuclear hydrolysis species, the solubility constant can be expressed by

$$[Pu(IV)]_{tot} = (K_{sp}^{'} / [OH^-]^4)(1 + \sum K^{'}_{sp} b^{'}_{1y} [OH^-]^y) \quad (17)$$

Using equation (17) and the hydrolysis constant of Pu(IV), the solubility products of Pu(IV) hydroxide or hydrous oxide can be calculated [Knop 99].

2.2.3 Redox chemsitry, complexation, sorption, and colloids of plutonium

Redox chemistry of plutonium

The redox chemistry of plutonium is influenced by its oxidation state in the solution. Farr et al. [Farr 2000] shows that Pu(III) is rapidly oxidized by water at near neutral pH range because of its negative potential at higher pH values. From the redox potentials of plutonium (Figure 6) at neutral pH value, it can be concluded that Pu(IV), Pu(V), and Pu(VI) are the relevant oxidation states in the natural environment. Recently Cho et al. [Cho 2006a] have shown that the so called "disproportionation of Pu(IV)" is a two-step process, no disproportionation.

The redox reactions are influenced by the solution conditions (pH, Eh). Pu(V) is a stable species in neutral or basic solution and undergoes disproportion in acidic solutions. In natural aqueous systems, the oxidation state of plutonium is mainly governed by the pH and Eh in the solution. An increasing pH favors the higher oxidation states and the Eh is influenced by the amount of dissolved oxygen; so higher Eh favors higher oxidation states.

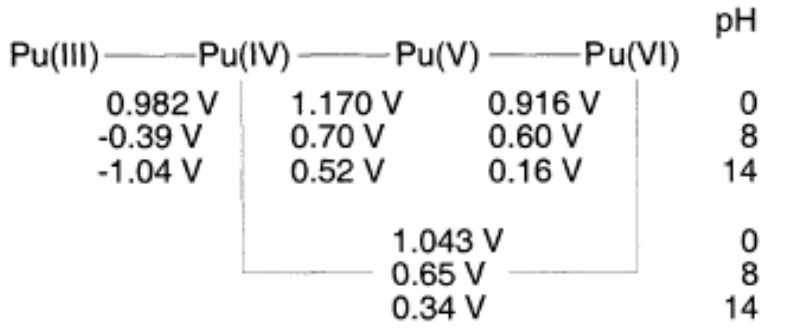

Figure 6: Redox potentials for all oxidation states of plutonium in acidic, neutral and basic solution [Flur 2003]

Complexation

In all oxidation states, plutonium exists as a hard Lewis acid and therefore, ionic and electrostatic bonds with hard Lewis bases are formed. Ionic bonds primarily depend on the

effective charge of the oxidation states. The electrostatic interaction is governed by steric interferences, structure and numbers of water molecules in the first coordination sphere in the plutonium ions. Plutonium forms complexes with inorganic ligands like fluoride, chloride, sulfate, carbonate, nitrate, silicate, etc. in the natural system. The order of decreasing tendency for complex formation is Pu(IV) > Pu(VI) > Pu(III) > Pu(V), the same tendency as for hydrolysis reactions. The Eh-pH diagram shown in the Figure 7 includes both F^- and CO_3^{2-} complexes with plutonium. These complexes are most important under conditions at Eh and pH values relevant to natural waters (Figure 7). Under oxidizing conditions, fluroide complexes with Pu(IV) are stable at lower pH; and the $Pu_2CO_3^{2-}$ complexes are stable at higher pH values.

Complexation of plutonium by organic molecules is dominated by hard-hard lewis interaction as in the case of inorganic complexes, thus the most important functional groups are carboxylate and phenolic groups. Complexation with a single carboxylate group is somewhat weaker than with an inorganic carbonate group, but when the organic molecules contains several functional groups able to bond simultaneously with plutonium, much stronger complexes are formed [Katz 86].

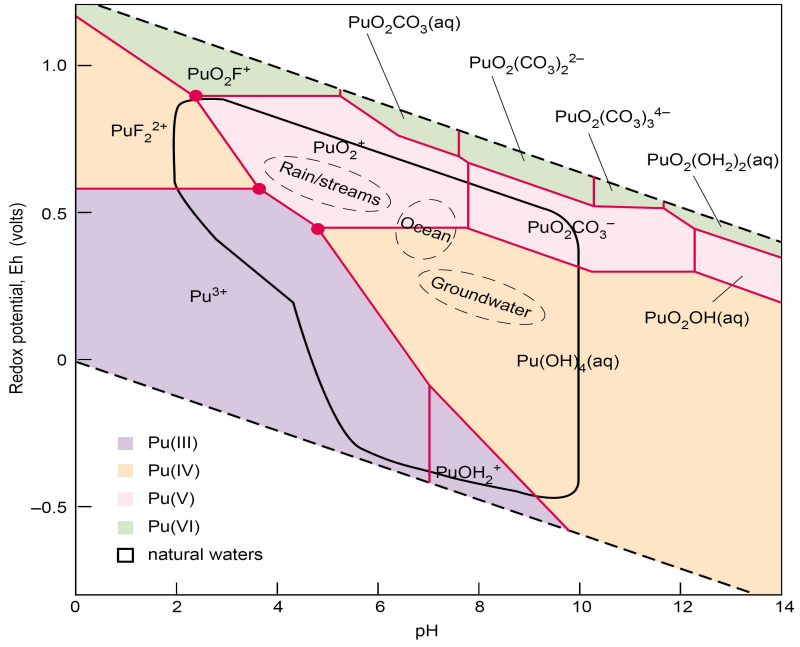

Figure 7: Eh Vs. pH diagram for plutonium in groundwater containing hydroxide, carbonate and fluoride [Rund 2000].

Sorption

Tetravalent plutonium is immobile in the subsurface because of its tendency to sorb strongly onto mineral surfaces and organic matter to form $Pu(OH)_4$ (am) and PuO_2 (cr) solid phases. Plutonium sorbs stronger, several orders of magnitude, in the Pu(III) and Pu(IV) oxidation state than in the higher oxidation states Pu(V) and Pu(VI). In the Baltic sea, 99 % of the total plutonium sorbed onto sediments is present in the form of Pu(IV) [Holm 95].

Several studies have been performed to understand the sorption of plutonium onto minerals or subsurfaces. Most sorption studies have been carried out with Pu(V) and Pu(VI) as initial species, because Pu(III) species is only stable in an anaerobic systems and Pu(IV) tends to precipitate as $Pu(OH)_4$. In the literature, a strong sorption of Pu(V) is described on geological materials like manganese oxides, zeolite, calcites, albite, quartz. Soprtion of plutonium onto smecties [Naga 97], manganese oxides, and calcites may be enhanced by the presence of carbonate found in natural systems. Kudo et al. [Kudo 2001] have discussed plutonium sorption studies onto materials where Pu(V) is reduced to Pu(IV). Sorption of Pu(V) on several minerals like kaolinite, silica, alumina, and goethite has been studied and a reduction of Pu(V) was found during the sorption onto the minerals [Sanc 85].

Colloids

Colloids may play an important role in the distribution and movement of plutonium in natural systems. The influence of colloids on the migration of plutonium is not yet well understood. The tendency of the formation of plutonium intrinsic colloids has been described by Kim et al. [Kim 91a] to be proportional to the effective charge of plutonium ions: Pu(IV) > Pu(VI) > Pu(III) > Pu(V). The mechanism of formation and growth of plutonium colloids is explained as a precipitation process, thus the concentration of plutonium must exceed the solubility product for the formation of a solid phase.

The colloids of Pu(IV) have been briefly described in the literature [Clev 79]. Pu(IV) colloids are formed during the neutralization of an acid solution, yielding a characteristics absorption spectrum. Pu(IV) intrinsic colloids have light green color, completely different from the dark brown color that Pu(IV) ions exhibits. Lloyd and Haire have shown that Pu(IV) colloids consist of very small particles that can be either amorphous or crystalline [Lloy 78].

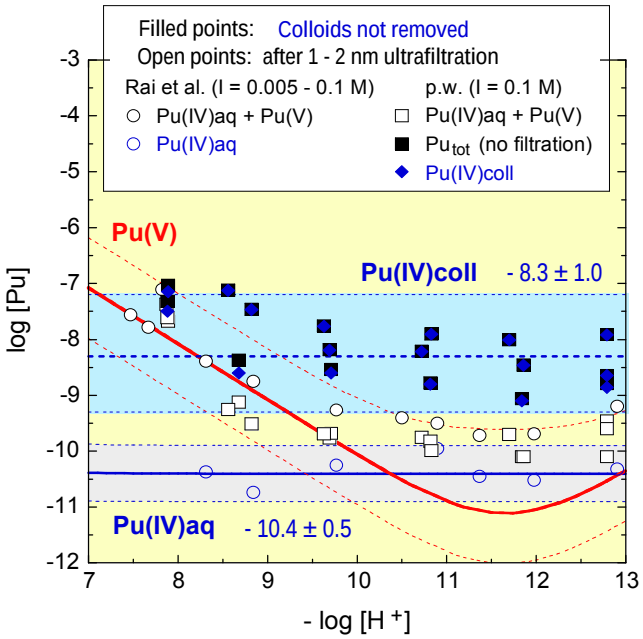

Figure 8: Formation of tetravalent plutonium colloids in aqueous solution [Neck 2006]

The stability of Pu(IV) colloids depend on their size, pH, and the ionic strength of the solution. Various techniques have been used for the determination of the size of plutonium colloids in the literature: filtration, ultrafiltration, centrifugation, chromatographic techniques, and laser induced break down spectroscopy. Recently, Neck et al. [Neck 2006] have investigated the formation of Pu(IV) colloids and the detection of colloids at low concentrations in the solution . Figure 8 shows the formation of Pu(IV) colloids at higher pH even at low concentration (10^{-8} M).

2.3 Radioactive Waste Disposals and Repository

The deposition of "nuclear waste" formed in the nuclear fuel cycle is one of the most demandable environmental problems for the 21st century, a heritage from the atomic age of the 20th century [Ewin 99]. The International Atomic Energy Agency (IAEA) defines: "radioactive waste is any material that contains or is contaminated with radionuclides at concentrations or radioactivity levels greater than the exempt quantities established by the competent authorities and for which no use is foreseen [Fuku 2003]".

However, radioactive waste generation is a reality and a consequence of various ways:

- nuclear power generation for electricity and propulsion
- nuclear fuel cycle; nuclear reactor,
- accidental arising of waste from incidents such as Chernobyl;

- military defense programmes of a number of countries;
- application of radioactivity in medicine and industry;
- enhancement of naturally occurring radionuclides due to human activity.

At the moment, 444 nuclear reactors are in operation worldwide producing a total of about 368 GW electric power, generating annually about 8500 tons of spent fuel [Fuku 2003]. Most of the produced nuclear waste still consists of the original uranium (~95 %), while about 4 % has been converted to fission products (^{93}Zr, ^{99}Tc, ^{129}I, ^{137}Cs, ^{107}Pd etc.) and about 1 % to transuranic elements like ^{237}Np, ^{238}Pu, ^{239}Pu, ^{240}Pu, ^{241}Pu, ^{242}Pu, ^{241}Am, ^{242}Am, ^{244}Cm, etc.
A general principle of radioactive waste management is that waste should be handled safely and appropriately managed and treated.

2.3.1 Types of radioactive waste

Different types of radioactive waste have been proposed by the IAEA. Very often, the radioactive wastes are divided according to the activity level: Very low-level waste (VLLW), Low and intermediate level waste (LILW), High-level waste (HLW) (Figure 9).

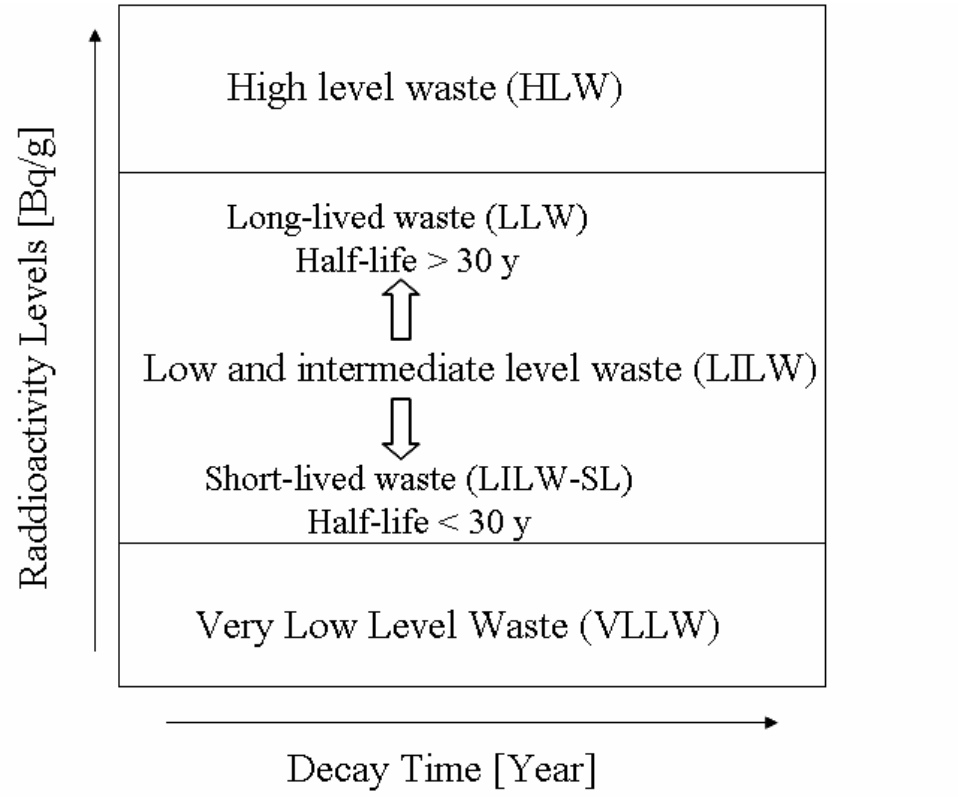

Figure 9: A scheme for the classification of radioactive waste

Very low-level waste (VLLW)

Very low-level waste is defined as waste containing a low concentration of radionuclides which can be exempted from the nuclear regulatory in accordance with clearance levels, and contains negligible radiological hazards. Many studies have been performed and it was concluded this type of waste contributes to an annual dose to the public of less than 0.01 mSv [IAEA 89].

Low and intermediate level waste (LILW)

LILW has the activity levels above clearance level and thermal power below 2 kW/m^3. A contact dose rate of 2 mSV/h has been used to differentiate two classes: low level waste (LLW) and intermediate level waste (ILW). Low-level waste (LLW) has been defined, as the radioactive waste that contains low concentration of beta/gamma radiation and does not require shielding during normal handling and transportation.

Intermediate level waste (ILW) has been defined as the waste containing higher concentrations of beta/gamma contamination and sometimes alpha emitters and requiring shielding but needed little or no provision for heat dissipation. LILW may be subdivided into short-lived waste (LILW-SL) and long-lived waste (LILW-LL). Short-lived low and intermediate level waste (LILW-SL) contains a high concentration of short-lived radionuclides, (half-life less than 30 years) and a low concentration of long-lived radionulcides. This type of waste is disposed in near surface and geological sites at varying depths, typically a few ten meters.

Long-lived low and intermediate level waste (LILW-LL) contains a high concentration of long-lived radionulcides and short-lived radionulcides, half-life of the radionulcides more than 30 years. This type of waste is disposed in near surface and geological sites at depths of several hundred meters. Some countries, such as USA and Canada do not use this classification category.

High-level waste (HLW)

High-level waste (HLW)) contains large quantities of short and long-lived radionulcides, fission products as well as actinides, which are separated during chemical processing of irradiated fuel and spent fuel. It generates significant quantities of heat from the radioactive decay, and normally continues to generate heat for several centuries. This type of waste has a high concentration of beta/gamma emitting fission products and alpha emitting actinides. Specific activities of these wastes depend on some parameters such as the type of

radionuclide, the decay period and the conditioning techniques. Typical activity levels are in the range of 5×10^4 to 5×10^5 TBq/m^3, corresponding to a heat generation rate of about 2 to 20 kW/m^3 [IAEA 89].

In some countries, the definition of HLW encompasses spent-fuel. Some countries categorize alpha bearing waste separately. For example in the USA, "Transuranic Waste" (TRU), is defined as: *"waste containing more than 100 nanocuries of alpha-emitting transuranic isotopes, with half lives greater than twenty years, per gram of waste "*. Figure 10 shows the radiotoxicity of different transuranic isotopes and fission products as a function of time. A dominant contribution to the radiotoxicity over storage times of up to one million years is associated with plutonium isotopes.

State of radioactive waste disposal

The principle of deep geological disposal for high level waste and spent fuel, and long-lived intermediate level waste is recognized internationally and reflected in the radioactive waste policies of many countries. Deep disposal ensures that these wastes remain isolated from the human environment for a very long time, despite the surface scouring action of possible future glaciations, and the return of activity to the surface through groundwater movement.

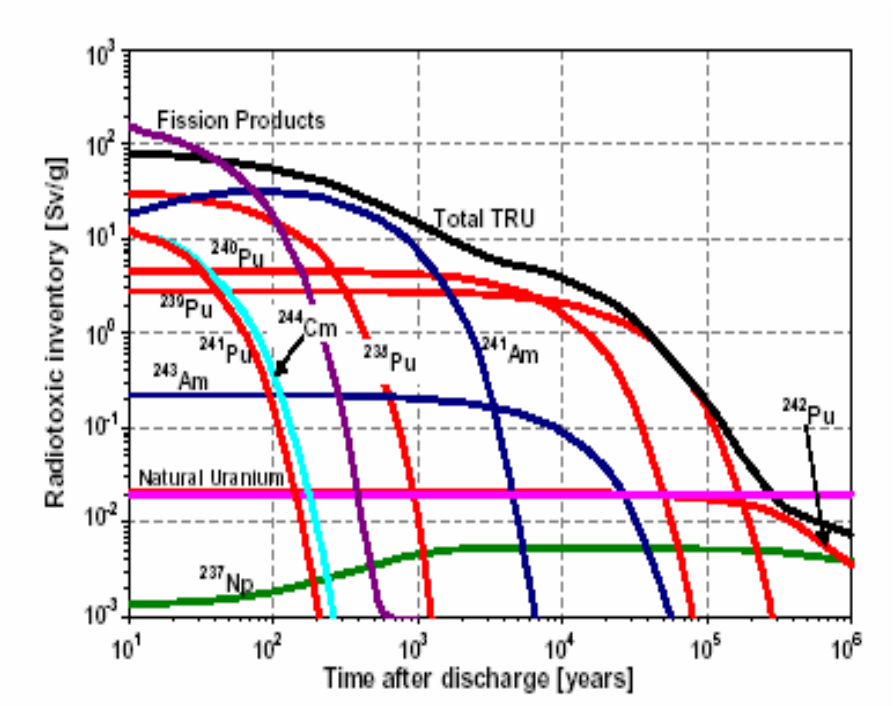

Figure 10: Radiotoxicity inventory in Sv per gram spent fuel of the most important actinides and fission products, compared with the radiotoxicity of natural uranium needed to produce 1 g of 3.7 % ^{235}U-enriched uranium oxide (~20 mSv/g) [Selt 2005].

Deep repository design concepts vary and are determined to a large extent by the geology being considered. Many countries realize that an indispensable part of the final design process involves the use of *in situ* investigation facilities or underground research laboratories (URL). In most cases, the concept of the URL is felt to be a necessary part of the final site characterization exercise. A number of countries have decided to locate repositories in existing underground mines with the advantage of ready-made access facilities to *in situ* laboratories. In some cases where no final site selection has taken place, a "reference" URL has been constructed (as in Canada) or is being considered (Japan). Others are considering constructing a URL at later stages of the site selection process (France, UK, and USA).
In Germany, heat generating wastes comprise spent fuel assemblies, vitrified reprocessing wastes, fuel rods, separators and assembly end pieces, and other reprocessing wastes; 51,000 m^3 of such waste are expected till 2080. Depending on the existing geological situation, different rock formations are being examined with regard to their suitability as repositories for high-level waste. Concepts for disposal in salt, granite, clay and other host rocks have been developed.

Approximately 65 % of low- and intermediate-level wastes come from nuclear power plants and other plants which are directly linked with the production of electricity. The remaining 35 % are produced by hospitals, industrial companies, and research institutes. 98 % of heat developing medium- and high-level wastes and irradiated fuel assemblies come from power generation and the so-called fuel cycle, the remainder is produced during the operation of research reactors. In the Federal Republic of Germany, all types of radioactive waste are planned to be disposed in deep geological formations. There are thee repository sites that have been considered:

Gorleben Site

The Gorleben site in the northeast of Lower Saxony, Germany, has been investigated for its suitability to host a respository at depths between 840 m and 1200 m for all types of radioactive waste [Beck 2004]. Since 1977, the Gorleben salt dome has been investigated for the disposal of heat-generating radioactive waste. Two shafts are now linked at depth and the underground infrastructure is in place.

Table 7: Radioactive waste storage and their distribution in the world [Law 91]

Country	Responsible agency	Transport	Storage	Disposal
Belgium	ONDRAF/NIRAS	ONDRAF	ONDRAF	ONDRAF
Canada	N/A	Waste producers	Waste producers	None, but AECL undertaking R&D on disposal
Germany	BfS (DBE)	Performed by industry after permit from BfS	By industry and/or Federal centers	BfS (DBE)
Finland	Posiva Oy	N/A	Utilities	Posiva for spent fuel; utilities for LILW
France	ANDRA	ANDRA	Industry	ANDRA
Korea	N/A	Industry	Waste producers	None as yet. (KAERI and NETEC)
Japan	Science & Technology Agency (Govt)	Industry	Waste producer	JNFL (LLW) not decided for HLW and others
Spain	ENRESA	ENRESA	ENRESA	ENRESA
Sweden	SKB	SKB	SKB	SKB
Switzerland	NAGRA	-	-	HLW
Taiwan	N/A	Industry	Waste producer	Taipower (LLW)
United Kingdom	UK NIREX	Industry	Waste producers (nuclear industry)	UK NIREX (ILW and alpha wastes) No decision on HLW.
United States	US DOE – OCRWM for HLWEM State Compacts for LLW	Industry	Waste producers	US DOE OCRWM at Yucca Mountain for HLW; US DOE EM at WIPP(TRU);State Compacts for LLW

Konrad Site

Konrad was previously an iron ore mine and in 1976, the Federal Government asked GSF (Federal Research Centre) to investigate its suitability for a non-heat generating waste repository (LLW, ILW).

Morsleben Site

Since the start of operation in 1970, some 24,000 m^3 of mostly LLW have been disposed. The overall regulation of radioactive waste management is controlled by the Federal Regulating authorities, but licensing is a matter of the state.

Table 7 shows the radioactive waste storage and disposal in different countries in the world. Storage of radioactive waste and their disposal is dependent mainly on the types of waste. Therefore, different countries have different agreements to handle radioactive waste.

2.4 Actinides in the Environment

In the actinide series, the elements of greatest interest as environmental contaminants are uranium, neptunium, plutonium, americium, and curium because of the presence of these elements in relatively high concentrations in ecosystems [Watt 83].

The importance of these elements as environmental contaminants depends upon factors related to their production, half-life, chemistry, mode of dispersion, and biological availability. Choppin et al. [Chop 98] and Lieser et al. [Lies 91] have discussed this topic including hydrosphere, geosphere, atmosphere, ground and seawater. As an example, Table 8 shows the actinide isotopes concentration in seawater.

Table 8: Concentration of actinide isotopes in seawater [Chop 98]

Actinide isotope	Concentration [mol/L]
^{232}Th	4.3×10^{-13}
$^{234,238}U$	1.3×10^{-8}
^{238}Pu	3.0×10^{-18}
^{239}Pu	1.0×10^{-14}
^{240}Pu	3.0×10^{-15}
^{241}Pu	8.0×10^{-17}
^{241}Am	4.0×10^{-17}
^{237}Np	2.0×10^{-14}
^{244}Cm	3.0×10^{-22}

Plutonium is distributed globally as a result of nuclear weapons tests, nuclear accidents, nuclear fuel reprocessing and the destruction of thermoelectric generators in satellites. There are different anthropogenic sources of plutonium in the environment. High-level amounts of plutonium are present at the nuclear weapons testing sites such as in the Marshall Island, Mururoa Atoll, Nevada, Semipalatinsk. Plutonium has also been released into the environment through accidents from nuclear facilities such as Sellafield/UK, Kyshtym/Russia, and Chernobyl/Ukraine. The high level waste disposal in the deep sea around the Farallon Islands (California/USA) and in the North Atlantic would be potential contamination sources in the marine environment. In 1964, ^{238}Pu was released into the atmosphere from the accidental burn up of the SNAP-9A satellite.

Plutonium in the earth's surface consists of five isotopes: ^{238}Pu ($t_{1/2}$ = 87.74 y), ^{239}Pu ($t_{1/2}$ = 24110 y), ^{240}Pu ($t_{1/2}$ = 6563 y), ^{241}Pu ($t_{1/2}$ = 14.4 y), and ^{242}Pu ($t_{1/2}$ = 373,000 y). The isotopes ^{238}Pu, ^{239}Pu, ^{240}Pu, and ^{242}Pu decay by emission of α particles, while ^{241}Pu undergoes β^- decay. Among these, ^{239}Pu and ^{240}Pu are the two most abundant plutonium isotopes in the environment. Plutonium in the environment exists in different physical and chemical forms. The estimated quantities of the plutonium isotopes from various sources are listed in Table 9.

Table 9: Sources and quantities of atmospheric plutonium [IAEA 98]

Source	**Alpha emitters**				
	^{238}Pu [kg]	**^{239}Pu [kg]**	**^{240}Pu [kg]**	**^{242}Pu [kg]**	**Total [kg]**
Weapons Testing	0.5	3260	590	100	3950
Satellite Accidents	0.9	-	-	-	0.9
Total civil Reprocessing	~0.5	~300	-	-	~300
Chernobyl Accident	<0.1	12	~3	-	~15
Natural Sources	-	4	-	-	~4
Total	2	~3600	600	100	~4300

The deposition of plutonium in the environment has occurred at different times. The largest amount of plutonium was deposited during 1950 and early 1960 from the atmospheric nuclear weapons testing. Since the first nuclear test detonation in New Mexico in 1945, approximately 3500 kg of plutonium were released into the atmosphere and another 100 kg in underground tests [Chop 2001].

About 0.6 PBq of ^{238}Pu was released into the atmosphere from the destruction of the SNAP-9 satellite power source in 1964. 0.58 PBq of ^{239,240}Pu has been released into the Irish Sea from the Sellafield (UK) reprocessing plant from 1971 to1999. Plutonium is mainly found in the environment in form of the oxide

The distribution of plutonium in the air is largely dependent on its particle size and dispersion mechanism. It was estimated that less than 0.1 % plutonium are soluble in soil and the low soluble fraction of plutonium is expected to be dissolved over a period of years. The presence of wet organic matter in the soil tends to increase solubility because of its higher content of humic matter.

Environmental plutonium can enter the human body mainly via two routes: inhalation of respirable plutonium-containing dust particles or aerosols and through food and water. The plutonium, taken up by plants is either directly consumed by human or eaten by animals whose meat forms part of the food chain [Tayl 95].

2.5 Aqueous Chemistry

2.5.1 Humic Chemistry

The terminology of humic chemistry has a long history dating from the early work of Achard (1786) who extracted peat with alkali to yield a precipitate that we would now call humic substances (HS). Humic substances occur in most natural systems and are involved in mineral weathering, mobilization, and transportation of metal ions, sorption formation of aggregates and cation-exchange processes of soils. In the case of a radionulcide waste repository, HS have a strong interaction and influence to the speciation of radionuclides due to their strong redox, complexing, and sorption properties.

The definition of humus, as a decomposed organic matter, originates from 1761 [Stev 82]. The first relevant study of the sources and chemical nature of HS was performed by Sprengel in 1839 [Pena 2005]. Research on the chemical properties of HS was extended by the Swedish scientist Berzelius, whose main contribution was the isolation of two light-yellow-colored HS from mineral water and slimy mud rich in iron oxides [Berz 1839].

Since HS have a diversity in the composition, it is difficult to define mixtures that compose mainly soil organic matter (SOM), natural organic matter (NOM), dissolved organic matter (DOM), or the particulate organic matter (POM) of waters. Figure 11 shows the possible flow path of the HS in the natural environment. It can be seen that all HS are interconnected through the water that means HS are primarily transported by water in the natural environments.

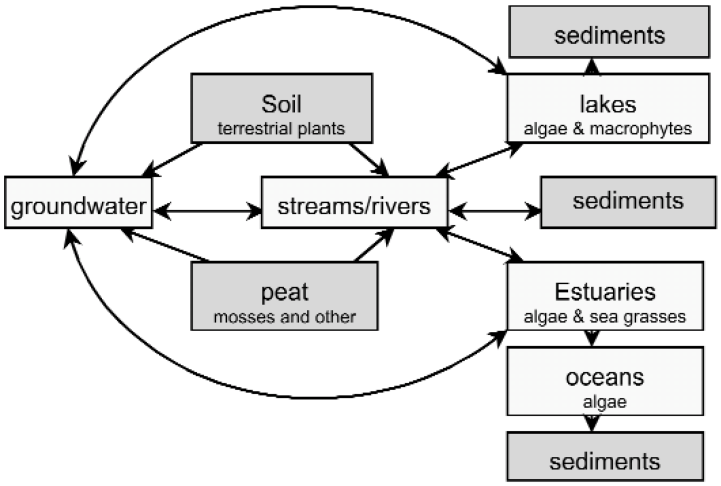

Figure 11: Scheme of the occurrence and possible environmental flow paths of humic substances [Koop 2001]

There are various definitions of HS with respect to their solubility in aqueous solution. Aiken et al. stated that humic substances are a general category of naturally occurring heterogeneous organic substances that can generally be characterized as being yellow to black in color, of high molecular weight, and refractory [Aike 85]. Hayes and Swift defined as humic substances the amorphous, macromolecular, brown-colored components of soil organic matter which bear no morphological resemblances to the plant or animal tissues from which they are derived, and which can be differentiated into general classes on the basis of solubility differences in aqueous acids and bases [Haye 78].

Humic substances are usually divided into three fractions due to their solubility in aqueous solutions at different pH values (Figure 12) [Aike 85, Haye 78, Chop 78, Chop 88]. Humic acids (HA) and Fulvic acids (FA) are extracted from soil organic matter or sediment samples as the sodium salts by treating with sodium hydroxide and acid solution. The fraction of HS that is not soluble at all pH values is referred as humin. HA is defined as “the fraction of HS

that is not soluble at pH < 3 but becomes soluble at higher pH value" and FA is the fraction of HS that is soluble at all pH values.

FA has the highest content of carboxylic groups compared to the other fractions (HA, humin) resulting in a high solubility in aqueous solution. It has the lowest molecular weight (between 300 to 1200 dalton).

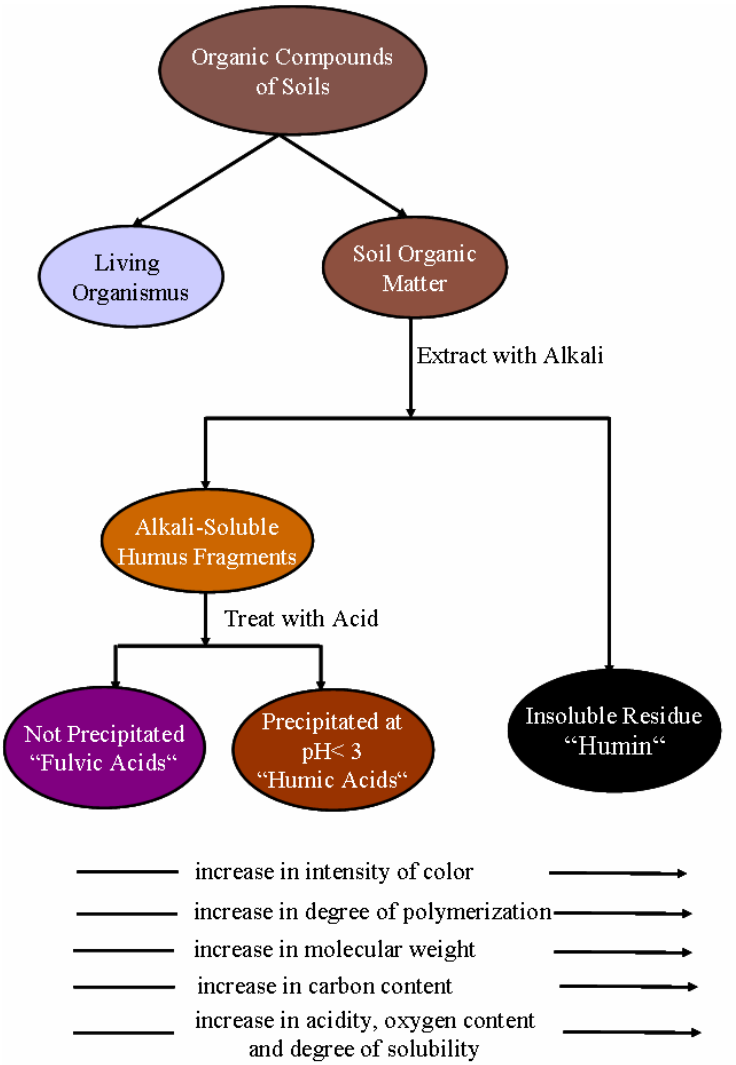

Figure 12: Scheme for the fractionation of humic substances and the general properties of the different types of humic substances

Humic acid has a lower carboxylic content and a higher molecular weight than fulvic acid and is insoluble in acidic solutions. The molecular weights of HA vary between 1000 to 20,000 dalton [Schn 72, Bürg 2005b]. Humin represents more than 50 % of the total organic carbon of soils, but is not very well investigated. Schnitzer et al. assumed that the elemental composition and functional group of humin are similar to that found in humic acid [Schn 72].

The formation process for humic substances is still not well understood. Several hypotheses have been proposed in the last years; for example the “sugar amine condensation theory”, “lignin theory”, and the “polyphenol theory” but nowadays most scientists suppose that humic substances are originated from lignin [Pena 2005].

Humic substances are high molecular weight polyelectrolytes containing a range of functional groups including carboxylic, phenolic, carbonyl, hydroxyl, aromatic and aliphatic alcohols, aldehyde, amine, amino, ketone, ether, ester, methoxy groups and sulfhydryl. In the last decades, analytical methods and computer technology have been used to elucidate the molecular structure of HA and FA. Stevenson (1982), Buffle et al. (1977), Schulten (1993) and in more recent studies Kujawainski et al. (2002) and Stenson el al. (2003), have proposed several molecular structures of humic and fulvic acid. Stevenson proposed a structural model of HA that is formed from the aggregation of almost all functional groups and is illustrated in Figure13.

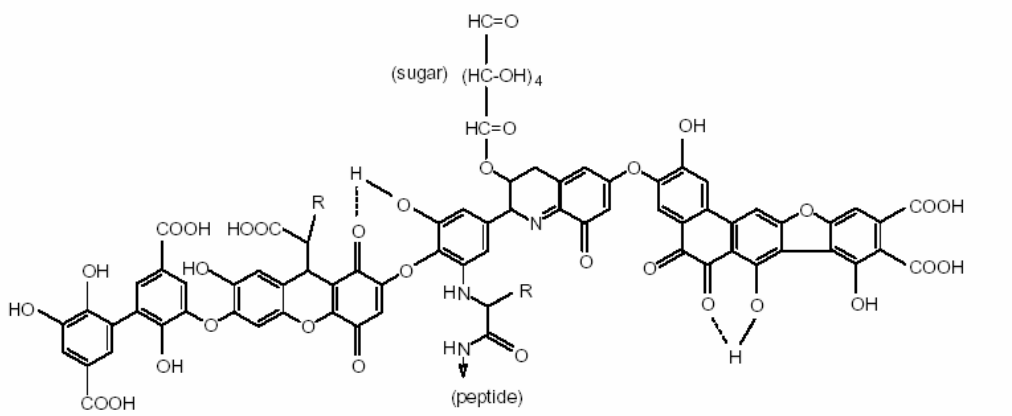

Figure 13: Model structure of humic acid according to Stevenson [1982], R can be alkyl, aryl or aralkyl.

Among the variety of functional groups, carboxylic and phenolic groups are the largest portions. Due to this polyfunctionality, humic substances are one of most important organic ligand to for the formation of complexes with actinides like plutonium, thorium, neptunium etc.

2.5.2 Actinide complexation with humic substances

To quantify the influences of humic substances on the geochemical behavior of actinide ions, many investigations have been performed for tri [Kim 93], tetra [Nash 81], penta [Marq 96], and hexa [Czer 94] valent actinides. Different models have been proposed to interpret the

metal ion-humic substance interaction [Chop 97a]. A schematic feature for the different models was proposed and discussed by V. Pirlet in her doctoral thesis [Pirl 2003a]. Depending on the binding sites of the humic substances, which can be used for the determination of complexation constants, the models are proposed (Figure 14).

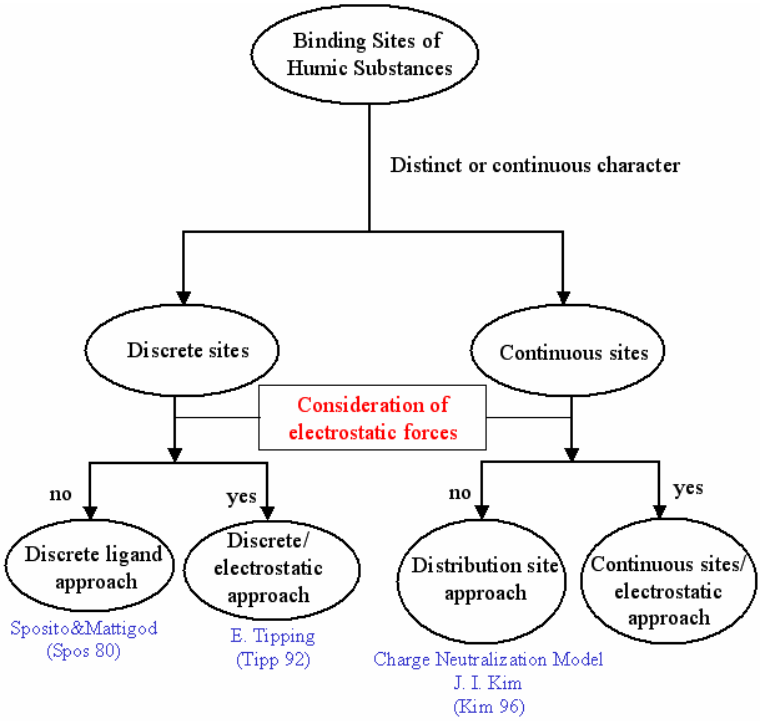

Figure 14: Scheme of proposed models for the interpretation of the metal ion-humic substance interaction [Pirl 2003a]

The main reason for the lack of complexation studies for tetravalent actinides with HS is the high hydrolysis, the solubility constant, and colloid formation of An(IV). Almost no complexation data are available for the Pu(IV) and Np(IV) interaction with humic substances. Solvent extraction technique has been applied for the determination of the binding constant of Th(IV) with soil humic acid [Nash 80, Chop 81]. It was found that the complexation constants increase with an increase of the ionization of HA.

In the case of plutonium, $Pu(OH)_4$ is expected to be the dominant species in the absence of humic acids in ground water. In presence of humic substances, Pu(IV) forms mixed complexes like $Pu(OH)_3HA(I)$ as reported by Czerwinski et al. [Czer 97]. Table 10 shows the published data on the interaction of tetravalent actinides with HS.

Table 10: Overview of the published studies on the interaction of tetravalent actinides with humic substances [Pirl 2003a]

Actinide	Origin of HS	pH	Model	Logß	Authors
Th(IV)	Lake Bradford HA	3.95 to 5	Two types of binding sites (degree of ionization)	$\log\beta_1$= 10.7-13.2 $\log\beta_2$= 10.7-13.2	[Nash 80, Chop 81]
	Aldrich HA	3.98		$\log\beta_1$= 11 $\log\beta_2$= 16.4	
	Aldrich FA	3.98 to 5		$\log\beta_1$= 9.5-10.8 $\log\beta_2$= 12.8.7-15	
Th(IV)	Guangdong HA	6	Two types of binding sites	$\log\beta_1$= 10.1	[Zuyi 94]
Th(IV)	Henan FA	6	Two types of binding sites	$\log\beta_1$= 9.5 $\log\beta_2$= 11.7	[Zuyi 94]
Th(IV)	HA	4, 7, 10	Discrete/electrostatic approach	logβ= 5.9 (pH 4) logβ= 10.4 (pH 7) logβ= 13.4 (pH 10)	[Tipp 93]
Th(IV) Pu(IV)	Soil HA HA	3.95	Estimated by calculation	logβ= 56.94	[Ibar 77] [Czer 97]
Pu(IV)	HA	4 and 7		logβ= 12.4, 17.2 (pH 4) logβ= 18.8, 20 (pH 7)	[Carl 89]
U(IV)	Soil HA	2 to 9	Scatchard plot (Two types of binding sites)	logβ= 6.6-7 (pH 6) (Strong) logβ=4.5-4.9 (pH 6) (weak)	[Li 80]

Moreover, Bondietti et al. [Bond 76] describes the apparent interaction between plutonium and humic substances. Pirlet [Pirl 2003b] has estimated the complexation constants of tetravalent Np species with fulvic acid and Boom clay HA (Table 11). Marquardt et al. (1996) demonstrated that at low concentration (10^{-13} M) Np(V)-humate forms 1:1 complex at pH 8 with logβ = 4.2. Np(V) is considered as chemical analog to Pu(V) [Marq 96]. At higher actinide concentration (10^{-4} M), stability constants for Np(V) with humic acid of logβ = 2.5 [Rao 95], 3 [Kim 91a], and 3.6 [Moul 92] were determined.

Table 11: Complexation constants of various Np(IV)-HS species at pH 6 to 9 [Pirl 2003b]

Np(IV)-HS Species	$\log b_{LC}$ (pH 6 to 9)
NpFA(IV)	7.67
Np(OH)FA(III)	21.4
$Np(OH)_2FA(II)$	32.2
$Np(OH)_3HA(I)$	46.5
$Np(OH)_4HA$	51.6

2.5.3 Kaolinite

Kaolinite is a clay mineral, which is a component of many soils and backfill materials [Payn 2004] and contains mainly hydroxylated sites of Si and Al. Kaolinite is one of the most widespread clay minerals in soils. It can be formed by hydrothermal alternation of feldspars or other silicates. Kaolinite has not only geochemical but also an industrial importance. It is mainly used in the manufacture of ceramic ware, and also used as a filter in paper and paints.

Kaolinite ($Al_2(OH)_4Si_2O_5$) is a dioctahedral 1:1 layer aluminumsilicate. The structure is compiled of an extending silica tetrahedral sheet ($Si_4O_{10}^{4-}$) and an alumina octahedral sheet ($((OH)_6Al_4(OH)_2^{4+}$), attached to each other via shared oxygen. Two thirds of the octahedral positions are filled with Al atoms, and therefore, kaolinite is referred to have a dioctahedral structure. These two layers are held together by weak hydrogen bonds [Rose 2002].

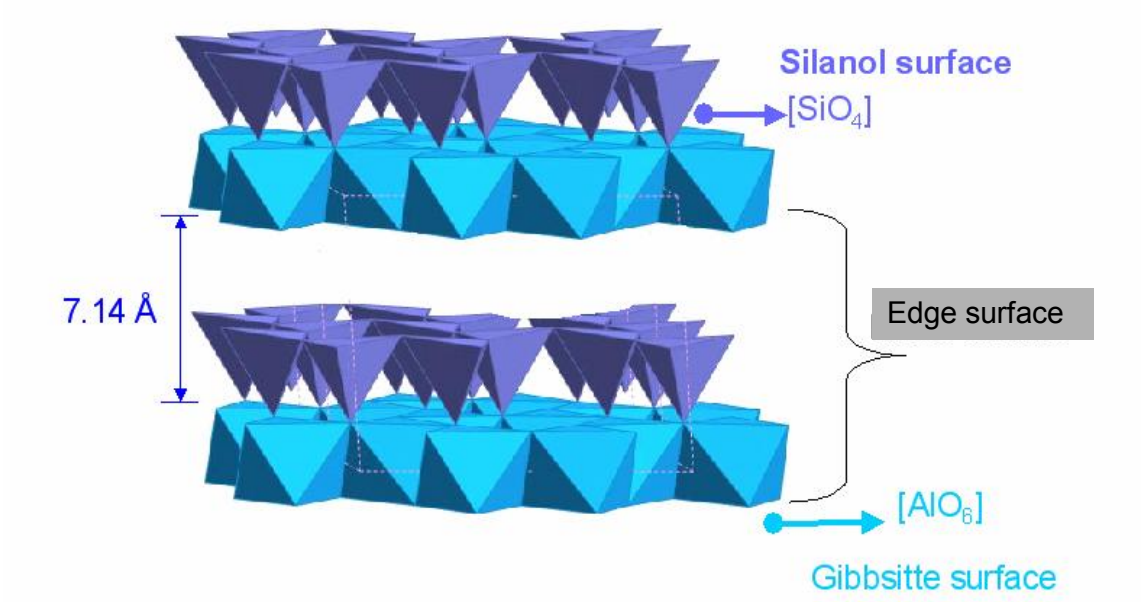

Figure 15: Structure of kaolinite with the gibbsite surface plane, a silanol surface plane and an edge surface plane [Amay 2006]

The kaolinite surface consists of three morphologically different surface planes with different chemical compositions namely a gibbsite surface plane (AlO_6), a silanol surface plane (SiO_4) and an edge surface plane represented by a complex oxide of $Al(OH)_3$ and SiO_2 (Figure 15).

In the gibbsite plane, the octahedral sheet is slightly distorted, in order to fit the tetrahedral sheet, which results in slightly altered Al-O bond length and site density. In consequence, all OH groups are coordinated with two Al atoms ($\equiv Al_2OH$). In addition to permanent, negatively charged $\equiv X^-$ sites, kaolinite has amphoteric, variable charged ≡SOH sites at the crystal edges and on the octahedral alumina sheet. ≡SOH sites represents silanol ≡SiO(H) sites at the crystal edges (contributing only to the negative charge through the formation of $\equiv SiO^-$) and aluminol ≡AlOH(H) sites at the crystal edges and on the octahedral sheet (both protonation and deprotonation can occur to form $\equiv AlOH_2^+$, ≡AlOH, and $\equiv AlO^-$). $\equiv Al_2OH$(H) sites also exist at the gibbsite basal plane and contribute to the positive surface charge in the lowest pH regime through the formation of $\equiv Al_2OH_2^+$ (Figure 16) [Huer 98].

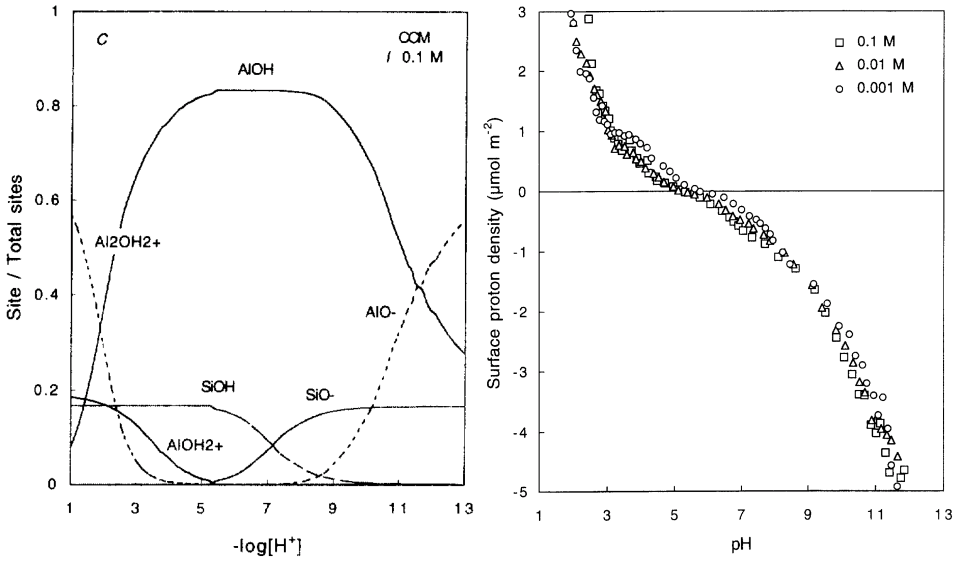

Figure 16: Speciation of kaolinite surface (KGa-1b) as a function of the pH values (without CO_2 contact) for I = 0.1 M (left) and surface charge of kaolinite with point of zero charge at pH » 5.5 (right) [Huer 98].

2.5.4 Interaction of actinides with kaolinite

Sorption studies of actinides onto kaolinite have been accomplished to obtain data on the distribution coefficient (K_d) that is regarded as an important parameter in the safety assessment of the geological disposal of radioactive wastes. Sorption behavior mainly depend

on the concentration of actinides, minerals, the ionic strength, pH of the solution, sorption capacity of the mineral, and the total surface area of the mineral. [Tors 88]. The sorption of actinides onto clay minerals significantly depends on the oxidation states of the actinide ions. Therefore, the sorption edges of actinide ions vary with their oxidation states. In the literature, the sorption edges are given for Th(IV) at pH 2.5, Am(III) at pH 5.8, , Np(V) at pH 7.3 onto γ-alumina (Figure 17). The sorption of Th(IV) onto mineral surfaces has been investigated with silica, alumina, iron oxides [Reil 2002]. It is well established that the sorption is mainly dependent on the net charge of the metal ion as well as on steric effects. Plutonium sorption onto mineral surfaces follows the order: Pu(IV) > Pu(VI) > Pu(III) > Pu(V) [Chop 2001].

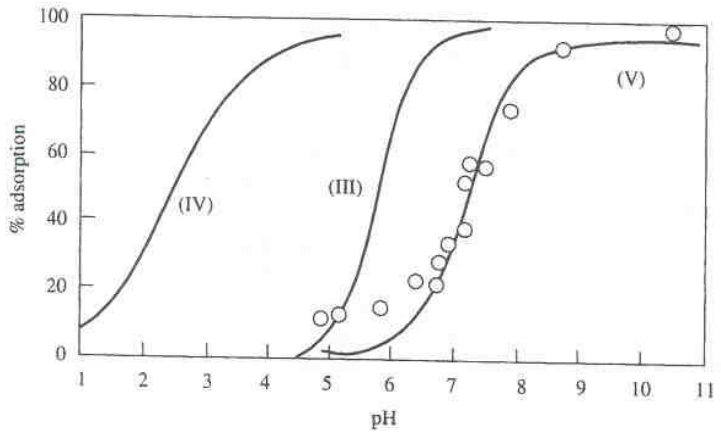

Figure 17: Comparison of the sorption of actinide ions of different oxidation states onto alumina. The solid lines refers to the amount of sorption of Th(IV), Am(III), Np(V) onto γ-alumina [Bido 89].

The strong hydrolysis of Pu(IV) in neutral water causes extensive sorption onto mineral surfaces and determines the migration of plutonium in the environment [Mors 91]. Pu(IV) and Pu(V) sorption onto various mineral surfaces has been investigated [Kenn 85)]. A high sorption was observed for Pu(IV) onto carbonate minerals, FeOOH surfaces, and MnO_2 surfaces [Mitc 95]. Lu et al. have studied the time dependence of the Pu(V) sorption onto oxide and clay colloids and concluded there was no time dependence [Lu 2003].

2.5.5 Interaction of kaolinite with organic matter

Clay-humic substances mixtures are widely distributed in natural environments and play an important role in regulating the transport and retention of hydrophobic organic matters in solids and waters. Hydrophobic fractions [Meie 99, Ghab 2004] are preferentially sorbed onto the clay surfaces. Humic acid –clay minerals interactions are extensively affected by the pH,

the ionic strength and also by the concentration of both species. The surface bondings occur due to specific covalent interaction between metals on the clay minerals and humate molecules and via weaker hydrogen bonds (Figure 18). As a result of the interactions, the surface property of both clay and humate are altered and influence their reactivity. Davis and Zachara et al. concluded that the metal sorption onto a mineral surface in the presence of humic acid could be significantly influenced during the sorption in the aquatic system [Davi 84, Zach 94].

The sorption mechanisms of HS on kaolinite have not yet been well understood. Murphy et al. cited that the sorption of humic acid occurs by a ligand and exchange reaction between the hydrolyzed groups of kaolinite and functional groups of humic acid [Murp 92]. Niitsu et al. suggested that sorption of colloidal HA species on mineral surfaces is governed by a long-range van der Waal's interaction and electric diffuse double layer repulsion [Niit 97]. Other possible sorption mechanisms have been proposed such as weaker hydrogen bonding and metal bridge formation [Tayl 95]. It is known from the literature that the sorption of HS onto mineral surfaces strongly depends on the pH [Lipp 2005]. It has been reported that the sorption of HS onto clay minerals first increases and then decreases with increasing pH values.

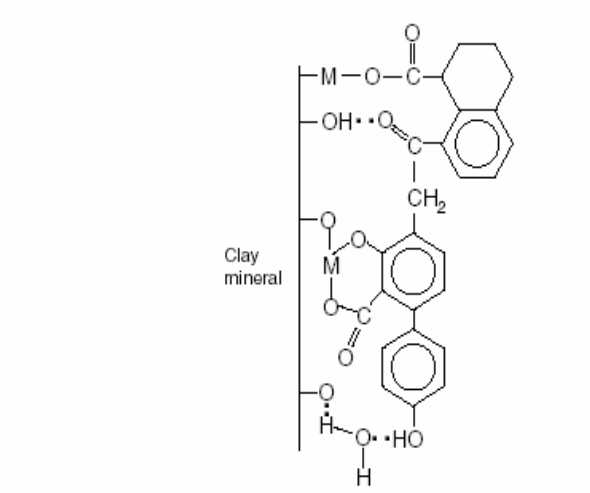

Figure 18: Types of bonding interaction involved in forming the clay-humate complex

Investigation of the sorption behavior of fulvic acid (FA) onto minerals, like kaolinite, has not been published at all. However, the understanding of the interactions of humic acid and fulvic acid with kaolinite in natural aquifer systems is important for the assessments of nuclear waste repositories.

Effects of humic substances on the sorption of actinides on clay minerals

The sorption of metal ions onto mineral surfaces, such as clay minerals or oxides, and the influence of HS on the sorption properties have been investigated [Reil 2002]. The presence of a competing ligand like HS can strongly influence the sorption of metal ions onto mineral surfaces. In 1997, Labonne-Wall et al. showed that the sorption decreases with increasing pH in the Am(III)-Silica-HA system, if the concentration of HA exceeds the saturation of the mineral [Labo 97].

Reiler et al. studied the influence of humic acid on the sorption of Th(IV) onto hematite and assumed that the sorption of Th(IV), considered as an analogue of tetravalent actinides (Np, Pu), can be influenced by the presence of HS even at low concentrations of HS in deep geological media [Reil 2002]. Ho and Miller reported that the addiation of HA altered the sorption of U(VI) onto hematite and showed that the uranium sorption was enhanced at low pH , whereas the sorption was lowered at higher pH [Ho 85]. A similar behavior was observed by Allard et al. [Alla 82] for the sorption of Am(III) onto alumina, by Moulin et al. Moul 89] for the sorption of Am(III) onto silica, by Niitshu et al. [Niit 97] for the sorption of Np(V) onto kaolinite, and by Righetto et al. [Righ 91] for the sorption of Am(III), Th(IV), and Np(V) onto alumina and amorphorous silica . The sorption of actinide ions onto kaolinite and other mineral surfaces has also been investigated [Zava 2005, Yama 2004, Atun 2003, Righ 91]. The results show that the sorption depends significantly on the type of metal ions (their oxidation state), pH, ionic strength, temperature, aerobic or anaerobic conditions, and the type of mineral surface. Sorption studies of plutonium and other tetravalent actinides onto goethite [Sanc 85], calcite [Zava 2005], or other soils [Tana 2002] were carried out. The sorption behavior of Am(III) and Eu(III) on hematite in the presence of HA as a function of ionic strength from 0.05 to 0.5 M has already been studied [Saku 2002]. Effects of humic acid on the sorption of Am(III) and Cm(III) onto kaolinite have also been briefly discussed by Samadfam et al. and shown the presence of HA enhanced the sorption at pH values about 5 [Sama 2000].

2.5.6 Speciation of actinides in aquatic systems

Speciation studies of actinides are primarily intended to investigate the nature of the species (physical/chemical), which exists in aqueous systems. Most of the actinide ions tend to hydrolysis and complexation with the ligands which are present in the aqueous solution. Chemical speciation involves the determination of soluble species of the actinide ions, their oxidation state, complexation with ligands (inorganic or organic) and redox behavior.

Physical speciation involves the investigation of sorption behavior on colloids present in the ground water and, e.g., clay mineral in the aqueous systems. The chemical and physical speciation of actinides is important for the understanding of the migration behavior of actinides in the far field. Direct and indirect speciation methods can be used for the speciation of actinides in aqueous solutions.

Indirect speciation methods like solvent extraction, ion-exchange chromatography, and ultrafiltration techniques must be coupled with radiometric or spectroscopic detection, used for ultratrace analysis of actinides. These methods are relatively simple and the techniques are well developed. However, there are limitations because the redox equilibrium can be changed in the solution [Chop 2003].

2.5.7 Speciation of actinides by direct methods

For the speciation of actinides the following direct methods are used: absorption spectroscopy, laser spectroscopy (fluorescence, photoacoustic, etc) and mass spectrometry. In Table 12, the direct methods for the speciation actinides in aqueous solutions are summarized. Classical UV-Visible absorption spectroscopy has been applied for the speciation of americium [Czer 96], neptunium [Marq 98], and plutonium [Chop 2004, Wils 2005] at the concentration range of about 10^{-6} M under natural conditions.

Table 12: Direct methods for the speciation of actinides in aqueous solutions and their detection limits [Chop 2003].

Direct speciation method	Detection limit for actinides [mol/L]
Nuclear Magnetic Resonance (NMR)	10^{-1} - 10^{-4}
X-Ray Absorption Spectroscopy (XAS)	10^{-1} – 10^{-4}
UV-Visible Absorption Spectroscopy (UV-Vis)	$\geq 10^{-5}$
Laser Induced Photoacoustic Spectroscopy (LPAS)	10^{-5}-10^{-9}
Time Resolved Laser Induced Fluorescence (TRLIF)	10^{-5}-10^{-9}
Thermal Lensing Spectroscopy (TLS)	10^{-5}-10^{-9}
Electospray Mass Spectroscopy (ES-MS) [Moul 2005]	Up to 10^{-6}

For improving the detection limit of actinides, Laser Induced Photoacoustic Spectroscopy (LPAS) has been introduced for speciation of actinides $<10^{-8}$ M. LPAS was successfully applied for the determination of neptunium and plutonium at a detection limit of 10^{-7}-10^{-8} M. Table 13 shows the speciation of plutonium in solution by direct methods.

Table 13: Direct methods for the speciation of plutonium in aqueous solutions and their detection limits; LCW UV-Vis: liquid core wave-guide coupled to a fiber optic UV-Vis .

Direct speciation method	Detection limit Pu [mol/L]
UV-Vis [Chop 2004]	10^{-5} - 10^{-6}
LCW UV-Vis [Wils 2005]	10^{-5} – 10^{-7}
LPAS [Stum 84]	10^{-8}
TLS [Moul 2001]	10^{-7}

2.5.8 Speciation of actinides by indirect methods

Indirect methods are mainly based on use of separation methods (dialysis, ultrafiltartion, centrifugation, chromatography, electrophoresis, extraction, etc.) in combination with sensitive detection techniques namely: atomic absorption spectroscopy (AAS), inductively coupled plasma with atomic emission spectroscopy (ICP-AES) or mass spectrometry (ICP-MS), or radiochemical and electrochemical methods [Moul 2005]. Chromatography or capillary electrophoresis has been successfully coupled with ICP-MS (HPLC-ICP-MS or CE-ICP-MS), for the speciation of actinide ions at very low concentrations. Redox speciation (oxidation state) of actinides by solvent extraction, co-precipitation, and ultrafiltration in combination with radiochemical (LSC, α, and γ spectroscopy) and mass spectroscopic detection techniques was already successfully used at the ultratrace level, e.g., the distribution of the oxidation states of plutonium in natural media such as river, ocean, and lake at a concentration down to 10^{-16} M [Moul 2005]. Table 14 shows the indirect speciation methods for actinides in solution.

Table 14: Indirect methods for the speciation of actinides in aqueous solutions and their detection limits

Indirect speciation method	Detection limit for actinides [mol/L]
Solvent extraction-radiometric detection [Nits 88, Chop 97b]	10^{-8} - 10^{-14}
Ultrafiltration-radiometric detection [Seib 2001]	10^{-9} – 10^{-14}
Chromotography-radiometric detection [Gehm 86]	10^{-8}-10^{-11}
HPLC-ICP-MS	10^{-8}-10^{-9}
Electrophoresis- radiometric detection [Marq 96]	10^{-8}-10^{-12}
CE-ICP-MS [Amba 2005]	10^{-7}-10^{-10}

The speciation of Np(V) with humic substances at a metal concentration of 10^{-8}-10^{-13} M was investigated by electrophoretic ion exchange, anion exchange chromratography, and ultrafiltration in combination with radiometric detection [Marq 96, Seib 2001]. Ambard et al. have determined the plutonium species by CE-ICP-MS at a concentration of 10^{-10} mol/L [Amba 2005]. More recently Bürger et al. have developed a new indirect speciation CE-RIMS method for plutonium ions [Bürg 2005b]. This method will be briefly discussed in this thesis.

2.6 CE-ICP-MS

For the speciation of actinides in natural groundwater, the online coupling of Capillary Electrophoresis (CE) with Inductively Coupled Plasma Mass Spectrometry (ICP-MS) has been developed [Kucz 2003]. With this method, different oxidation states of actinides (III-VI) are separated on their radius/charge ratio with subsequent detection by ICP-MS. A detection limit of 20 ppb, i. e., 10^{9}-10^{8} atoms for one oxidation state of plutonium, has been obtained.

The process of capillary electrophoresis (CE) is defined as the differential movement or migration of ions by attraction or repulsion in an electric field. The separation mechanism is based on the charge of the ions as well as the size of the analyte. An electrical field is applied across a capillary filled with an electrolyte [Kann 2002]. The CE system mainly consists of a fused silica narrow bored capillary, electrolytic solution (buffer), two electrodes (cathode and anode), a high voltage power supply (0 to 30 kV) and a detector (Figure 19).

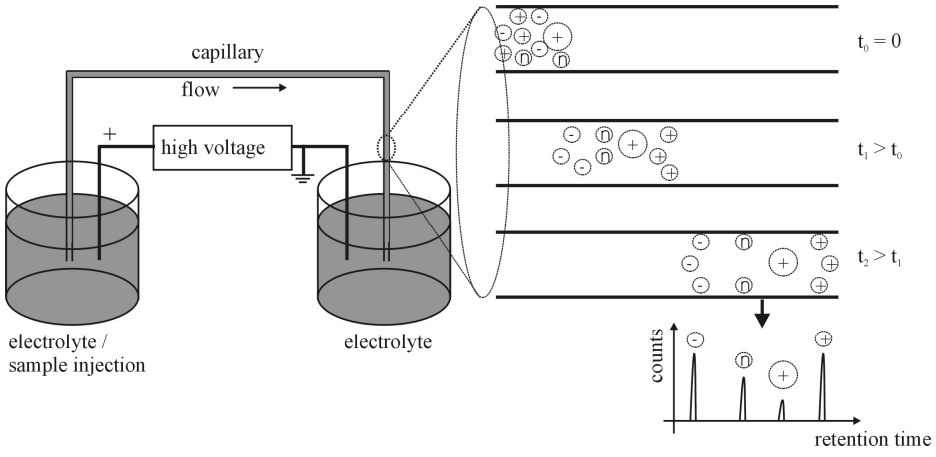

Figure 19: Schematic arrangement of the main components of a CE instrument [Land 97]

The migration of ions in a capillary is controlled by two phenomena: the electrophoretic mobility and the elctroosmotic mobility. The electrophoretic mobility is related to the charge to size ratio of the analyte.

The electrophoretic mobility can be expressed as follows:

$$v_{ion} = m_{ion} E \tag{18}$$

where v_{ion} is the migration velocity of the ions (ms^{-1}), μ_{ion} is electrophoretic mobility ($m^2\ V^{-1}\ s^{-1}$) of the ions and E is the electric field strength ($V\ m^{-1}$).

The force ($F_E = qE$) caused by the electrical field is proportional to the effective ion charge, q, and the electric field strength, E. The transversal movement of the ion is opposed by a retarding frictional force ($F_f = f v_{ion}$), which is proportional to the velocity of the ion, v_{ion}, and the friction coefficient, f.

$$qE = fv_{ion} \tag{19}$$

The friction coefficient of the moving ion is related to the hydramic radius (Stokes radius) of the ion, r_{ion}, and the viscocity, η, of the surrounding medium expressed as:

$$f = 6\pi\eta r_{ion} \tag{20}$$

Rearranging of equations (18), (19) and (20) yields

$$m_{ion} = \frac{V_{ion}}{E} = \frac{q}{6\pi\eta r_{ion}} \tag{21}$$

The migration time and ion mobility are described as:

$$m_{ion} = \frac{l}{tE} = \frac{lL}{tV} \tag{22}$$

Here l is the effective capillary length [m], L is the total capillary length [m], t is the migration time [s], E is the electric field [V], and V is the applied voltage. Most capillaries are made of fused silica, which mainly contains reactive surface silanol groups [Heig 92]. These silanol groups dissociate and form a negative charge on the wall of the capillary.

The electroosmotic flow (EOF) arises from the interaction between the ions and the negatively charged capillary wall. When the capillary is filled with an electrolyte buffer solution, the negatively charged capillary wall attracts positive ions from the electrolyte solution, producing an electrical double layer and a potential difference (zeta potential) close to the capillary wall, as described by Stern's model in Figure 20. The zeta potential is the potential at a given point in the double layer; it decreases exponentially with increasing distance from the capillary wall surface.

In fused silica capillaries an increase in the zeta potential and the EOF mobility occurs at higher pH values due to the formation of SiO^- whereas at low pH the silanol groups are not ionized (Figure 21) with the consequences that the EOF mobility is diminished and the zeta potential is decreasing. Therefore, the observed migration velocity of the ion may not only depend on its elecrophoretic mobility (μ_{ep}) but also on the elctroosmotic flow (μ_{EOF}).

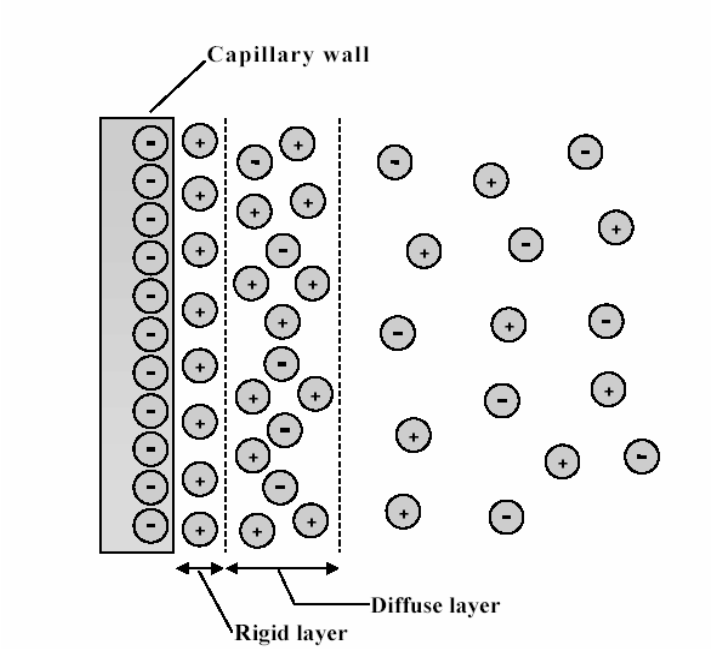

Figure 20: Stern's model of the electrical double layer charge distribution in the negatively charged capillary wall leading to the generation of zeta potential and EOF.

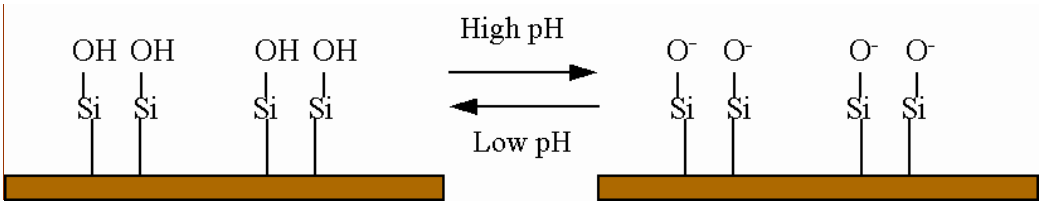

Figure 21: Dissociation processes of silanol groups in the capillary at varying pH

The ion mobility, (μ_{ion}), of a solute is the vector sum of the electrophoretic mobility, (μ_{ep}), of the solute and the electroosmotic flow, (μ_{EOF}) of the solution.

$$m_{ion} = m_{ep} + m_{EOF} \quad (23)$$

The ion velocity in the solution is,

$$v_{ion} = (m_{ion} + m_{EOF})E \quad (24)$$

One of the main advantages of CE is that extremely small volumes of sample can be injected (nanoliter). There are two injection methods: hydrodynamic and electrokinetic. Hydrodynamic injection is accomplished by the application of a pressure difference between the two ends of the capillary. Hence the Hagen-Poiseuille equation can be applied,

$$v_{inj} = \frac{\Delta P p r^4 t_{inj}}{8 h L_{cap}} \qquad (25)$$

where v_{inj} is the injection volume, ΔP is the pressure difference between the ends of the capillary, r is the inner radius of the capillary, t_{inj} is the injection time, η is the sample viscosity, and L_{cap} is the total length of the capillary.

2.6.1 Online coupling of capillary electrophoresis (CE) with ICP-MS

The advantages of CE method are high resolution, low sample quantity, and low working cost [Amba 2005]. The coupling of CE with a classical detector as a UV detector is not suitable for actinide speciation studies under environmental conditions due to its high detection limit (10^{-5}-10^{-7} mol /L). In order to improve the detection limit, CE is coupled to ICP-MS.

A homemade CE system coupled to a commercial ICP-MS has been used in this work. The interface from the CE to ICP-MS is made of PEEK as a four way fitting and is based on the concept of Schaumlöffel et al. [Scha 99]. Figure 22 shows the CE-ICP-MS apparatus as developed by Kuczewski et al. [Kucz 2003]. Hydrodynamic injection was applied to introduce the sample into the capillary with a pressure of 50-1000 mbar.

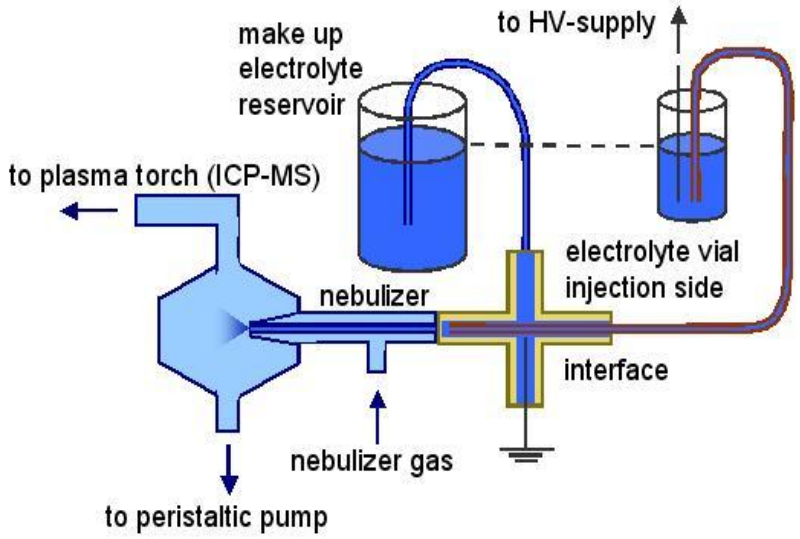

Figure 22: Principle of online coupling of CE to ICP-MS [Kucz 2003]

This equipment was designed in such a way that different components such as nebulizer, spray chamber, and capillary could be tested. About 44 nL (± 5%) of the sample was injected within 10 sec at 100 mbar. A fused-silica capillary with inner diameter of 50 µm and outer diameter 363 µm and 60 to 70 cm length was used. 2 % HNO_3 (with 10 ppb Rh as ICP-MS marker) was used as a make-up solution. As microconcentric nebulizer, a MicroMist 50 or 200 connected to a Cinnebar small volume cyclonic spray chamber was applied. The operational conditions for online coupling of CE to ICP-MS are given in Table 15.

Table 15: Experimental and operating conditions for the CE-ICP-MS system [Bürg 2005b]

CE system homemade	**Operation conditions**
Capillary	fused silica, 50 µm inner diameter, 60 to 70 cm length
Nebulizer	MicroMist 50 or 200, GlassExpansion, West Melbourne, Australia
Spray chamber	Cyclone spray chamber (Cinnebar Cyclonic Small Volume) or standard Scott type spray chamber
CE voltage	+30 kV
Injection	hydrodynamic, 50 to 1000 mbar
Sample injection	5 to 10 s at 50 to 100 mbar
CE electrolyte buffer	1 M AcOH, pH ≈ 2.4
ICP-MS system HP 4500 (Agilent)	
RF power	1000 – 1100 W
Plasma gas flow rate	15.5 L/min
Nebulizer gas flow rate	1 to 1.2 L/min
Detection mode	peak jump
Internal standard / make-up solution	10 ppb Rh / 2% HNO_3
Data acquisition	dwell time 100 ms for marker Rh-103, 900 ms for Pu-239

For the optimization of the CE-ICP-MS apparatus, model ions of different elements with oxidation states I-VI were analyzed. A good separation of all six oxidation states could be achieved as can be seen from Figure 23.

The migration time depends generally on the charge, size and shape of the ionic species. The CE-ICP-MS system enables the separation of Pu(III), Pu(IV), Pu(V), Pu(VI) as well as of Np(IV), and Np(V) with a high reproducibility (Figure 24). This CE-ICP-MS system has been routinely applied for the speciation of plutonium and neptunium in ground water [Kucz 2003].

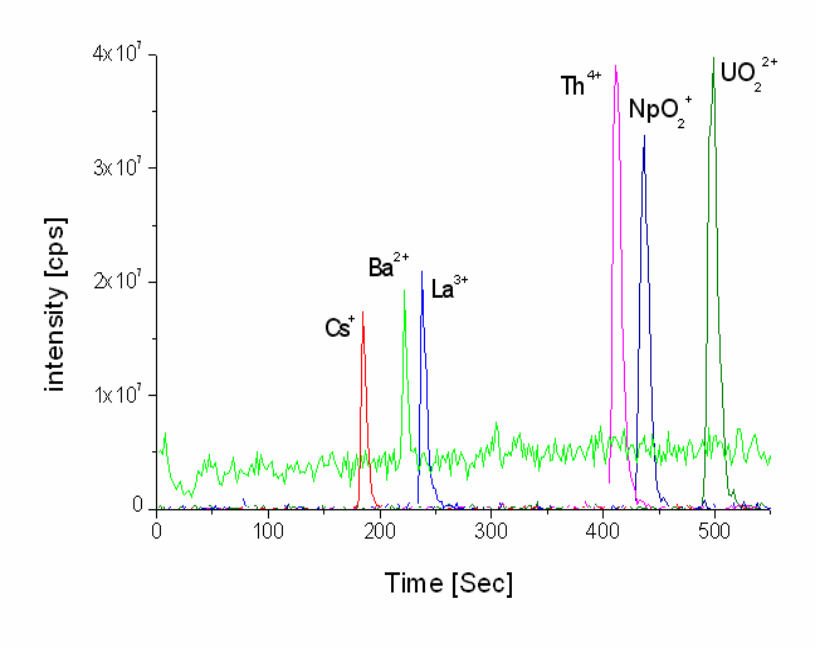

Figure 23: Separation of Cs(I), Ba(II), La(III), Th(IV), Np(V) and U(VI) ions in 1 M acetic acid by CE-ICP-MS.

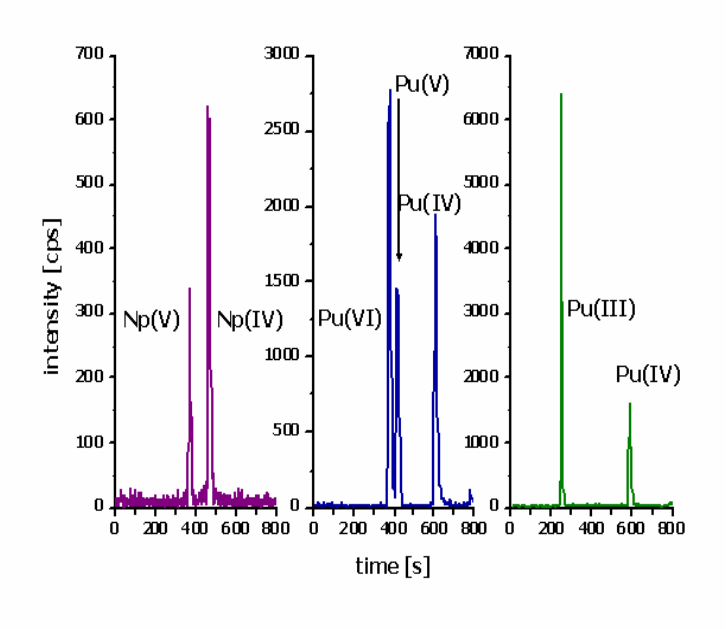

Figure 24: Separation of the different oxidation states of neptunium and plutonium by CE-ICP-MS [Kucz 2003].

2.7 Resonance ionization mass spectrometry (RIMS)

Resonance ionization mass spectrometry (RIMS) is an extremely sensitive and elemental selective technique for ultra-trace analysis of long-lived radionulcides in environmental, biological, and technical samples. RIMS consist of a pulsed laser system in combination with a time of flight mass spectrometer. Three titanium : sapphire (Ti : Sa) are pumped by a commercially available Nd-YAG pump laser (Clark-MXR ORC-1000). The three Ti : Sa laser beams travel through a single quartz fiber and cross the region where the atomic beam evaporates from the filament (Figure 25). By using laser light of three Ti : Sa lasers at λ_1 = 420.77 nm, λ_2 = 847.25 nm and λ_3 = 767.53 nm the plutonium atoms are excited into a Rydberg state and subsequently field ionized. The ions are accelerated to 3 keV and detected by a time-of-flight spectrometer with a mass resolution m/Δm of ~ 600 at 240 amu.

The overall efficiency of the RIMS apparatus is ≥ 10^{-5}, resulting in a detection limit of 10^6 - 10^7 atoms of plutonium [Trau 2004].

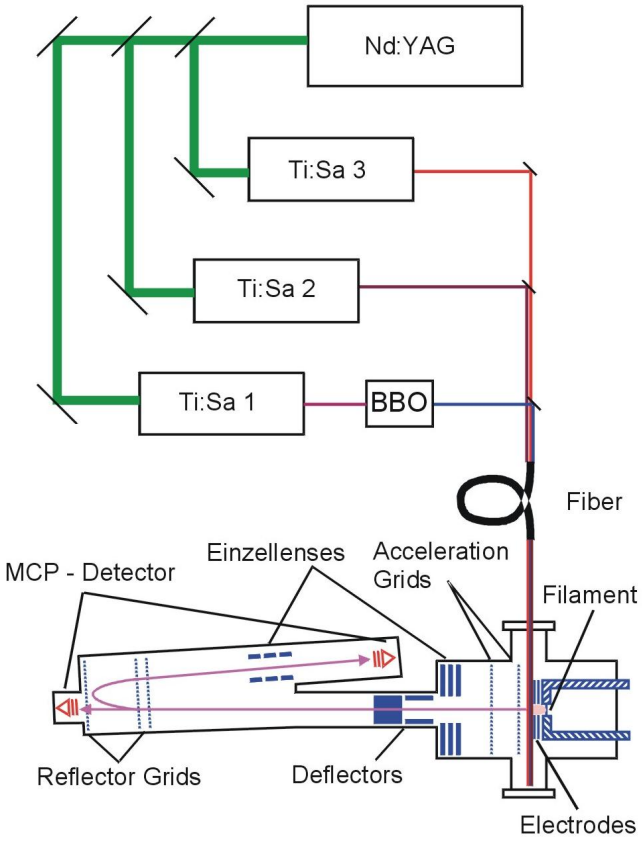

Figure 25: Instrumental set-up for RIMS measurements with a reflection type time-of-flight mass spectrometer [Nunn 98, Trau 2004]

For the production of an atomic beam, a special filament must be prepared (Figure 26). Plutonium hydroxide is electrochemically deposited on a tantalum backing from a 20 % $(NH_4)_2SO_4$ solution. The sample is covered with a thin titanium layer (1 µm) by sputtering (Figure 26).

When the filament is heated in vacuum, the plutonium hydroxide is converted to the oxide and is reduced to the metallic state during diffusion through the titanium layer and in such a way, an atomic beam is evaporated from the filament. [Nunn 98, Trau 2004]

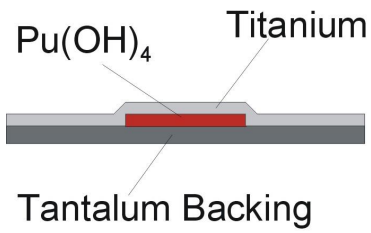

Figure 26: Filament for RIMS measurement.

2.7.1 CE-RIMS

For the speciation of actinides (especially plutonium) in the underground nuclear waste repositories site, ultratrace levels are necessary. For that, a new speciation method for plutonium has been developed with their higher sensitivity and selectivity compared to conventional speciation methods. In order to improve the sensitivity of the speciation method for actinide analysis, off-line coupling of CE to RIMS has been successfully applied for the first time by Bürger et al. in 2005 [Bürg 2005b]. Compared to the on-line coupling of CE to ICP-MS, samples for RIMS measurements have to be taken off-line and filaments [Nunn 98, Trau 2004] must be prepared by electrodeposition. From these filaments, the actinides (Pu, Np) can be atomized by thermal evaporation into vacuum. In comparison with CE-ICP-MS, the detection limit for Pu could be improved by at least two orders of magnitude with CE-RIMS.

The principle of coupling CE to RIMS is based on collecting fractions of the different oxidation states eluted from the capillary at different, but known retention times [Kuzc 2003]. The fractions of the different oxidation states are collect by vials and the filaments are prepared by electrodeposition. A schematic diagram for the offline coupling of CE to RIMS is illustrated in Figure 27.

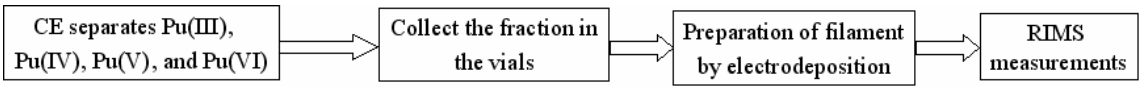

Figure 27: Schematic diagram for the off line coupling of CE to RIMS

The separation conditions for the different oxidation states of plutonium have been determined by CE-ICP-MS (Figure 28, upper part). For the RIMS measurements, the high voltage needs to be switched off for several seconds to change the collecting vials at the end of the capillary. Pu(VI) and Pu(V) fractions are collected in one vial due to their similar migration time. Figure 28 (lower part) represents the separation of the plutonium oxidation states with short high voltage breaks.

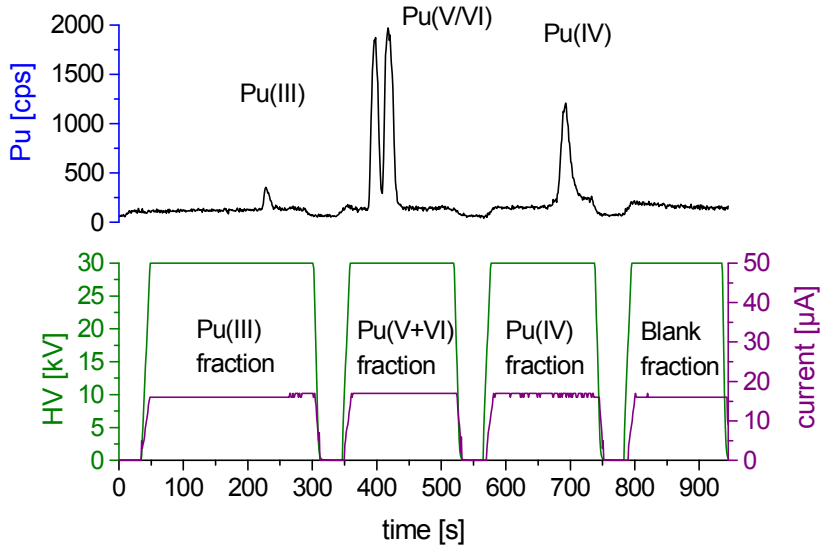

Figure 28: Separation of the plutonium oxidation states with short high voltage breaks for the collection of the fractions of the oxidation states Pu(III), Pu(V+VI), and Pu(IV) in different vials and detection by RIMS.

Before measuring the separated fractions by RIMS, the fractions have been analyzed by alpha spectroscopy to verify the method. Table 16 shows a comparison of the plutonium fractions Pu(V)/Pu(VI), Pu(III), and Pu(IV) determined by different coupling methods.

The coupling of CE to RIMS was tested by determining the plutonium oxidation states of a mixture of Pu(IV), Pu(V), and Pu(VI) by CE-ICP-MS at a plutonium concentration of approximately 4×10^{-6} mol/L and the determination by RIMS at a plutonium concentration of ca. 2.5×10^{-7} mol/L after separation and fractionation by CE.

Table 16: Comparison of different coupling methods for the determination of the oxidation states of plutonium [Bürg 2005a]

Coupling Method	**Pu(III) [%]**	**Pu(V+VI) [%]**	**Pu(IV) [%]**
CE-ICP-MS	30.9±5.2	5.5±1.0	63.6±4.5
CE-ICP-MS with HV-break	36.8±3.7	8.7±0.9	54.5±5.5
CE-α-spectroscopy	31.9±4.8	10.8±1.6	57.2±8.6

Table 17 gives the measurements by online coupling CE-ICP-MS and CE offline coupled to RIMS. The detection limit of RIMS is 2-3 orders of magnitude more sensitive compared to the ICP-MS. Thus, speciation of the oxidation states of plutonium at level of 10^{-9} to 10^{-10} mol/L appears to be possible.

Table 17: Comparison between the determination of the oxidation states of plutonium CE-ICP-MS (ca. 4×10^{-6} mol/L plutonium) and by RIMS (ca. 2.5×10^{-7} mol/L) after separation by CE in different fractions (CE-RIMS offline) [Bürg 2005b]

Coupling method	**Pu(V+VI) [%]**	**Pu(IV) [%]**
CE-ICP-MS (online)	19.2(2.0)	80.8(3.0)
CE – RIMS (offline)	15.2(5.0)	84.8(5.0)

3.0 Experimental Part

3.1 Chemicals and Reagents

Chemicals

All chemicals were of p.a. quality or better and were obtained from Merck (Darmstadt, Germany) or Riedel de Haen (Seelze, Germany). Milli-Q deionized water was used to prepare all the solutions. The Milli-Q deionized water (18 MΩ) was filtered through a filter from Millipore (Schwalbach, Germany). For all column experiments, the anionic ion exchanger AG 1-X8 from BIORAD® (Richmond, USA) was used.

Capillary

A fused-silica capillary with an inner diameter of 50 μm and an outer diameter of 363 μm (PolyMicro Technologies, Phoenix, AZ) and 60 to 70 cm length was used in the CE experiments. Prior to use, the capillary was always purged with 0.1 M HCl/ 0.1 M NaOH, and Milli-Q deionized water for 5 min at 1 bar.

pH measurements

The pH measurements were performed with a pH meter (φ-310, Beckmann, Germany) in combination with a reference electrode (Beckman, Germany). The pH-meter was calibrated daily with certified commercial buffers (Merck, KGaA, Darmstadt, Germany) at pH = 2, pH = 4, pH = 7, and pH = 9.

Radionuclides

Plutonium-238

The plutonium solution was evaporated to dryness and dissolved in 8 M HCl. The solution was purified by an anion exchange (BIO RAD® AG 1-X8, 3 mm × 130 mm). Purification is described as follows:

Purification of ^{238}Pu

The purification of plutonium-238 followed the procedure proposed by Fowler et al. [Fowl 86]. An appropriate aliquot of ^{238}Pu (usually in 2 M HNO_3) was evaporated in a glass beaker on a hot plate and the residue was dissolved in 8M HCl (10 mL). The plutonium solution (8M HCl) was transferred to an anion exchanger column ((BIO RAD® AG 1-X8, 3 mm × 130 mm) that had been pre-treated with 8M HCl and a few drops of nitric acid. After a washing step

with 8 M HCl, plutonium was eluted from the column with 8 M HCl containing 2 % NH_4I and 3 % $NH_2OH.HCl$. The eluate was collected and boiled. 2 mg of Fe^{3+} ($FeCl_3.6H_2O$ salt) were added and iron hydroxide was precipitated with NH_4OH.

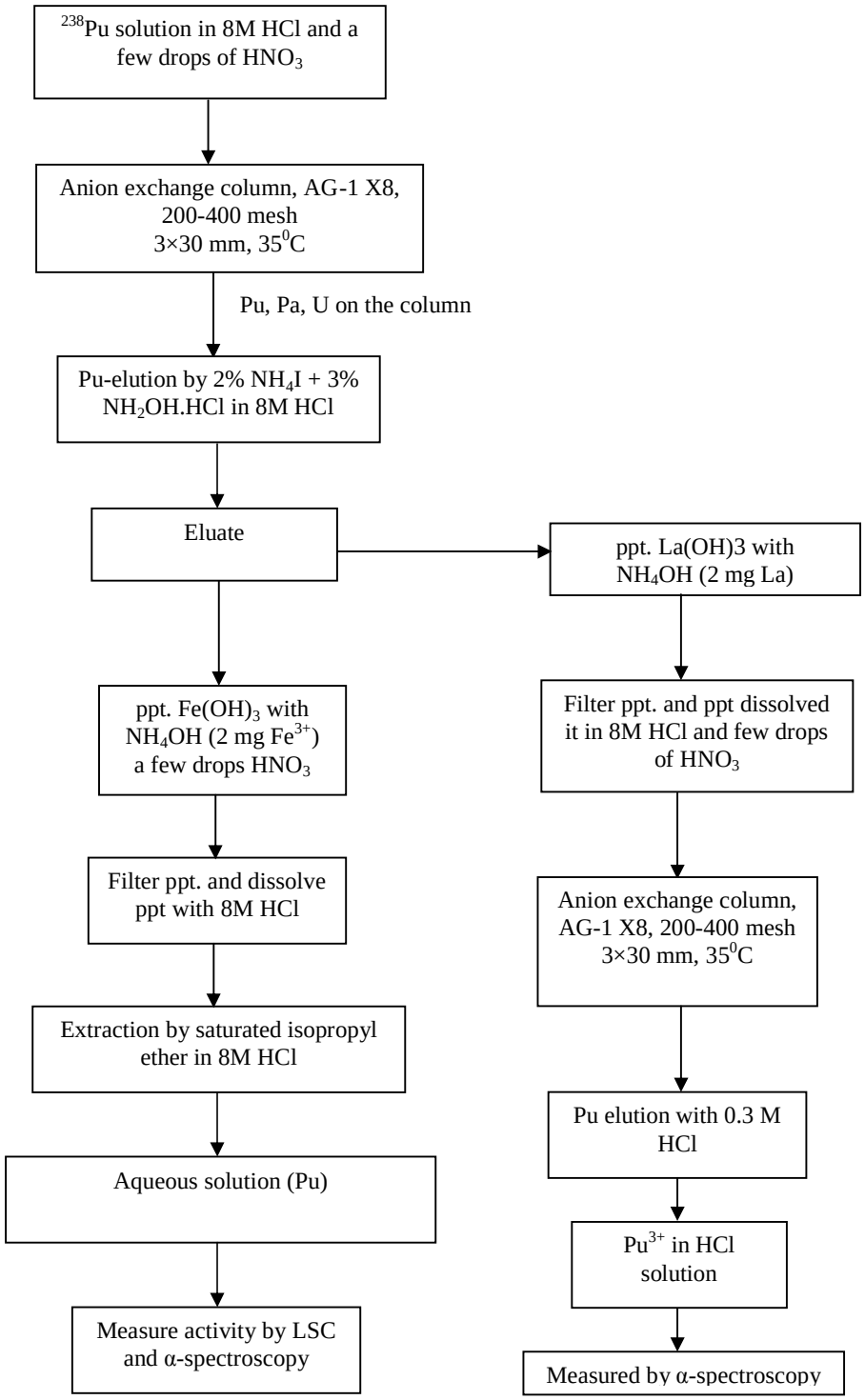

Figure 29: Scheme for the separation of ^{238}Pu from the other actinides

An alternative procedure is a $La(OH)_3$ co-precipitation (Figure 29). The precipitates were filtered and the Pu dissolved in 8 M HCl. Iron was removed by extraction with isopropyl ether. This extraction was done twice.

The aqueous fraction was evaporated to dryness and dissolved in 1 M $HClO_4$. An aliquot of the plutonium solution was electrodeposited [Bajo 2003] and measured by alpha spectroscopy for purity control. The activity was controlled by LSC. Figure 30 shows an alpha spectrum of purified Pu-238. The yield of ^{238}Pu recovered by column chromatography was 95 %. ^{238}Pu was used in the sorption experiments.

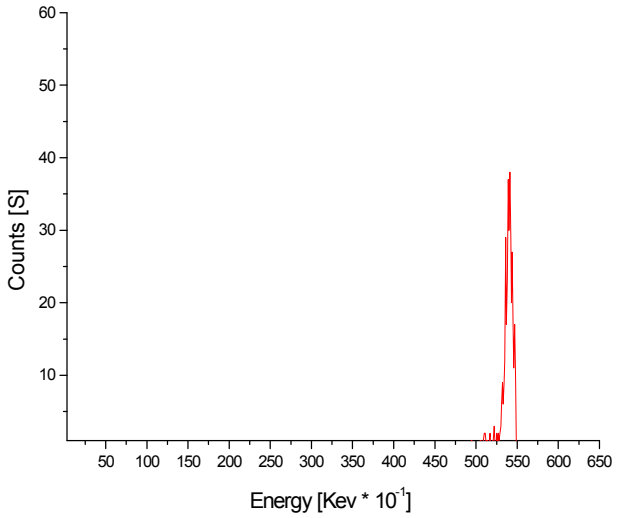

Figure 30: α-spectrum of Pu-238 after separation on ion exchange column

Plutonium-239

For the experiments carried out with plutonium-239, a 99.1 wt% ^{239}Pu stock solution, with small amounts of other isotopes (0.888 wt% ^{240}Pu, 0.014 wt% ^{241}Pu) and known specific activity was used. The plutonium solution was evaporated to dryness and fumed with HNO_3 (conc.) and 30 % H_2O_2. The residue was dissolved in 8 M HCl and the solution was fed onto an anion exchanger. After a washing step, plutonium was eluted with 0.36 M HCl/ 0.05 M HF. The eluate was evaporated to dryness and fumed two times with 1 M $HClO_4$ in a PTFE beaker. The resulting solution consisted of different oxidation states of plutonium. The tetravalent oxidation state of plutonium was obtained by potentiostatic electrolysis. The purity was verified by UV-Vis spectroscopy by the characteristic absorption bands at 400 to 870 nm [Cohe 61 (a, b)]. The electrolysis procedure of plutonium is described in chapter 3.7.

Plutonium-244

The plutonium solution was evaporated to dryness and dissolved in 8M HCl. The solution was purified via the anion exchange procedure (Dowex AG 1-X8, 4 mm × 150, 35^0C).

Purification of ^{244}Pu

A column was prepared with anion exchange resin (e.g., Dowex 1X8, 150 mm by 4 mm diameter, 35^0C) and preconditioned with 8M HCl. The plutonium cocktail was taken up in 8 M HCl in a 25 mL glass beaker and the activity was controlled by LSC. A few drops of nitric acid were added to the plutonium solution which was then transferred to the column. The column was washed with two column volumes of 8 M HCl. Then plutonium was eluted with two columns volumes of 0.2 M HCl and the eluate was collected in a glass beaker. Figure 31 shows the scheme for the separation of ^{244}Pu from impurities. A part of the eluate was electroposited and measured by alpha spectroscopy. From the alpha spectra, only $^{239/240}$Pu and ^{238}Pu could be identified. The Pu-isotope ratios of the cocktail are shown in Table 18.

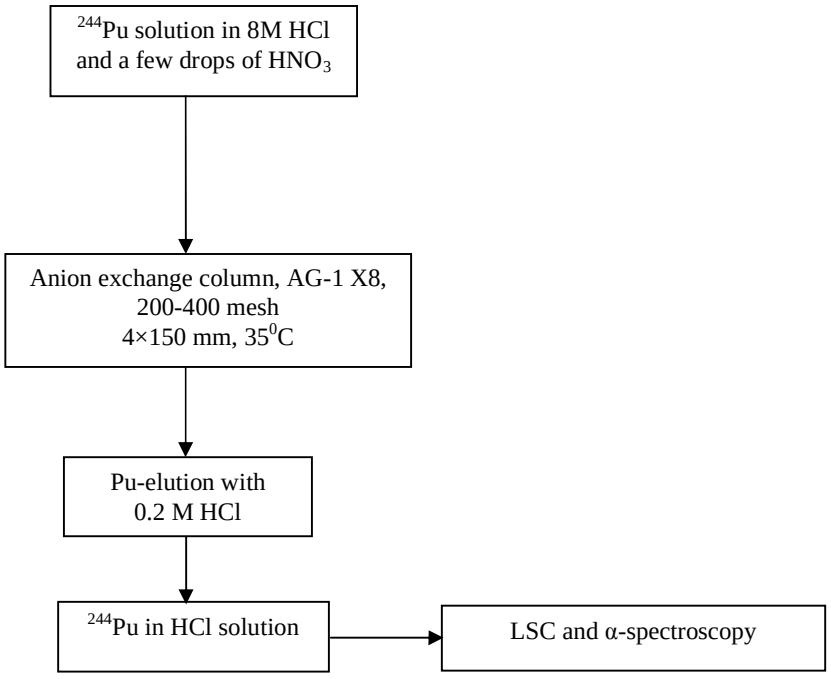

Figure 31: Scheme for the separation ^{244}Pu

Table 18: Isotope ratio of the plutonium cocktail [Erdm 97]

Plutonium isotope	Certified value (mass spectrometry) [%]	RIMS-measurements [%]
Pu-238	0.01	-
Pu-239	0.04	0.03 (1)
Pu-240	2.7	2.60 (5)
Pu-241	0.4	0.29 (2)
Pu-242	9.0	8.0 (1)
Pu-244	87.8	89.4 (5)

Neptunium-237

The neptunium solution was evaporated to dryness and dissolved in 8 M HCl. The solution was purified via anion exchange (BIO RAD® AG 1-X8). After a washing step with several millilitres of 8 M HCl, plutonium contaminations were removed with a fresh solution of 150 mg NH_4I in 5 mL 8 M HCl. Subsequently, neptunium was eluted from the ion exchanger with 4 M HCl/ 0.05 M HF and evaporated to dryness in a PTFE beaker. To obtain a solution containing only Np(V), the solution was fumed two times with 1 M $HClO_4$ and the residue was dissolved in deionized water. This stock solution could be stored at a pH value of 3 for several days. Neptunium (IV) was prepared using a zinc-amalgam treatment.

Thorium-234

^{234}Th was separated from ^{238}U by ion exchange column chromatography in 8 M HCl following the procedure described by Albinsson et al. [Albi 2002]. After purification, stock solutions were prepared in 0.1 M $HClO_4$. Gamma spectroscopy was used to verify the purity by monitoring the gamma lines at 93 and 63 keV.

Purification of ^{234}Th

Uranyl nitrate was dissolved in 8 M HCl in a 25 mL volumetric flask. This solution was transferred to an anion exchanger column (Dowex AG 1-X8, 4 mm × 150, 35^0C) that had been pre-treated with 8 M HCl. Uranium is sorbed onto the column whereas thorium passes through with 8 M HCl. The eluate was collected in a glass beaker as purified ^{234}Th and measured by gamma spectroscopy (Genie 2000).

Lanthanum-140

Lanthanide nitrate [98.1 % ^{139}La, 311.5 mg $La(NO_3)_3$. $6H_2O$ i.e. 100 mg $^{139}La^{3+}$] was dissolved in 100 mL HNO_3 (0.001 mol/L) resulting in a concentration of 0.0072 mol/L. 1

mL of this solution was irradiated in the Mainz TRIGA-Reactor for six hours at a flux of 7.0×10^{11} n/ s cm^2. The resulting activity of ^{140}La was about 1.76 kBq ^{140}La/ mg ^{139}La.

3.1.1 Humic substances

Aldrich humic acid

The commercially available Aldrich humic acid was obtained from Aldrich Company (Munich, Germany). Before use, the sodium salt of Aldrich humic acid (charge no. 01816-054) was purified according to the purification method described by Kim and Buckau in order to remove inorganic contaminants [Kim 88].

The proton exchange capacity (PEC) is 4.6×10^{-3} eq/g [Kim 88, 90]. The elemental composition (C, H, N, O and S) and content of inorganic constituents of Aldrich humic acid is presented in Table 19. After purification, the humic acid was stored in the dark. Solutions of the humic acid were prepared by dissolution of a definite amount and adding a small amount of 1 M NaOH in an ultrasonic bath. The solution was adjusted to pH 7 with 0.1 M $HClO_4$/0.1 M NaOH and stored in the refrigerator for less than 1 month.

Table 19: Element composition of different origin humic and fulvic acids [Wolf 2004, Kim 88, Kim 90]

Elements content	Aldrich HA [%]	Gohy-573 FA [%]	Gohy-573 HA [%]
C	54.47	54.14	56.6
H	3.82	4.23	4.66
N	0.75	1.38	1.73
O	29.29	38.94	43.93
S	3.80	1.32	0.42
Ash content	3.7	n.d	n.d

Gorleben humic acid and fulvic acid

The natural humic acid and fulvic acid from ground water of the deep borehole Gohy-573 in the Gorleben site (lower Saxony, Germany) were isolated, purified and characterized according to Wolf et al. [Wolf 2004]. Elemental composition (C, H, N, O and S) and content of inorganic constituents of Gohy-573 HA and FA are shown in Table 19. Preparations of Gohy-573 HA and FA solution were carried out according to the procedure described above. The Proton Exchange Capacity (PEC) value of Gohy-573 HA and FA is 5.38×10^{-3} eq/g and 6.82×10^{-3} eq/g, respectively, [Wolf 2004, Kim 88], see Table 20.

Table 20: Characteristic parameters of humic and fulvic acid used in the experiments [Seib 99, Wolf 2004, Kim 88, Kim 90]

	Aldrich HA	**Gohy-573 FA**	**Gohy-573 HA**
PEC [meq/g]	4.6	6.82	5.38
-COOH [meq/g]	4.3	-	4.75
$-OH_{(Phenolic)}$ [meq/g]	2.9	-	1.86

3.1.2 Kaolinite

Well-crystallized standard kaolinite KGa-1b was obtained from the Clay Mineral Society (CMS) Source Clays Repository (Washington County, Georgia, USA) [Prue 93, Payn 2004]. Chemical and mineralogical properties of kaolinite have been reported in the literature [Prue 93]. The cation exchange capacity (CEC) of KGa-1b is 2.0 meq/100 g and the surface area is 11.7 m^2/g. Kaolinite suspensions were prepared in a solution of 0.1 M $NaClO_4$. The chemical composition of standard kaolinite KGa-1b is given in Table 21.

Table 21: Chemical composition of standard kaolinite (KGa-1b) [Prue 93]

Chemical components	**Percentage ratio [%]**
SiO_2	44.2
Al_2O_3	39.7
TiO_2	1.39
Fe_2O_3	0.13
FeO	0.08
MnO	0.002
MgO	0.03
CaO	n.d
Na_2O	0.013
K_2O	0.05
F	0.013
P_2O_5	0.034

3.2 Radiometric Techniques

The concentration of radionuclides (Th, Np, Pu) in solution and the solid phase can be determined by different radiometric techniques such as α-and γ spectroscopy, liquid scintillation counting (LSC), and delayed neutron activation analysis (DNAA). The activity of ^{234}Th was measured by γ spectroscopy. The concentration of plutonium in the solid phase was

determined by DNAA of ^{239}Pu. LSC was used for the determination of ^{234}Th, ^{237}Np ^{238}Pu, ^{239}Pu, and ^{244}Pu in the liquid phase.

a- **spectroscopy**

For alpha spectroscopy, silicon surface barrier detectors (ORTEC Company) with an active area of 450 mm^2, a detector resolution of < 25 keV at 5.5 MeV were used. The detector efficiency varied between 10-15 %. The detector efficiency was controlled regularly by measuring a calibrated ^{241}Am source. α-spectroscopy requires special sample preparation. Therefore, a small volume ~ (2-5) µL of the sample was deposited on a titanium foil and evaporated to dryness carefully. Counting times up to 24 h were chosen. The detection limit for ^{239}Pu is 350 µBq, with a counting error of ≤ 4 %.

g- **spectroscopy**

For all gamma measurements a high purity germanium detector (HPGe) was used (GEM series HPGe Detector Model No. GEM 23185 P-Plus, ORTEC Company). The detector crystal had a diameter of 54.5 mm and a length of 48.9 nm. The detector had a resolution of 1.85 keV at 1.33 MeV.

Liquid scintillation counting (LSC)

Lquid scintillation counting (LSC) has been used as a simple radiometric method for the detection of the total activity in the solution. Alpha and beta emitter can be also detected by LSC. In Figure 32, a schematic diagram is presented for the basic scintillation process used in LSC.

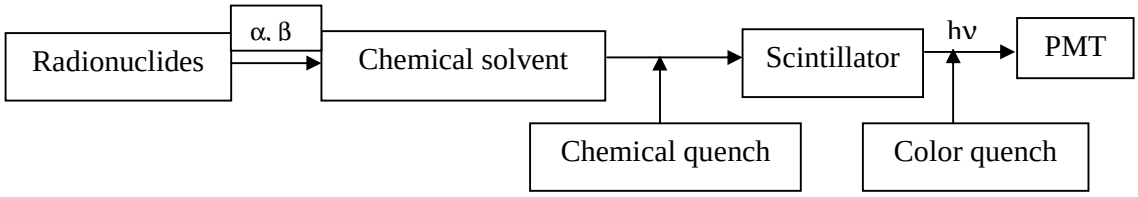

Figure 32: A scheme for the basic scintillation process [Annu 98]

The scintillation cocktail consists of a solvent Diisopropylnaphthalene (DIN), pseudocumene or a linear alkylbenzene together with a fluor solute such as a 2,5-diphenyloxazole (PPO) dissolved in a concentration of approx. 2-10 g/L. A commercially available scintillation cocktail Ultima GOLD AB (Canberra Packard, Rüsselsheim) has been used throughout the

experiments. For sample analysis, discrimination of α, β were always considered. For the neptunium experiments at the Institut für Nuklear Entsorgung (INE), Forschungszentrum Karlsruhe, a commercial LSC instrument Tri-Carb 2500 TR/AB and the scintillation cocktail Ultima GOLD XR (Canberra, Packard) were used. The maximum sample volume was 1 ml in 10 mL scintillation cocktail.

Delayed neutron activation analysis (DNAA)

The amount of sorbed plutonium onto kaolinite was determined for some of the samples by beta-delayed neutron activation analysis [Rudo 77]. The samples were irradiated at the TRIGA reactor at Mainz with a thermal neutron flux of 1.7×10^{12} n/(s cm^2) for two minutes and the beta-delayed neutrons were counted 30 sec later for one minute with a home-made helium-3 detector using the ^{3}He(n,p) reaction. Twelve concentrically arranged ^{3}He-tubes embedded in paraffin were used as neutron detector. The DNAA has a detection limit of 6×10^{11} atoms (3σ) of ^{239}Pu and is independent of the matrix.

3.3 Other Techniques

3.3.1 UV-Vis spectroscopy

UV-Vis absorption spectroscopy has been used for the speciation and characterization of actinides in solution. The sharp absorption bands of actinides occur due to the transition of their f electrons. The absorption bands are characteristic of the actinides and their oxidation states. The concentration of different oxidation states of actinides in the solution can be determined by means of the Lambert-Beer's law,

$$A = \varepsilon c b \qquad (28)$$

where A is the absorbance, ε the molar absorption coefficient [$M^{-1}cm^{-1}$], c the concentration of the actinide in the solution [M], and b the beam path length [cm]. The Pu and Np samples were measured in 1 cm quartz cuvettes or polystyrene semimicrocuvettes. The absorption spectra measured with Cary5 or Cary50 (Varian) of Pu(III), Pu(IV), Pu(V), and Pu(VI) ions are given in the Figure 33 and show different bands at different wavelengths. The plutonium solutions were prepared in 1 M $HClO_4$ except for Pu(V). The Pu(V) solution was prepared (INE, Karlsruhe, Germany) in 0.001 M $HClO_4$ because of its instability in more acidic solutions. Plutonium oxidation states, their characteristics absorption band and the absorption coefficients are given in Table 22.

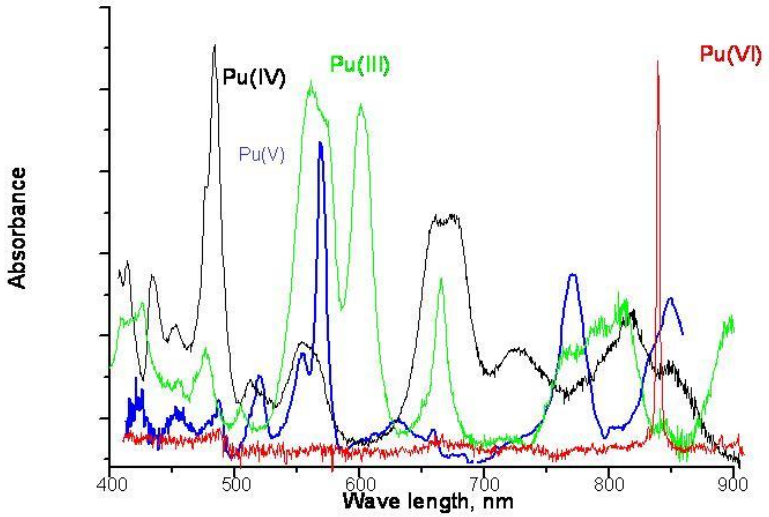

Figure 33: Absorption spectra of the four oxidation states of plutonium in $HClO_4$ medium, at concentrations between 10^{-4} and 10^{-5} M (verified by Carry5 or Carry50).

Table 22: Molar absorption coefficients ($M^{-1}cm^{-1}$) for the different oxidation states of plutonium at the major absorption bands [Katz 86]

Plutonium oxidation state	**Major absorption bands [nm]**	**Molar absorption coefficients [$M^{-1}cm^{-1}$]**
Pu(III)	600	35.3
	900	19.30
	470	49.6
Pu(IV)	655	34.4
	1070	27
Pu(V)	569	17.10
	775	9.87
Pu(VI)	831	550

For the neptunium characterization in solution, all samples were prepared in 2 M HCl solution and measured by UV-Vis spectrophotometer Cary5 (Varian) at the Institute für Nukleare Entsorgung (INE), Karlsruhe, Germany. The absorption spectra of the oxidation states of neptunium in solution are shown in Figure 34. The molar absorption coefficients for the different oxidation states of neptunium are given in Table 23.

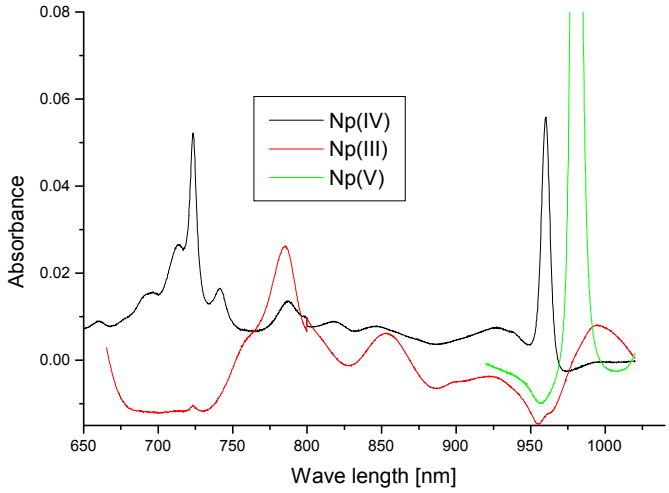

Figure 34: Absorption spectra of the oxidation states of neptunium in 2 M HCl, at concentrations between 10^{-3} and 10^{-4} M (verified by Carry5).

Table 23: Molar absorption coefficients ($M^{-1}cm^{-1}$) for the different oxidation states of neptunium at the major absorption bands [Katz 86]

Neptunium oxidation state	Major absorption bands [nm]	Molar absorption coefficients [$M^{-1}cm^{-1}$]
Np(III)	786	44*
Np(IV)	723	127
	960	162
Np(V)	980	395

* at 50-60 ^{0}C

3.3.2 Inductively coupled plasma mass spectrometry (ICP-MS)

Nowadays, ICP-MS is a very popular and powerful analytic method for the determination of long-lived radionuclides at ultratrace levels. It has been used for the determination of multielements and isotopic ratios in radioactive samples [Beck 2002a, b]. The basic principle of a typical ICP-MS is shown in Figure 35.

Sector field ICP-MS is now used to determine Pu activities and isotope ratios. Different types of ICP-MS facilities are summarized in Table 24. For the ICP-MS measurements described here, the sample which must be in a liquid form, is pumped at 1 mL/min (usually with a peristaltic pump) into a nebulizer, where it is converted into a fine aerosol with argon gas at about 1 L/min.

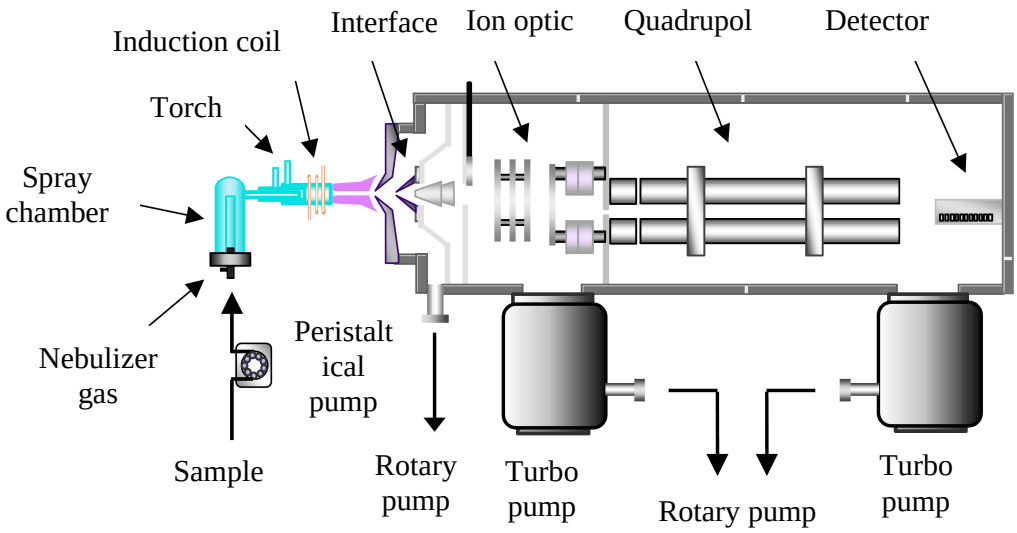

Figure 35: Instrumental setup for a typical ICP-MS (Agilent-HP4500).

The fine droplets of the aerosol, which represent only 1 – 2 % of the sample, are separated from larger droplets using a spray chamber. The fine aerosol then emerges from the exit tube of the spray chamber and is transported into the plasma torch via a sample injector.

Table 24: Different types of ICP-MS for the determination of long-lived radionuclides at ultratrace level [Beck 2002a]

Types of ICP-MS	Detection limit [ng/L]	Precision for isotope ratio [%]
ICP-QMS	0.01-0.6	0.1-0.5
DF-ICP-MS	0.00004-0.005	0.02-0.1
ICP-QMS	0.003-0.01	0.07-0.1
MC-ICP-MS	0.0001-0.0002	0.002-0.02

As microconcentric nebulizer (MicroMist 50 or 200, GlassExpansion, West Melbourne, Australia) was used and as a spray chamber (Cinnebar Cyclonic Small Volume) or a standard Scott type spray chamber was applied. A peristaltic pump was operated for removing waste from the spray chamber. All experiments were done using HP 4500 (Agilent, Waldbronn, Germany) ICP-MS system.

3.3.3 X-Ray absorption fine structure spectroscopy (XAFS)

X-ray absorption fine structure spectroscopy (XAFS) is a powerful tool to determine the chemical state and the local atomic structure of atomic species. It provides information

regarding the oxidation state of the species, coordination chemistry, bond-lengths, coordination number and the atoms surrounding the specified atom. A schematic view a XAFS setup gives Figure 36.

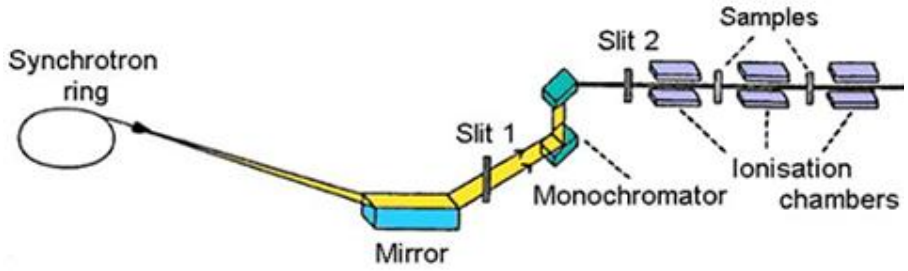

Figure 36: A schematic view of a typical XAFS setup.

The XAFS spectrum is usually divided into two regions: x-ray absorption near-edge spectroscopy (XANES) and extended x-ray absorption fine structure spectroscopy (EXAFS). XANES provides information about the oxidation state and the coordination chemistry (octahedral, tetrahedral coordination) of the absorbing species while EXAFS delivers information regarding bond length, coordination number, and species of the neighbors of the absorbing atoms. For the XAFS measurements with plutonium, wet pastes of sorbed plutonium onto kaolinite were placed in Teflon sample holders, which were sealed with a Kapton film. For safety purposes, all sample holders were double-sealed in PE bags. The plutonium samples were measured at the synchrotron radiation facility ANKA, Karlsruhe, Germany. Pu L_{III}-edge XAFS data were collected at room temperature in the fluorescence mode using a Ge solid-state detector with (5-12) scans. For the analysis of XAFS data, the software packages EXAFSPAK and FEFF were used.

3.3.4 X-ray photoelectron spectroscopy (XPS)

XPS is a surface method that can analyze samples at a depth of 2 to 5 nanometers. XPS enables the analysis of chemical elements at the surface and the nature of their chemical bonds. It can detect all elements except hydrogen and helium.

In XPS, a sample is bombarded with X-rays. Some electrons become excited enough to escape from the atom (photo emission), see Figure 37.

Figure 37: Principle of XPS.

An electron analyzer collects the electrons and measures their kinetic energy thus producing an energy spectrum of intensity (number of photoelectron with time) versus binding energy (the binding energy of the electron). In this work, XPS was performed at the Institut für Nukleare Entsorgung (INE), Karlsruhe, Germany for analyzing the formation of neptunium fulvate colloids. Samples of Np-FA were prepared in inert glove boxes. Np-FA colloids were separated by ultrafiltration from the solution and spread onto aluminum foil using a clean brush. The samples were mounted onto sample holders and moved into the XPS spectrometer (PHI model 5600) without air contact by using a transfer vessel (PHI model 04-110). The samples were transferred into the vacuum of the introduction recipient and evacuated over night to remove residual water. A vacuum of about 1.0×10^{-4} Pa was achieved. The analysis recipient is continuously pumped by an ion pump (oil-free) and occasionally by a Ti-sublimation pump; the background pressure usually is in the range of 7.0×10^{-8} Pa [Schi 2000]. The spectrometer is equipped with a monochromator for Al K_α X-rays (1486.6 eV) and spot size around 1 mm^2. A neutralizer, i.e., a source of low energy electrons, is applied to compensate surface charging. The binding energy scale of the spectrometer was calibrated by making use of the well-known binding energies of Cu $2p_{3/2}$, Ag $3d_{5/2}$ and Au $4f_{7/2}$ lines of sputter cleaned pure metal foils [Seah 98].

3.4 Liquid-Liquid Extraction Technique

Speciation studies of plutonium in groundwater from a nuclear waste repository site are difficult because of the low plutonium concentration [$\sim10^{-6}$ M]. There are very few sensitive methods (direct) available for such investigations. Therefore, indirect methods were used for the determination of plutonium in underground waste repositories [Nits 88]. The liquid-liquid extraction technique was applied to determine the plutonium oxidation states at low concentration levels. Different complexing agents (TTA: 2-thenoyltrifluro-acetone; PMBP: 4-benzoyl-3-methyl-1-phenyl-pyrozolin-5-one; HDEHP: phosphoric acid bis-(2-ethyl-hexyl) ester) were combined [Marq 2004, Nits 88, Nits 94, Bert 81]. The steps for the separation of the different oxidation states of plutonium are outlined in Figure 38.

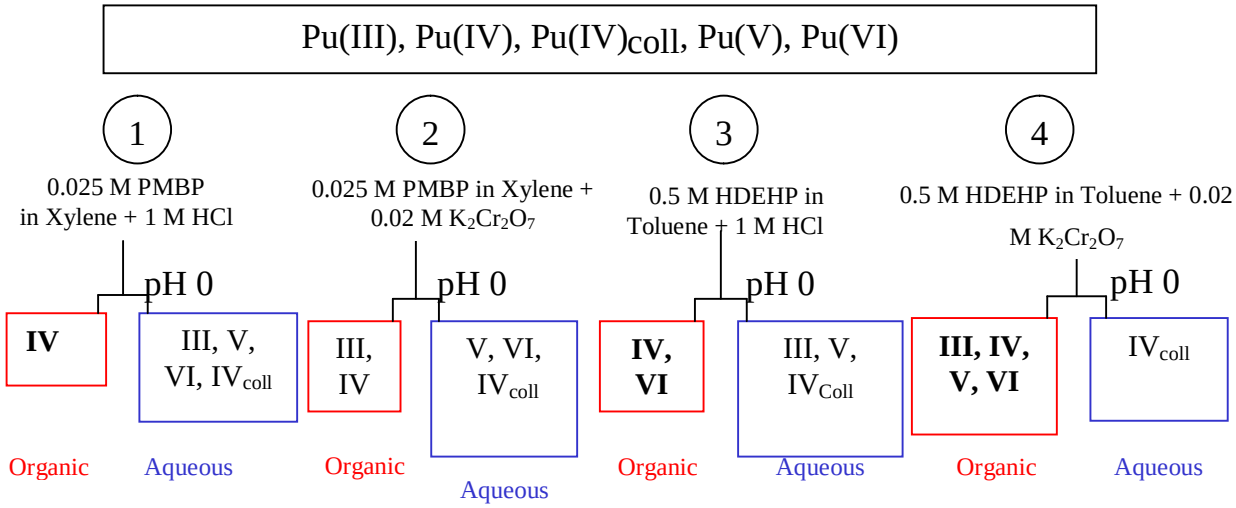

Pu(IV) = Step 1 (organic)
$Pu(IV)_{coll}$ = Step 4 (aqueous)
Pu(III) = Step 2 (organic) - Pu(IV) and Pu(III) = Step 1 (aqueous)- Step 2 (aqueous)
Pu(VI) = Step 3 (organic) - Pu(IV)
$Pu(V) = Pu_{tot}$ - Pu(IV) -$Pu(IV)_{coll}$ - Pu(III) - Pu(VI)

Figure 38: Scheme for the speciation of the plutonium oxidation states by liquid- liquid extraction

3.5 Ultrafiltration and Centrifugation Method

Ultrafiltration

Molecules or ions can be separated by ultrafiltration based on their particle size. If they are smaller than the cut-off of the ultrafilter membrane, they pass through it, and if they are bigger, they are retained on the filter membrane. All ultrafilters (Microsep^{TM}) in the experiments were supplied by the Pall Filtron Company (Northborough). Prior to use, the ultrafilters were rinsed several times with milli-Q water in order to remove glycerol used by the manufacturer to prevent the membrane from drying out.

For the characterization of Aldrich humic acid, ultrafilters with cut-off ranges from 1 to 1000 kD were used. Characterization of Aldrich humic acid with different cut-off filters was performed at different ionic strengths (Figure 39). For the determination of complexation constants by ultrafiltration, a cut-off of 1 kD was used.

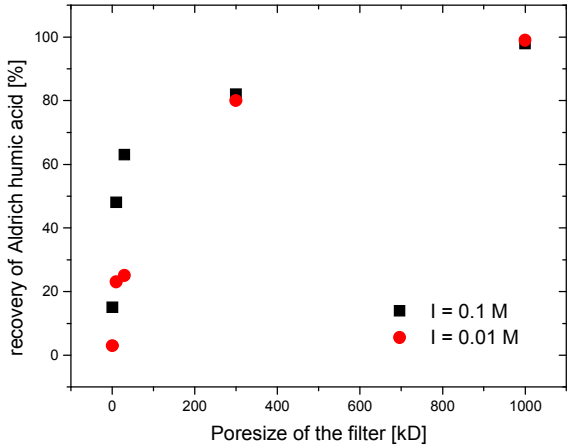

Figure 39: Ultrafiltration of Aldrich humic acid at different ionic strength ($NaClO_4$) at pH 6 [Seib 99]

The humic acid or the complexed ions are almost completely retained on the filter whereas non-complexed metal ions pass through the membrane. Using 1 kD (~1000 amu) filter, free metal ions (Pu) and metal humate (plutonium humate) were separated by performing centrifugation for 20 min. After the ultrafiltration of 1 mL sample volume, 100-200 µL of the filtrate was added to the LSC cocktail for measuring the content of plutonium in the filtrate.

Centrifugation

All sorption experiments were performed by separating the solid from the liquid phase. The centrifugation method was also used for the determination of the complexation constants of La(III) with Gohy-HA.

3.6 Batch Experiments

The batch experiments were carried out using 15 ml polypropylene centrifuge tubes at room temperature and in presence of light. A suspension of 4 g/L kaolinite was chosen for all experiments, preconditioned in 0.1 M $NaClO_4$ and shaken continuously for 48 h. The sorption experiments were carried out in presence of O_2 and CO_2 (aerobic) and anaerobic (in a glove box; 2 ppm O_2). For aerobic sorption studies at pH > 7.0, the appropriate amount of $NaHCO_3$ was added to the system to achieve CO_2 equilibrium with the atmosphere at the desired pH (Table 25).

Table 25: Amount of $NaHCO_3$ added at different pH value to achieve CO_2 equilibrium with the atmosphere in 10 mL sample solution ($NaHCO_3 \Leftrightarrow CO_2 + NaOH$)

pH	1(M) $NaHCO_3$ [µL]
7.0	0.75
7.5	2.150
8.0	6.7
8.5	21.75
9.0	68.5
9.5	250
10	560
11	1120

3.6.1 Binary system

Sorption of plutonium onto kaolinite

All experiments were conducted at pH 0-11, 0.1 M ionic strength, and at ambient temperature (22 ± 2^0C). In the binary experiments for the sorption of plutonium onto kaolinite, the plutonium solution was added to the preconditioned kaolinite suspension. In kinetic experiments, pre-equilibrated solutions were combined and the time required for re-establishing the equilibrium was measured. The time dependence of sorption has been investigated at varying contact times. The pH of the solutions was controlled and readjusted by adding 0.1 M $HClO_4$ or 0.1 M NaOH. Experimental parameters and operating conditions for the sorption studies of plutonium onto kaolinite are shown in Table 26.

Table 26: Experimental parameters and operating conditions for the sorption studies of plutonium and thorium onto kaolinite

Parameter	Conditions
Kaolinite, [KGa-1b]	4 g/L
[^{239}Pu(IV)]	3.5×10^{-7} - 6.9×10^{-9} M
[^{234}Th(IV)]	6.6×10^{-13} M
Ionic strength	0.1 M ($NaClO_4$)
pH	0 – 11
Preconditioning time	48 - 64 h
Contact time of kaolinite with plutonium	120 h
pCO_2	$10^{-3.5}$ atm
Phase separation (centrifugation)	1 h (~ 2500 rpm)
Detection	LSC, DNAA, Gamma spectroscopy

The solid and liquid phases were separated by centrifugation (2500 rpm for 1 h). After centrifugation, the supernatants were analyzed to determine the content of free plutonium ions in the liquid phase by liquid scintillation counting (LSC). The sorbed amount of Pu (air-dried kaolinite, solid phase) was also measured for some samples by beta delayed neutron activation analysis (DNAA).

From both measurements, the total amount of plutonium was controlled, yielding consistent results. For all sorption experiments, < 10 % sorption on the centrifuge tube walls depending on pH values was found and a mathematical correction was applied.

Sorption of thorium onto kaolinite

The sorption of thorium onto kaolinite was investigated in the same way as for plutonium (Table 26). The pH of the solutions was controlled regularly. The solid and liquid phases were separated afterwards by centrifugation (2500 rpm for 30 min). After centrifugation, the supernatants were analyzed by liquid scintillation counting (LSC). The sorbed amount of thorium on kaolinite (solid phase) was measured by gamma spectroscopy. Using the LSC data for the liquid phase and gamma data for the solid phase, the amount of free and sorbed thorium from both phases was calculated. From both measurements, the total amount of thorium was controlled, yielding consistent results. < 1 % sorption on the centrifuge tube walls was found.

Sorption of humic substances onto kaolinite

The sorption experiments of humic substances onto kaolinite were conducted at pH 1, 3, 6, and 9 for Gohy-573 fulvic acid (FA) and at pH 3, 6, 9, and 11 for Aldrich humic acid (HA) with 4 g/L of kaolinite suspension.

Table 27 summarizes the parameters and operating conditions for the sorption of humic substances onto kaolinite. Varying contact times (3, 5, 7 days) were used for measuring the kinetics. The solid and liquid phases were separated by centrifugation (2500 rpm for 1 h) and 2 mL of the supernatant solution were used to determine the content of free humic substances (both HA and FA) in the liquid phase by UV-Vis spectroscopy (at a wavelength of 320 nm). For data analysis, blank probes (only HA/FA solution at different pH values) were measured.

Table 27: Experimental parameters and operating conditions for the sorption of humic substances (HS) onto kaolinite

Parameter	Conditions
Kaolinite, [KGa-1b]	4 g/L
[HA, FA]	10-150 mg/L
Ionic strength	0.1 M ($NaClO_4$)
pH	1-11
Preconditioning time	48 h
Contact time of kaolinite with HS	3, 5 , 7days
pCO_2	$10^{-3.5}$ atm
Phase separation (centrifugation)	1 h (~ 2500 rpm)
Detection	UV-Vis spectroscopy (at 320 nm)

3.6.2 Ternary system

Sorption of plutonium onto kaolinite in presence of humic substances

In the ternary systems, similar experiments have been performed as in the binary experiments. Table 28 summarizes the experimental parameters and operating conditions for the sorption studies of plutonium onto kaolinite in the presence of humic and fulvic acid.

Table 28: Experimental parameters and operating conditions for the sorption studies of plutonium onto kaolinite in presence of humic and fulvic acid

Parameter	Conditions
Kaolinite, [KGa-1b]	4 g/L
[^{239}Pu(IV)]	6.0×10^{-8} M
[HA, FA]	10, 50, 100 mg/L
Ionic strength	0.1 M ($NaClO_4$)
pH	3, 6, 9 (for HA)
	1, 3, 6, 9 (for FA)
Preconditioning time of kaolinite	64 h
Precondition time of kaolinite with HS or plutonium (Binary system)	2 days
Contact time of kaolinite with HA, plutonium (Ternary system)	2-6 days
pCO_2	$10^{-3.5}$ atm
Phase separation (centrifugation)	1 h (~ 2500 rpm)
Detection	LSC

Here different experiments have been performed depending on the adding sequences of the reactants (Pu(IV), HS, and kaolinite). Mainly three adding sequences of reactants were used: 1) kaolinite-Pu(IV)-HS all together (at the same time), 2) kaolinite-HS equilibrium then adding plutonium solution, 3) kaolinite-Pu(IV) equilibrium then adding HS solution.

A plutonium concentration of 6.0×10^{-8} M and HS concentrations of 10, 50, and 100 mg/L were used at a constant ionic strength I = 0.1 M. After the appropriate equilibrium time, liquid and solid phases were separated by centrifugation (2500 rpm) for 1 hour. The supernatants were analyzed in order to determine the content of free plutonium ions in the liquid phase by liquid scintillation counting (LSC). For data analysis, the wall sorption of plutonium was always considered.

Sorption of thorium onto kaolinite in presence of humic substances

Table 29 summarizes the experimental parameters and operating conditions for the sorption studies of thorium onto kaolinite in the presence of fulvic acid.

Different experiment sets have been carried out depending on the adding sequences of the reactants (Th(IV), FA, and kaolinite): 1) kaolinite-Th(IV)-FA all together (at the same time), 2) kaolinite-FA equilibrium then adding thorium solution, 3) kaolinite-Th(IV) equilibrium then adding FA solution. After the appropriate equilibrium time, the liquid and solid phases were separated by centrifugation (2500 rpm) for 1 hour. The activity of ^{234}Th was measured by liquid scintillation counting and gamma spectrometry.

Table 29: Experimental parameters and operating conditions for the sorption studies of thorium onto kaolinite in presence of fulvic acid

Parameter	Conditions
Kaolinite, [KGa-1b]	4 g/L
[^{234}Th(IV)]	6.0×10^{-13} M
[FA]	10, 50, 100 mg/L
Ionic strength	0.1 M ($NaClO_4$)
pH	1, 3, 6, 9
Preconditioning time of kaolinite	64 h
Precondition time of kaolinite with FA or thorium (Binary system)	2 days
Contact time of kaolinite with FA, thorium (Ternary system)	2-6 days
pCO_2	$10^{-3.5}$ atm
Phase separation (centrifugation)	1 h (~ 2500 rpm)
Detection	LSC, Gamma spectroscopy

3.7 Production of the Plutonium Oxidation States by Electrolysis

The different plutonium oxidation states can be produced by electrolysis. In this work, the plutonium oxidation states were prepared electrochemically in $HClO_4$ medium [Cohe 60a, b]. This procedure was chosen because no disturbing substances are present in the electrolytic solution.

Electrolytic cell

For the electrolysis, a homemade glass electrolytic cell (Figure 40, left) with three separated compartments (U-shape) was used.

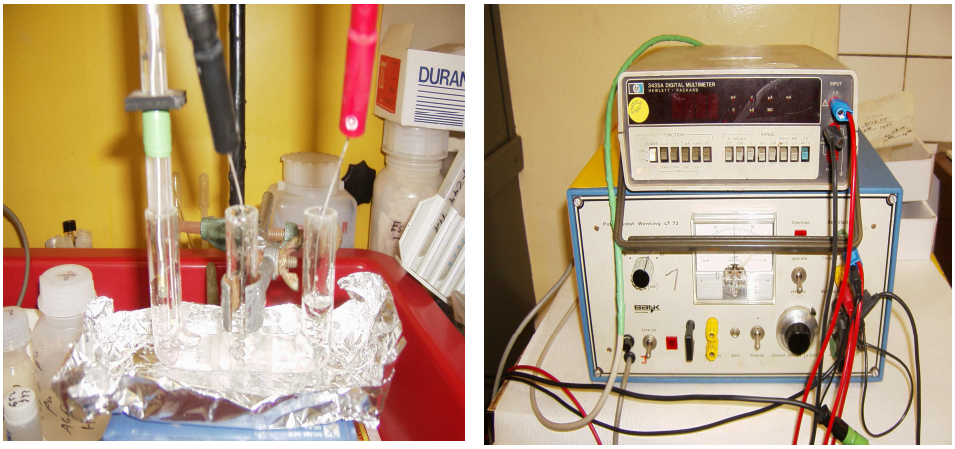

Figure 40: Set-up of the electrolytic cell for the preparation of a defined oxidation state of plutonium in $HClO_4$ solution. Electrolytic cell (left), Potentiostat (right)

The middle one (black color) was used as a working electrode (Pt), the right one (red color) contains a Pt counter electrode and the left one (green color) contains the reference electrode (Ag/AgCl) in 1 M $HClO_4$. These compartments were connected with a potensiotat for obtaining a constant potential (Figure 40, right) at the working electrode. All four oxidation states (III-VI) of plutonium (Figure 41) were electrolyzed in 1 M $HClO_4$ or 0.001 M $HClO_4$ at a constant potential. Table 30 represents the potential values for the preparation of the different oxidation states of plutonium by the electrochemical procedure.

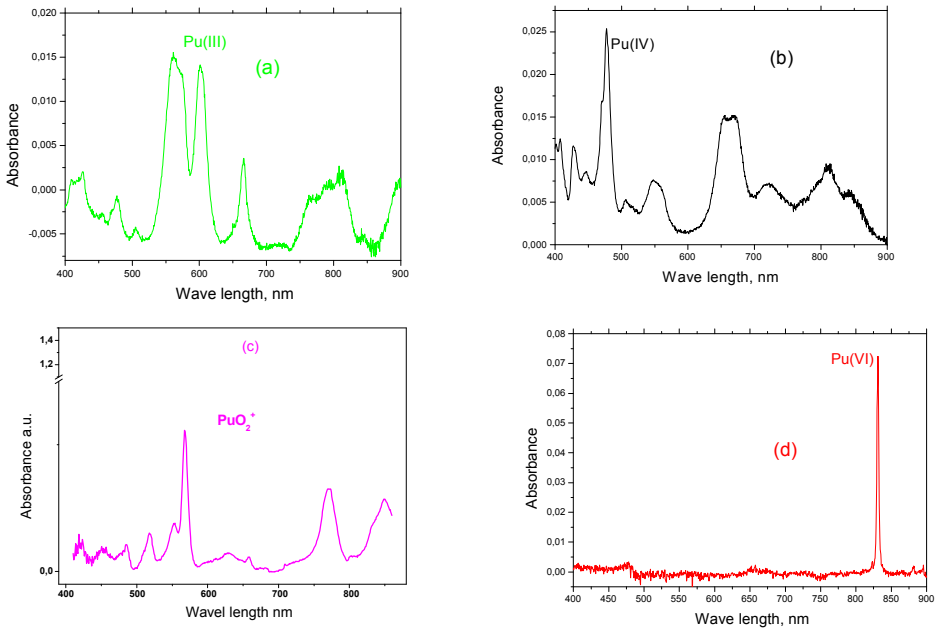

Figure 41: Absorption spectra of the different oxidation states of plutonium in $HClO_4$ media. a) Pu(III) at $2.0.10^{-4}$ M in 1 M $HClO_4$, b) Pu(IV) at $3.0.10^{-4}$ M in 1M $HClO_4$, c) PuO_2^+ at $3.0.10^{-4}$ M in 0.001 M $HClO_4$, d) PuO_2^{2+} at $4.0.10^{-4}$ M in 1 M $HClO_4$

Table 30: Electrolysis conditions for the preparation of the plutonium oxidation states [Marq 2000]

Desired oxidation state	**Starting oxidation state**	**Potential [V]**
Pu(III)	Possible from all oxidation state	
	Pu(IV), fast reaction	$E_{cathode}$ = - 0.6 V
	Pu(VI), slow reaction	E_{anode} = -0.196 V
Pu(IV)	Starting only from Pu(III), fast reaction	E_{anode} = 0.8-0.9 V
Pu(V)	Starting only from Pu(VI) in 0.02 M $HClO_4$	$E_{cathode}$ = 0.9 V
Pu(VI)	Starting from Pu(III) or P(IV)	E_{anode} = -1.95 V

3.8 Preparation of Neptunium(IV) by Chemical Treatment

A chemical treatment was used for the preparation of different neptunium oxidation states in HCl solution. This method was chosen to minimize the formation of colloids in the solution. As a chemical agent, zinc amalgam was used because of its high reducing power. A certain

amount of zinc metal and an amalgam solution were mixed together in order to prepare zinc amalgam.

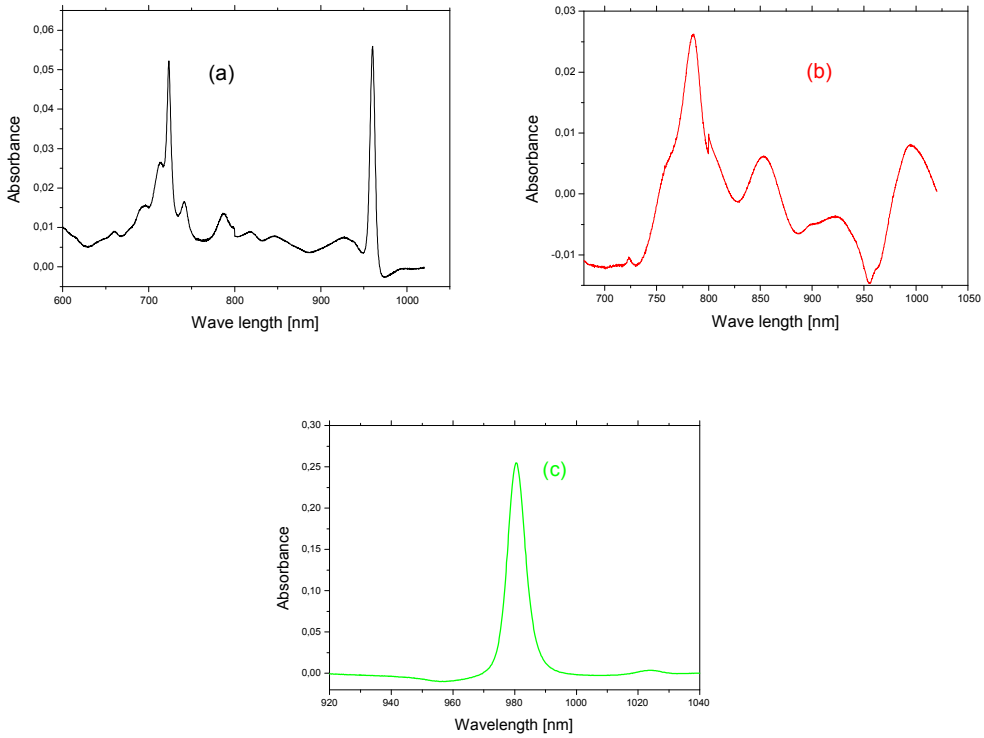

Figure 42: Absorption spectra of the different oxidation states of neptunium in HCl media. a) Np(III) at $8.0.10^{-4}$ M in 2 M HCl, (b) Np(IV) at $8.0.10^{-4}$ M in 2 M HCl, c) Np(V) at 2.10^{-3} M in 2 M HCl.

The reduction of neptunium by zinc amalgam was performed in 2 M HCl solution in a glove box under 100 % argon atmosphere. A Np(V) solution was brought in contact with zinc amalgam and shaken continuously about 20 min. Np(V) is reduced to Np(III) which is oxidized to Np(IV) with in 1-2 days. Figure 42 shows the absorption spectra of the different oxidation states of neptunium as characterized by UV-Vis spectroscopy (Carry5).

4.0 Results and Discussion

4.1.1 Reduction of Pu(VI) in contact with fulvic acid

Humic substances (HA, FA) play an important role for the migration of actinides in the natural aquatic systems due to their strong redox behavior and complex formation. From literature its is known that in the presence of humic acids, Np(V) is reduced to Np(IV) [Chop 99, Pirl 2003a, Zeh 99a,b] as well as U(VI) to U(IV) [Schm 2000]. From these studies, it has been seen that the reduction (U(VI), Np(V)) is significantly influenced by the origin of humic acids (eg; Aldrich HA, Synthetic HA). The higher reduction potential of synthetic humic acid can be explained by the higher phenolic/acidic OH group contents compared to natural humic acid. Choppin found that Pu(VI) is reduced to Pu(IV) in the presence of humic acid in natural aquatic systems [Chop 99, Chop 97b]. The reduction of Pu(VI) in contact with fulvic acid has thus far not been investigated. Therefore, the reduction of Pu(VI) in contact with fulvic acid is discussed in this work.

Table 31: Experimental conditions for the reduction experiments of Pu(VI) with Aldrich humic acid [Kucy 2003] and Gohy-573 fulvic acid.

Parameter	**Reduction of Pu(VI) with Gohy-573 FA**	**Reduction of Pu(VI) with Aldrich HA**		**Reduction of a Pu mixture with Gohy-573 FA**
	(Expt 1)	**(Expt 3)**		**(Expt 2)**
Pu oxidation state	VI	VI	VI	III, IV, V, VI
pH	1, 2.5, 5, 9	0.4, 2.8	2.5	1
Ionic strength		1 M (1 M $HClO_4$)		
[Pu]	2.5×10^{-6} mol/L	3×10^{-5} mol/L	5×10^{-5} mol/L	6×10^{-5} mol/L
[HS]	0.5 mg/L	10 mg/L		0 - 36 mg/L stepwise
Detection	CE-ICP-MS	UV-Vis-NIR (Cary5)		CE-ICP-MS
Conditions	All experiments were performed in contact with air and light, under room temperature and atmospheric pressure			

The reduction of Pu(VI) in contact with Gorleben fulvic acid (FA) has been investigated by online coupling of capillary electrophoresis to inductively coupled plasma mass spectrometry (CE-ICP-MS). Table 31 describes the experimental conditions and parameters for the redox experiments.

The reduction speed of Pu(VI) is greatly influenced by the pH, ionic strength, concentration and Eh of the solution. Figure 43 shows the reduction of Pu(VI) by Gorleben fulvic acid (FA) as a function of time.

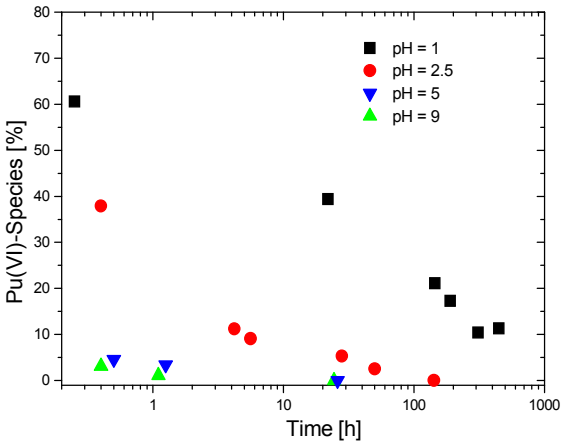

Figure 43: Reduction of Pu(VI) (2.5´ 10^{-5} M) in contact with Gorleben fulvic acid (Gohy-573, 0.5 mg/L) at ionic strength I » 1 M and different pH values as a function of time determined by CE-ICP-MS (Table 31, Expt1).

The reduction of Pu(VI) by Gohy-FA shows an approximately linear behavior (in half-logarithmic scaling) and a significant dependence on the pH value. The enhanced reduction of Pu(VI) by increasing the pH may be explained by the increased fraction of dissociated groups of FA. Therefore, the speed of reduction increases by increasing the pH [Jian 93]. In these redox experiments, E_h and temperature were not measured.

The kinetics of the Pu(VI) reduction by FA is slower at acidic pH compared to neutral pH. At neutral pH, a complete reduction of Pu(VI) by Gohy-FA within one day is observed. Consistently, a fast reduction of Pu(VI) by humic substances is reported by Choppin [Chop 2003] and for humic rich Gorleben groundwater by Marquardt [Marq 2004].

Redox kinetics of plutonium with Gorleben fulvic acid

To investigate the redox kinetics the different oxidation states of Pu with Gorleben fulvic acid (pH about 1), this acid has been added stepwise. The composition of the different oxidation states were checked by CE-ICP-MS (Pu(III) ≈ 5%, Pu(IV) ≈ 39%, Pu(V) ≈ 22%, and Pu(VI) ≈ 34%). Table 31 (Expt 2) lists the experimental conditions.

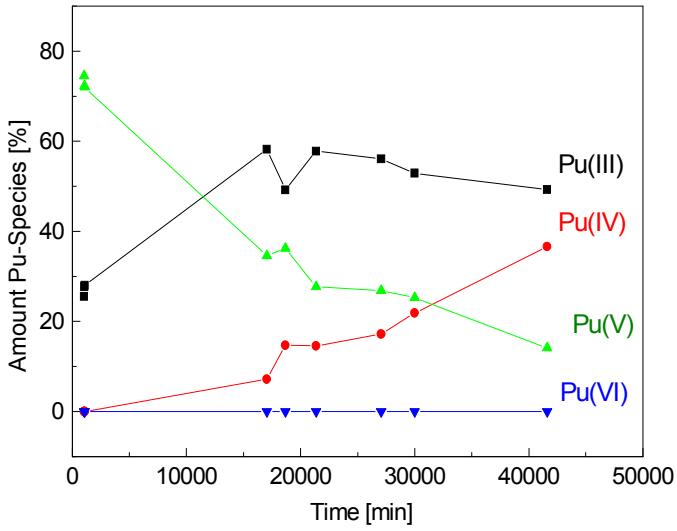

Figure 44: Redox kinetics of a mixture of the four naturally occurring plutonium oxidation states in solution (6 ´10^{-5} M) in contact with Gorleben fulvic acid (Gohy-573, 0 to 36 mg/L) at ionic strength I » 1 M and pH » 1 (Table 31, Expt 2).

Figure 44 shows the redox kinetics of a mixture of all four naturally occurring plutonium oxidation states in contact with Gorleben FA for a contact time up to one month. Within approx. 2 hours, the initial fraction of Pu(IV) and Pu(VI) is completely reduced and Pu(V) and Pu(III) are formed. After 1 month Pu(V) is reduced to Pu(IV) and approx. 80 % of the plutonium in solution can be found in form of Pu(III) and Pu(IV).

4.1.2 Reduction of Pu(VI) in contact with humic acid

The reduction of Pu(VI) in contact with Aldrich Humic acid (HA) has been investigated by UV-Vis spectroscopy [Kucz 2004]. For the experiment, Pu(VI) was added to HA at a concentration between 3.0×10^{-5} M and 5.0×10^{-5} M, at pH 0.4, 2.5 , 2.8. The reduction process was monitored by UV-Vis spectroscopy. The experimental conditions are presented in Table 31 (Expt 3). A pH dependence for the reduction process of Pu(VI) by HA has been found (Figure 45).

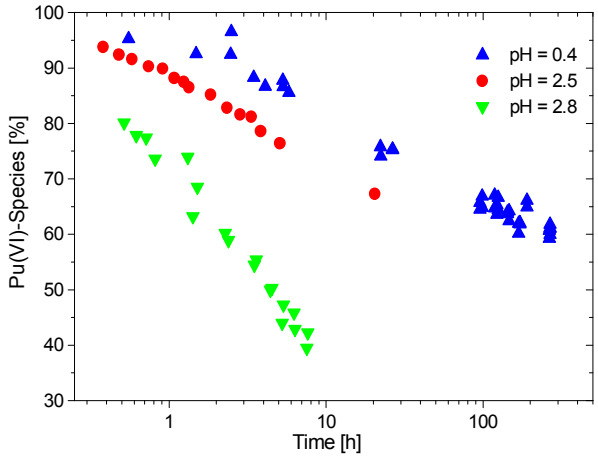

Figure 45: Reduction of Pu(VI) (3-5´ 10^{-5} M) in contact with Aldrich humic acid (AHA, 10 mg/L) at ionic strength I » 1 M and different pH values determined by UV-Vis spectroscopyy (Table 1, Expt 3) [Kuzc 2004].

The reduction of plutonium might be influenced by the precipitation and flocculation of HA at pH ≤ 3 [Chop 88] resulting in a co-precipitation of plutonium. To solve this problem, further experiments will be performed in contact with Pu(VI) and HA at higher pH values (> 3).

Redox kinetics of plutonium with Aldrich humic acid

The redox kinetics of the different oxidation states of plutonium (Pu(V) ≈ 25 %, and Pu(VI) ≈ 75 %) at pH 2.5 has also been investigated. Table 31 (Expt 3) gives the experimental conditions. Figure 46 shows the redox kinetics of a mixture of plutonium oxidation states in contact with Aldrich HA for a contact time of up to one month.

In these redox experiments, it was shown that the reduction of Pu(V) is slower compared to the reduction of Pu(VI). The investigation showed that the reduction of Pu(VI) to Pu(V) is fast compared to the reduction of Pu(V) to Pu(IV) and Pu(III) because of its reduction potential in solution (Table 32). Pu(V) is reduced slowly to Pu(IV). In the case of humic rich Gorleben ground water where the concentration of HA/FA was about 50-60 mg/L [Kuzc 2003], a similar reduction behavior of Pu(VI) was found.

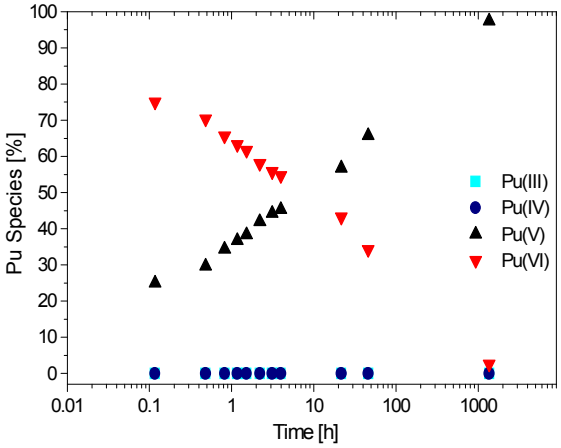

Figure 46: Redox kinetics of a mixture of all four naturally occurring plutonium oxidation states in solution (5 ´10-5 M) in contact with Aldrich humic acid (AHA, 10 mg/L) at ionic strength I » 1 M and pH » 2.5 (Table 1, Expt 3) [Kuzc 2004].

Table 32: Reduction potential of plutonium [Chop 97b]

Plutonium oxidation states	**pH (0) [volt]**	**pH (8) [volt]**
Pu(IV)/Pu(III)	0.982	-0.39
Pu(V)/Pu(IV)	1.170	0.70
Pu(VI)/Pu(V)	0.916	0.60
Pu(VI/Pu(IV)	1.043	0.65

4.1.3 Comparison of the reduction studies of plutonium by humic and fulvic acid

The experiments have shown that Pu(VI) is reduced by HA and FA to Pu(IV) and Pu(III) within a couple of days or weeks. Similar reduction behavior was found for humic rich Gorleben ground water [Kucz 2003]. The reduction of Pu(VI) with FA occurs faster with increasing pH values, and this was also found for HA [Kuzc 2004]. The studies have shown that the reduction of Pu(VI) to Pu(V) is fast compared to the reduction of Pu(V) to Pu(IV) and Pu(III). This can be explained by the redox potential of plutonium in solution (Table 32). The slow reduction of tetravalent plutonium to Pu(III) is due to the hydrolysis ($Pu(IV)(OH)_x^{(4-x)+}$), in particular at neutral pH ($Pu(OH)_4$), and the formation of eigen-colloids leading to a stabilization and thus decreasing the speed of reduction to the trivalent plutonium [Bürg 2005a].

For the Aldrich HA and the Gorleben FA, a complete reduction of plutonium (VI) in the aqueous phase within a few hours to weeks can be observed. Therefore, in contact with adequate concentrations of humic or fulvic acid the fraction of free hexavalent plutonium in natural aqueous solutions will be very low. A further reduction of the pentavalent to tetravalent and trivalent plutonium can be observed at acidic pH, as discussed here for Gorleben FA and reported by several authors for HA [Jian 93, Marq 2004, Andr 2000, Chop 88]. In a geogenic system with an adequate amount of humic or fulvic acid, the reduction of Pu(VI) and Pu(V) to Pu(IV) and Pu(III) would lead to an enhanced immobilization of the plutonium due to the strong sorption of these oxidation states onto mineral surfaces in comparison to Pu(V) and Pu(VI).

4.2. Complexation of tetravalent plutonium with humic substances

Metal-humic acid complexes considerably influence the migration behavior of actinides in the environment. In an earlier chapter it has been shown that in Gorleben groundwater, containing humic substances, Pu(VI) is reduced within minutes to Pu(V) and further, within a few hours or days, to Pu(IV) and Pu(III) [Kucz 2004]. Therefore, our current work has been focused on Pu(IV) complexation with Aldrich humic acid.

Table 33: Experimental conditions for the kinetics of plutonium complexation with Aldrich humic acid

Ionic-strength	0.01M $NaClO_4$
Buffer	0.01M MES
C_{HA}	0 mg/L; 1 mg/L; 10 mg/L
C_{Pu}	7.3×10^{-6} mol/L 7.3×10^{-7} mol/L 7.3×10^{-8} mol/L
Time	20 h; 168 h; 672 h
pH- Value	1.8
Filtration	Ultrafiltration; Pore-size 1k Dalton
Detection	Liquid Scintillation Counting (LSC)
Other Expt. Conditions	Continuously shaken; Room temperature

^{239}Pu(IV) was prepared electrochemically and the oxidation state was verified by UV-Vis spectroscopy. The time dependence of the complexation was investigated in order to find out when the equilibrium of the complexation was reached. Three different plutonium metal

concentrations and two humic acid concentrations were used. The experimental conditions are summarized in Table 33.

Humic acid and Pu(IV) were brought into contact at pH 1.8 and the mixture was shaken continuously. After a set time period (20 h; 168 h; 672 h) aliquots of the solution were filtrated using ultrafiltration (1k Dalton pore size), and the free plutonium ion concentration was determined by liquid scintillation counting (LSC).

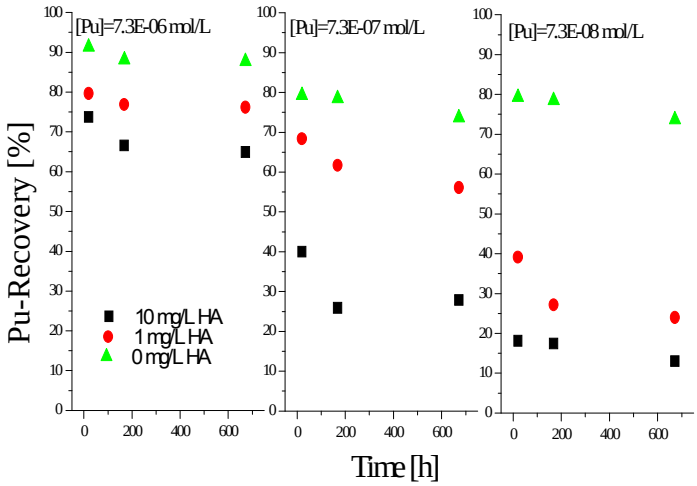

Figure 47: Recovery of free plutonium after addition of Pu(IV) to a solution containing Aldrich HA as a function of time as determined by ultrafiltration and LSC at various metal ion and humic acid concentrations at pH 1.8: black square: 10 mg/L, red circle: 1 mg/L, green triangle: 0 mg/L, Ionic strength = 0.01 M $NaClO_4$.

As shown in Figure 47, there is no significant change in the recovery of free Pu(IV) between one week and one month. The time between one day and one week was investigated in a second experiment (Figure 48, Expt.2). Here, the free plutonium was determined after 20 h; 48 h; 96 h; 168 h. From the results, shown in Figure 48, one can see that complex equilibrium is reached within one week

From the known deprotonation degree, a value for pH 1.8 was extrapolated by a Boltzmann fit, shown in Figure 49. The extrapolated deprotonation degree α is 2.7 %. Table 34 gives an overview of the calculated number of effective complexing sites of humic acid at pH 1.8.

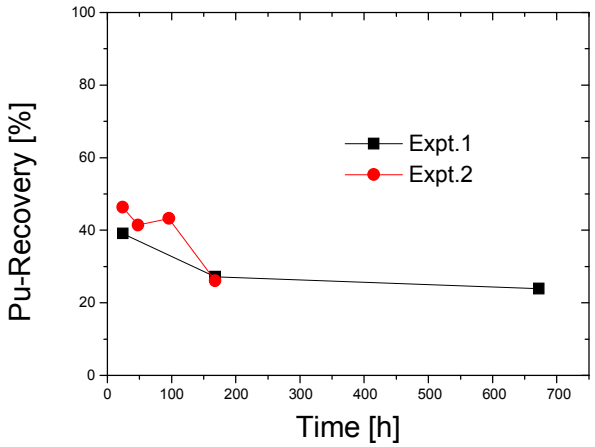

Figure 48: Time dependence of the complexation of Pu(IV) with Aldrich humic acid at varying contact times at pH 1.8, [Pu(IV)] = 7.3E-08, and [HA] = 1 mg/L.

Taking into account that under these conditions, two hydroxide ions are bound to plutonium(IV), at a plutonium concentration of 7.3×10^{-8} mol/L and a HA concentration of 1.0×10^{-3} g/L, the effective number of active humic binding sites yields an effective humic acid concentration of 12.4×10^{-8} eq/L (Table 34). This might be an explanation why it takes so long to reach complexation equilibrium. Figure 49 shows the degree of deprotonation of HA with varying pH values.

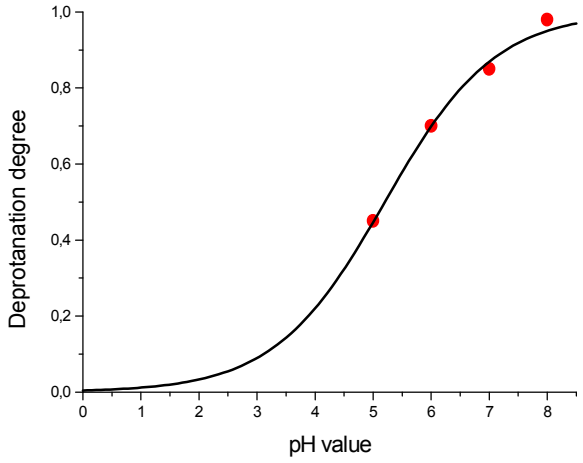

Figure 49: Extrapolation (Boltzmann-fit) of the deprotonation degree as a function of the pH value.

Table 34: Results for the effective PEC of HA in solution corrected by the extrapolated deportonation at pH 1.8

Parameter	Tabulated value	In solution	In solution, α corrected
[Pu(IV)]		7.3×10^{-8} mol/L	7.3×10^{-8} mol/L
[HA]		1.0×10^{-3} g/L	1.0×10^{-3} g/L
PEC	4.6×10^{-3} eq/g	4.6×10^{-6} eq/L	12.4×10^{-8} eq/L

4.2.1 Determination of loading capacity of Pu(IV) with Aldrich humic acid

It has been assumed that the complexation reaction is

$$Pu + HA(z) \rightarrow PuHA(z) \tag{29}$$

with z the charge of the complexing plutonium ion. The complexation with humic acid is described by the charge neutralization model [Kim 96]:

$$[HA(z)]_t = \frac{(HA)\cdot(PEC)}{z} \tag{30}$$

Here, (HA) is the concentration of humic acid in [g/L], (PEC) is the proton exchange capacity in [eq/g]. The loading capacity (LC) is defined as:

$$LC = \frac{[PuHA(z)]}{[HA(z)]_t} \text{ or } LC = \frac{z[Pu^{z+}]^*}{(PEC)(HA)]} \tag{31}$$

$[Pu^{z+}]^*$ is the maximum plutonium ions bound to the humic substances.

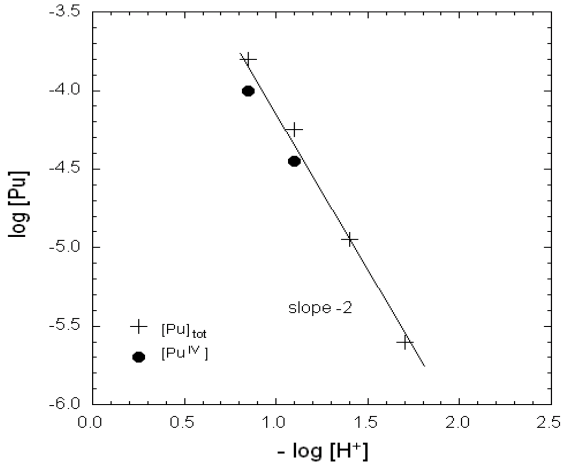

Figure 50: Formation of plutonium hydroxide species as a function of pH [Bite 2002].

Bitea et al. [Bite 2002] by LIBD and LAPAS observed that Pu(IV) exists as $[Pu(OH)_2]^{2+}$ at pH values from 0.3 to 2.0 in the aqueous solution. Figure 50 shows the formation of

plutonium hydroxides as a function of pH and from the slope -2 it is inferred that $[Pu(OH)_2]^{2+}$ is present in equilibrium with colloids (solubility product, $\log K_{SP} = -59.0 \pm 0.3$).

The corrected equation by the LC term for the complexation constant in that case can be expressed as follows:

$$ß_{LC} = \frac{[PuHA(z)]}{[Pu^{z+}]_f \cdot (([HA(z)]_t \cdot LC) - [PuHA(z)])} \quad (32)$$

$$ß_{LC} = \frac{[Pu(OH)_2HA(II)]}{[Pu(OH)_2{}^{2+}]_f \cdot (([HA(II)]_t \cdot LC) - [Pu(OH)_2HA(II)])} \quad (33)$$

The LC value is best visualized by plotting the mole ratios namely, $\frac{[Pu(OH)_2HA(II)]}{[HA(II)]_t}$ against $\frac{[Pu^{4+}]_t}{[HA(z)]_t}$ as shown in Figure 51. The loading capacities are found to be 3.3 % at pH 1.8, 4.5 % at pH 2.5, 9.2 % at pH 3.

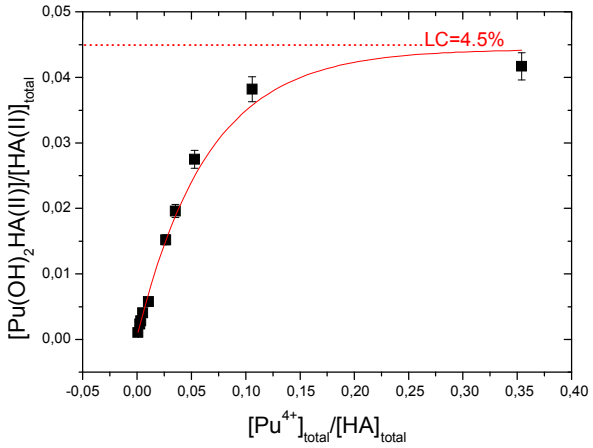

Figure 51: Determination of the loading capacity (LC) for the complexation of Pu(IV) with humic acid at pH 2.5, [Pu(IV)] = 6.6´10^{-7} M, [HA] = 0 - 25 mg/L and ionic strength 0.1 M $NaClO_4$.

4.2.2 Complexation constants of plutonium(IV) with Aldrich humic acid

The complexation constant is obtained as

$$ß_{LC} = \frac{[Pu(OH)_2HA(II)]}{[Pu(OH)_2{}^{2+}]_f \cdot (([HA(II)]_t \cdot LC) - [Pu(OH)_2HA(II)])} \quad (34)$$

where $[Pu(OH)_2HA(II)]$ is the concentration of Pu humate [mol/L] and $[Pu^{z+}]_f$ is the concentration of the free Pu [mol/L].

In the experiments the Pu(IV) concentrations were varied between 10^{-8} and 10^{-5} mol/L. Aldrich humic acid was used with concentrations between 0.01 and 25 mg/L. According to the results of the kinetic study (chapter 4.2.1.1) an equilibration time of one week was chosen. After that, the free plutonium-ion concentration was determined after ultrafiltration by means of liquid scintillation counting (LSC).

The $\log ß_{LC}$ values calculated are 6.5-7.9 at pH 1.8; 6.7-8.3 at pH 2.5; 6.4-8.4 at pH 3, see Figure 52. The scattering of the $\log ß_{LC}$ values are unusually large within two orders of magnitude. This may be due to co-precipitation effects, as the humic acid at the low pH values forms a precipitate. Furthermore colloid formation of Pu(IV) must be taken into account. The obtained complexation constants are compared with experimental data reported in the literature (Table 35).

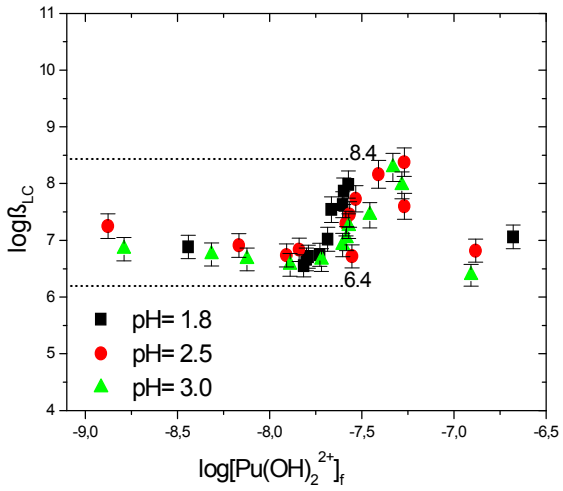

Figure 52: Humate complexation of Pu(IV) studied by ultrafiltration; $\log ß_{LC}$ values calculated and plotted as a function of the free Pu(IV) conc. at different pH values (1.8, 2.5, 3.0).

Table 35: $\log ß_{LC}$ values for Pu(III) and Pu(IV) at different pH values in comparison with Am(III) and Th(IV)

Actinides	Species	pH	$\log ß_{LC}$
Pu(III)	PuHA(III)	3.0-4.0	6.2 – 6.8 [Buda 2006]
Am(III)	AmHA(III)	3.0-6.4	6.3-6.5 [Czer 96, Kim 96]
Pu(IV)	$Pu(OH)_2HA(II)$	1.8-3.0	6.4 – 8.4
Th(IV)	ThHA(IV)	3.9	12.4 [Nash 81]

4.2.3 Complexation of tetravalent neptunium with humic substances

The complexation of Np(IV) with fulvic acid has also been studied. All experiments have been performed (INE, Karlsruhe) with ^{237}Np in a glove box under argon atmosphere at room temperature. Gorleben fulvic acid (GoHy-573 FA) with concentrations of 100 and 1000 mg/L was used. In first batch experiments, the fulvic acid concentration was kept constant (0.1 and 1 g/L) and the Np concentration varied from $3x10^{-5}$ to $3x10^{-4}$ M at pH 1 and 3.

To minimize the colloid formation of Np(IV), the experiments were started with colloidal-free Np(III) stock solutions at pH 1 and 3. Np(III) was prepared by reduction of Np(V) with liquid Zn-amalgam. After the removal of Zn-amalgam, a GoHy-573 FA solution was added to Np(III). Within 1-2 days the Np(III) is oxidized to Np(IV). Because of the strong interaction of Np(IV) with the fulvic acid, the uncomplexed Np(IV) concentration is kept below its solubility limit. Thus, this method will avoid colloid formation of tetravalent neptunium even at higher metal concentrations.

After 20 and 40 hours equilibration time, the solution has been characterized by absorption spectroscopy in the wavelength range from 920 to 1040 nm. Here, the absorption bands for the free Np(IV) ion (at 960 nm) and of Np(IV) fulvate species (> 960 nm) appear.

At pH 1 and 1000 mg/L FA, mainly the absorption band at 970 nm was observed after 20 h and after 40 h a small new peak at 978 nm arises. By decreasing the FA concentration to 600 mg/L, 3 peaks were observed at 960 nm for the uncomplexed Np(IV) and at 970 and 978 nm for the fulvate species.

At pH 3, the peak at 978 nm besides a small one at 970 nm dominates the spectrum (Figure 53). No free Np(IV) was detected at 960 nm. However, by increasing the Np(IV) concentration, a new band near 984 nm appeared. The nature of these fulvate species is so far unclear. Earlier studies by Pirlet [Pirl 2003a] showed also a dominating absorption band at 978 nm, although the preparation procedure and the pH values were different. In that work, Np(V)FA was reduced by dithionite to Np(IV)FA at about pH 7. We conclude that independent of the pH value in the range between 3 and 7 only one Np(IV) fulvate species prevails.

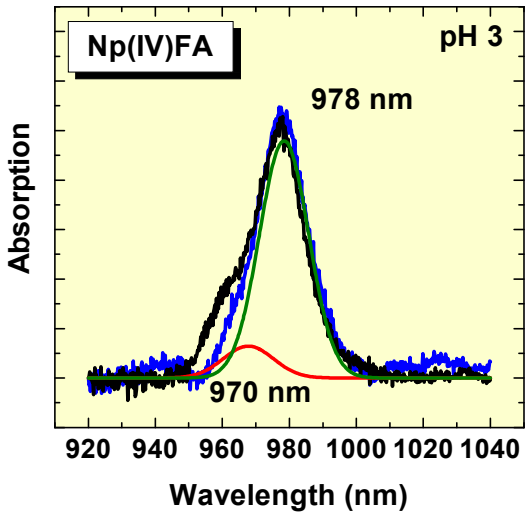

Figure 53: Absorption spectra and deconvoluted spectra of Np(IV)-FA at pH 3.

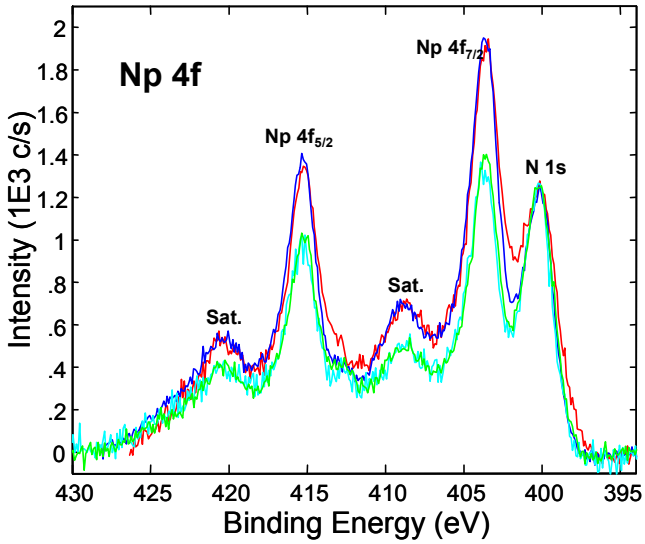

Figure 54: XPS spectra of Np(IV)-FA after a reaction time of 1 d (green) and 14 d (blue and red), [FA] = 1 g/L, [^{237}Np(IV)] = 1.0E-04 M, pH = 1, Ultrafiltration (10 kD filter) = 30 min.

To characterize the Np(IV)-fulvic acid complex, the Np(IV)FA was separated by ultrafiltration and analyzed by X-ray photoelectron spectroscopy (XPS). The resulting XPS spectra of two samples - 1 day and 14 days equilibration time - are shown in Figure 54. No significant differences could be observed. Further experiments are needed to characterize precisely the Np(IV)FA complex as a function of the reaction time.

4.3 Precipitation of Aldrich humic acid as a function of pH

Redox speciation and complexation of plutonium in contact with HA at low pH values have been investigated and presented in chapter 4.1. From the reduction kinetics and complexation experiments, it was concluded that co-precipitation of HA could influence the redox reaction and complex formation. Therefore, the precipitation of HA as a function of pH has been studied.

For this, Aldrich humic acid (HA) was used at concentrations of 1, 10, and 25 mg/L. The influence of the pH-value on the precipitation of HA at pH 1.8, 2.5, and 3.0 was studied by UV/Vis spectroscopy (Carry50) by measuring the change in concentration of HA in solution. The pH of the solution was checked regularly (Beckmann model-310 pH meter). Figure 55 shows the precipitation of HA at pH = 1.8 for three different humic acid concentrations (1, 10, and 25 mg/L).

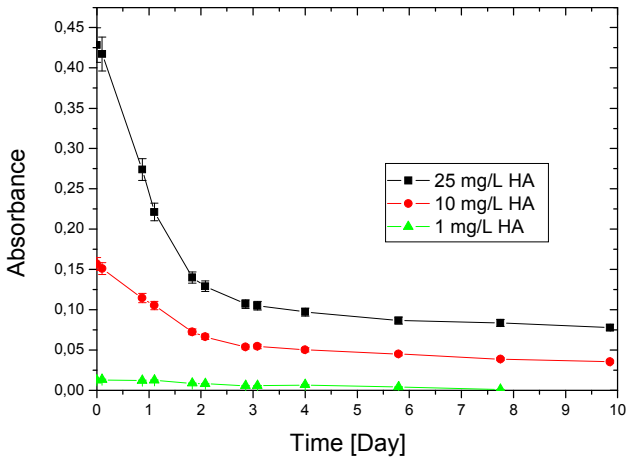

Figure 55: Precipitation of Aldrich humic acid for different concentrations (1, 10, and 25 mg/L) at pH 1.8 as a function of time.

The concentration of HA in solution decreases significantly with time. A precipitate of HA at the bottom of the cuvette is already observable by eye. A reduction of the HA concentration in solution (original concentration 25 mg/L) of 80 % at pH 1.8, 30 % at pH 2.5 and almost 0 % at pH 3.0 was found for the Aldrich humic acid after 240 h (Figure 56).

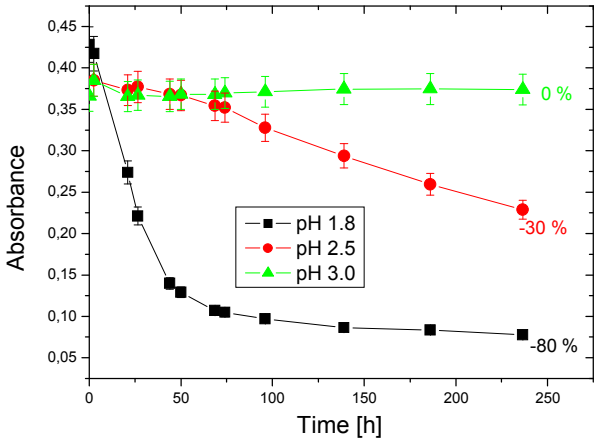

Figure 56: Decrease of HA concentration in solution at different pH-values (1.8, 2.5, and 3.0) as a function of time (values in percent define the decrease after 10 d) for a starting AHA solution of 25 mg/L.

4.3.1 Limitation of the ultrafiltration method for the determination of the complexation constants with humic substances

Fulvic acid is soluble in all pH ranges but humic acid precipitated at pH < 3. Therefore, fulvic acid could be used for determining the complexation constants of metal ions at low pH-values, where adsorption effects on filter materials are almost negligible. To verify the ultrafiltration method for the determination of complextation constants of metal ions with humic and fulvic acid, different metal ions (Ca(II), La(III), Zr(IV)) have been chosen. Experimental conditions and parameters are summarized in Table 36.

Table 36: Experimental conditions for the metal fulvate and humate complexation at pH 6

Parameter	Conditions
Ionic strength	0.01M $NaClO_4$
Buffer	0.01M MES
[FA, HA]	20, 50 mg/L
$[Ca^{2+}]$, $[La^{3+}]$, $[Zr^{4+}]$	10^{-4} mol/L
Contact time	20 h; 168 h
pH	6.0
Filtration	Ultrafiltration; Pore-size 1k Dalton
Detection	UV-Vis spectroscopy
Others	Continuously shaken; Room temperature

Fulvic and humic acid (20 and 50 mg/L) were brought in contact with different metal ions (Ca(II), La(III), Zr(IV), 10^{-4} M) at pH 6 and the mixtures were shaken continuously. After a preselected time (20 h; 168 h) aliquots of the solution were filtrated using ultrafiltration (1k Dalton pore size), and the concentration of the humic substances in the filtrate was determined by UV-Vis spectroscopy.

Figure 57 shows the percentage of fulvic acid in the filtrate in the presence and absence of metal ions. As can be seen, 20 to 60 % of FA passes through the filter depending on the FA concentration and the complexed element.

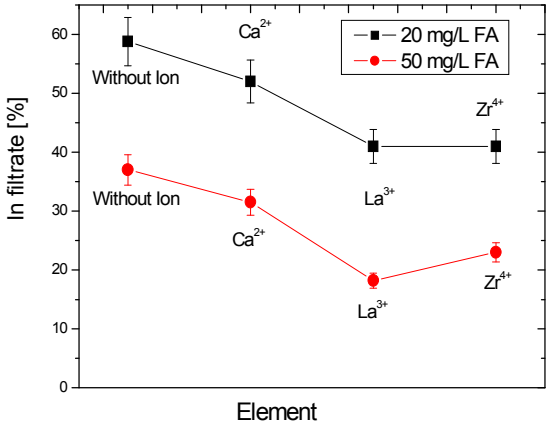

Figure 57: Percentages of fulvic acid in the filtrate in presence and absence of metal ions at pH = 6, contact time = 7 days, [Ca^{2+}, La^{3+}, Zr^{4+}] = 10^{-4} M.

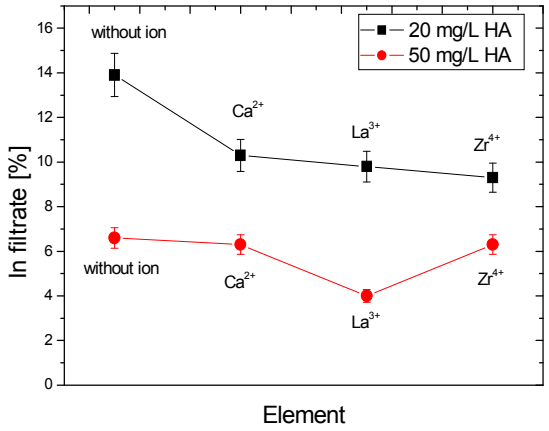

Figure 58: Percentages of recovered humic acid in the filtrate after formation of complex in presence and absence of metal ions at pH = 6, contact time = 7 days, [Ca^{2+}, La^{3+}, Zr^{4+}] = 10^{-4} M.

In the case of humic acid, only 5 to 15 % of HA pass through the filter depending on HA concentration (Figure 58). Figure 59 shows the percentage of humic and fulvic acid on the filter in the presence and absence of metal ions.

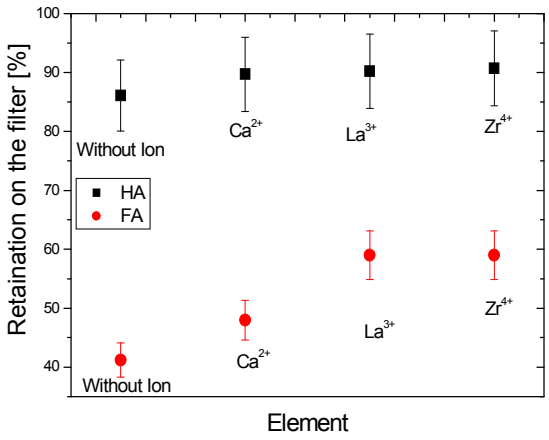

Figure 59: Percentage of humic (black dot) and fulvic acid (red dot) on the filter in presence and absence of metal ions at pH = 6, contact time = 7 days, [Ca^{2+}, La^{3+}, Zr^{4+}] = 10^{-4} M and [FA, HA] = 20 mg/L.

Thus, the ultrafiltration method is not suited for the determination of complexation constants with fulvic acid.

4.3.2 Limitation of the ultrafiltration method for the determination of complexation constants of Pu(IV) with humic substances

The recovery of Pu(IV) after ultrafiltration in the absence of humic acid was investigated, i.e., the amount of sorbed Pu on the filter and/or vessel material was determined. A concentration of 4.15×10^{-7} mol/L Pu was used at different pH-values (1.8, 2.5, 3.0, 3.8, and 4.8) with 0.1 M MES (2N-Morpholinoethane sulfonic acid) as a buffer and $NaClO_4$ to fix the ionic strength at 0.1 M. The pH-value of the Pu(IV) solution was adjusted with 0.1 M NaOH or 0.1 M $HClO_4$. The Pu solutions were ultrafiltrated using filters with different pore sizes (1, 3, 10 kDa) and the concentration of Pu in the filtrates was measured by liquid scintillation counting (LSC).

The percentage of plutonium recovery for the different pH-values is shown in Figure 60. The recovery is 85 % at pH 1.8, 59 % at pH 2.5, 48 % at pH 3.0, 18 % at pH 3.8, and 13 % at pH 4.8.

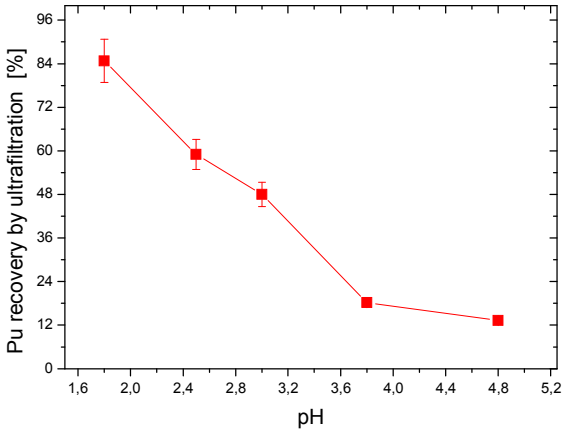

Figure 60: Percentage of plutonium recovery after ultrafiltration at varying pH-values (1 kDa filter pore size); [Pu(IV)] = 4.7E-07 M, I= 0.1 M $NaClO_4$.

No differences were observed for the different filter pore sizes (1, 3, 10 kDa). Referring to the decreasing percentages of recovery for Pu(IV) with increasing pH, a determination of the complexation constants with HS using the ultrafiltration method is not possible for higher pH-values without applying substantial corrections.

4.4 Sorption of tetravalent plutonium onto kaolinite

4.4.1 Speciation of Pu(IV) in aqueous system

The speciation of Pu(IV) in aqueous solution was calculated using a geochemical modeling software (PHREEQC, Version 2.0 [Park 99]). The required speciation data were obtained from different sources, mainly from Zavarin et al. [Zava 2005] and Knopp et al. [Knop 99]. The calculated relative distribution of Pu(IV) species in aqueous solution is shown in Figure 61. At pH < 1 Pu^{4+} is the predominant species. At pH > 1, the formation of the hydroxide species $Pu(OH)^{3+}$, $Pu(OH)_2^{2+}$, $Pu(OH)_3^{+}$, and $Pu(OH)_4$ is observed with increasing pH value. At pH > 8.5, negatively charged plutonium carbonate complexes are the dominant species in the form of $Pu(OH)_2(CO_3)_2^{2-}$ and $Pu(OH)_4(CO_3)_2^{4-}$. Thus, a significant influence on the sorption of plutonium onto the negatively charged kaolinite at pH > 8.5 due to the plutonium carbonate species can be expected.

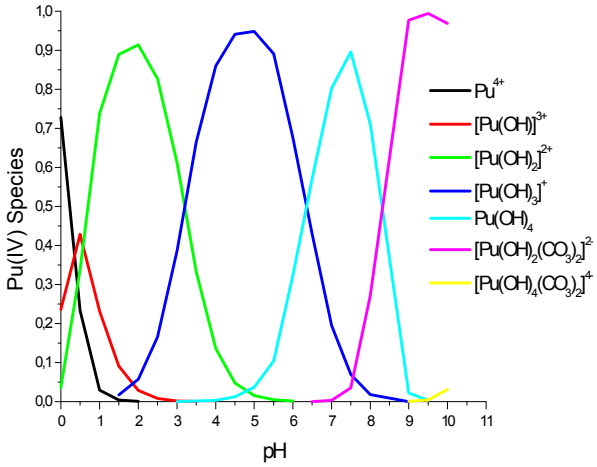

Figure 61: Species distribution of Pu(IV) in aqueous solution; [Pu(IV)] = 6.6E-06M, ionic strength 0.1 M ($NaClO_4$), at room temperature, and CO_2 in equilibrium with atmosphere.

4.4.1.1 Effect of contact time on the sorption of Pu(IV) onto kaolinite

The sorption experiments were performed with different contact times (64 to 120 h) at pH 1-12. No significant time dependence was observed at all pH values (Figure 62). For the sorption experiments described in the following, 120 h has been chosen as contact time.

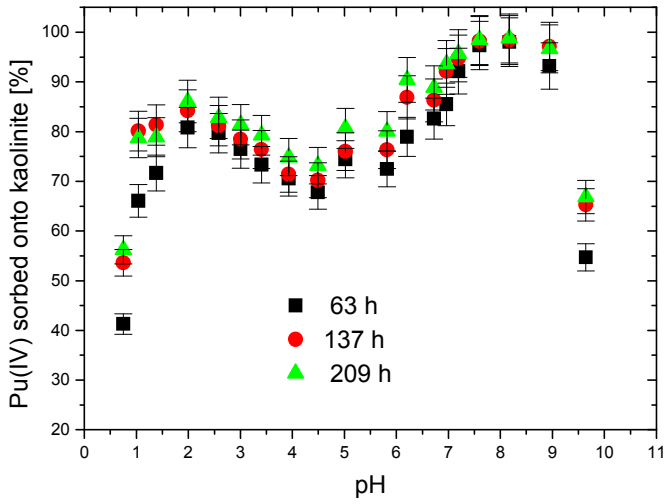

Figure 62: Pu(IV) sorption onto kaolinite as a function of pH and varying contact times (63 h, 137 h, 209 h); [Pu(IV)] = 3.56E-07M, ionic strength 0.1 M ($NaClO_4$), room temperature, and CO_2 in equilibrium with atmosphere.

4.4.1.2 Effect of pH on the sorption of Pu(IV) onto kaolinite

The sorption of tetravalent plutonium onto kaolinite was investigated as a function of pH and the obtained results are shown in Figure 63. A pH range of 0 - 11 was studied with Pu(IV) concentrations of 3.56×10^{-7} – 6.91×10^{-9} M and a solid phase concentration of 4 g/L with ionic strength I = 0.1 M ($NaClO_4$). Figure 63 shows that the sorption behavior of plutonium onto kaolinite is almost constant for varying concentrations of plutonium. The sorption of Pu(IV) in contact with kaolinite is strongly influenced by the pH. The sorption edge can be observed at pH ≈ 1. The sorption increases with increasing pH up to 85 % at pH 2 and then decreases down to 55 % at pH 4. At intermediate pH 4 - 6, an unexpected, lower sorption has been found. In order to shed light on the sorption behavior of Pu(IV) at pH 4 - 6, the oxidation state of the remaining Pu in the liquid phase after sorption onto kaolinite was determined by liquid-liquid extraction [Nits 88]. It has been found that at pH ≈ 4, Pu(V) is the dominant species in solution.

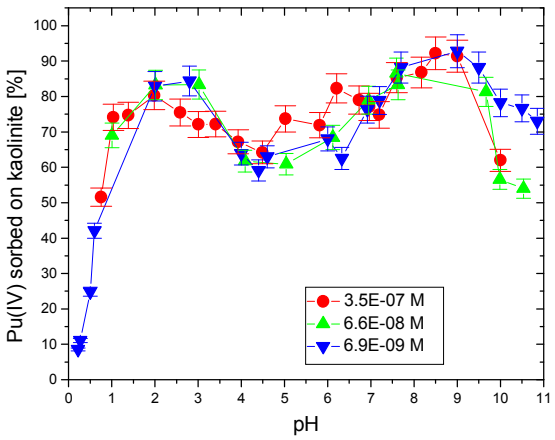

Figure 63: Sorption of tetravalent plutonium ions onto kaolinite (4.0 g/L) as a function of pH at I = 0.1 M ($NaClO_4$) and 25°C, after 120 h equilibration time with $pCO_2 = 10^{-3.5}$ atm using varying plutonium concentrations.

It seems that the initially added Pu(IV) is partially oxidized in the liquid phase to Pu(V) in contact with kaolinite at pH values 4 - 6 under aerobic and anaerobic conditions, which might be an explanation for the lower sorption in this pH range. Very recently the Pu(IV) sorption onto kaolinite was investigated by XANES at pH 1, 4, 9. The observed sorbed species on kaolinite was Pu(IV). Details will be discussed in chapter 4.4.4.

At pH > 8.5, the negatively charged plutonium carbonate species are predominant in the presence of CO_2, thus leading to a decrease of sorption of plutonium onto the also negatively charged kaolinite surface at that pH. The sorption of Pu(IV) onto kaolinite in the presence and absence of CO_2 is shown in Figure 64.

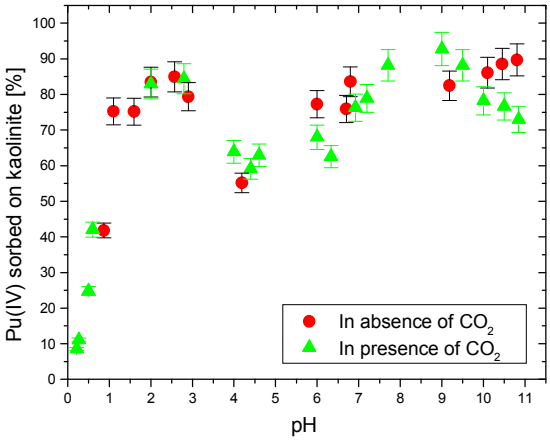

Figure 64: Influence of CO_2 on the sorption of Pu(IV) onto kaolinite as a function of pH; [Pu(IV)] = 6.6E-9 M , $pCO_2 = 10^{-3.5}$ atm, [KGa-1b] = 4 g/L, contact time = 120 h.

In the absence of CO_2 at pH > 8.5, a stronger sorption of Pu(IV) onto kaolinite has been found and compared to the sorption in the presence of CO_2.

4.4.1.3 Speciation of plutonium in contact with kaolinite by liquid-liquid extraction

In sorption studies of Pu(IV) with kaolinite, at intermediate pH values 4-6, an unexpected lower sorption was found. To understand the minimum in the sorption around pH values 4-6, the oxidation state of Pu in solution (after sorption onto kaolinite) was determined by liquid-liquid extraction. The experimental procedure has already been discussed in chapter 3.4.1. Three different samples (A, B, C) at pH 1, 4, and 9 were investigated. At pH 4 about 75 % of the plutonium in the aqueous phase was determined as Pu(V) whereas at pH 1 and 9, mainly Pu(III), Pu(IV), and $Pu(IV)_{colloids}$ were observed (Table 37).

In Figure 70 and 71 one can see that the sorption of Pu at low pH is weaker than that of Th which might be correlated with the 38 % presence of Pu(III).

Table 37: Oxidation states of plutonium species in solution after the sorption on kaolinite as a function of pH

Sample name	pH	Oxidation states of plutonium
A	1.0	Pu(III) = 38 % and Pu(IV) = 46 %
B	4.0	Pu(IV) = 14.0 % and Pu(V) = 75 %
C	9.0	Pu(IV) = 45.0 % and $Pu(IV)_{colloids}$= 49 %

4.4.1.4 Desorption of plutonium from sorbed kaolinite

Desorption experiments were carried out at different pH values under the same experimental conditions used in the sorption experiments. The Pu sorbed onto the kaolinite was desorbed in a fresh $NaClO_4$ solution of I = 0.1 M and buffered at the appropriate pH value. The desorption rate from kaolinite as a function of pH is shown in Figure 65.

About 1 - 10 % desorption of plutonium from kaolinite occurs. This indicates that the plutonium ions are bound strongly onto kaolinite (chemisorption rather than physisorption) and that sorption is only partially reversible.

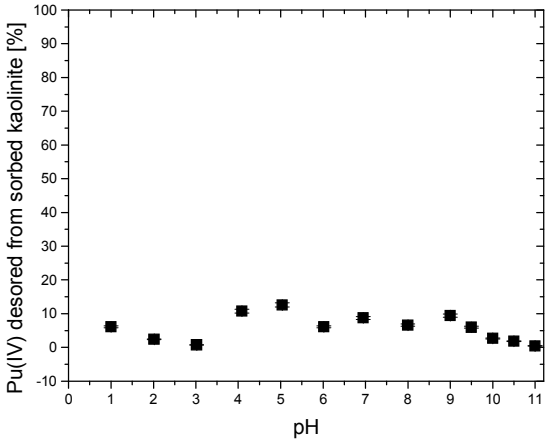

Figure 65: Desorption of plutonium from kaolinite. The desorption experiments were carried out at ionic strength I = 0.1 M $NaClO_4$; [Pu(IV)] = 6.6E-8 M , [KGa-1b] = 4 g/L, $pCO_2 = 10^{-3.5}$ atm, contact time = 120 h.

4.4.2 Sorption of Th(IV) onto kaolinite

The distribution of Th(IV) species for solutions in equilibrium with CO_2 was calculated using geochemical modeling software based on the most recent published Th(IV) complex

formation constants in the literature. The speciation data mainly obtained from Altmaier et al. [Altm 2005]. The calculated relative distribution of Th(IV) species in aqueous solution is shown in Figure 66. At pH < 3 Th^{4+} is the predominant species. At pH > 3, the Th(IV) speciation is dominated by the hydrolyzed species $Th(OH)^{3+}$, $Th(OH)_2^{2+}$, $Th(OH)_3^{+}$, and $Th(OH)_4$ in this order with increasing pH value. In the presence of CO_2, at pH > 8.0, negatively charged thorium carbonate complexes are the dominant species in form of $Th(OH)_2(CO_3)_2^{2-}$ and $Th(OH)(CO_3)_4^{5-}$.

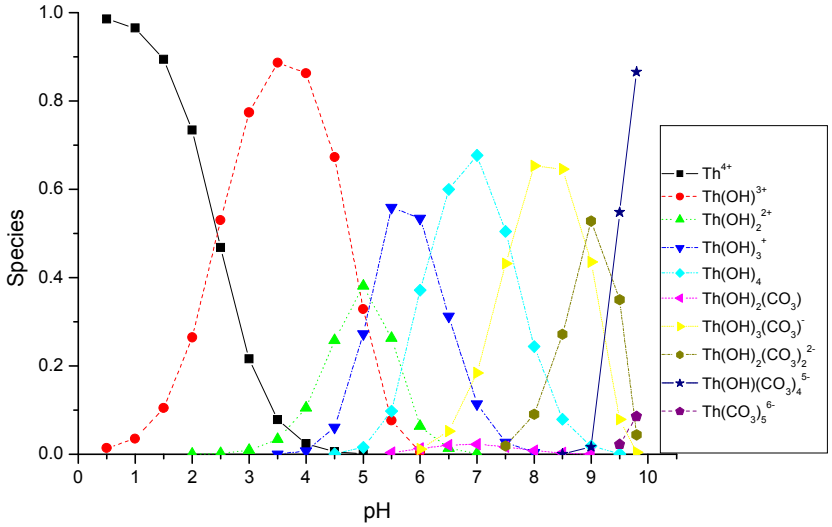

Figure 66: Species distribution of Th(IV) in aqueous solution; [Th(IV)] = 1.0E-09M, ionic strength 0.1 M ($NaClO_4$), at room temperature, and CO_2 in equilibrium with atmosphere.

4.4.2.1 Effect of contact time on the sorption of Th(IV) onto kaolinite

Kinetic experiments have been conducted to evaluate the time required for the sorption equilibrium. At contact times of 48, 72, 120 h, no significant time dependence was observed. Therefore, 72 h contact time has been used for the thorium sorption experiments.

4.4.2.2 Effect of pH on the sorption of Th(IV) onto kaolinite

The sorption of tetravalent thorium onto kaolinite was investigated as a function of pH and is shown in Figure 67. A pH range of 0 - 11 was studied with Th(IV) concentrations of 6.13×10^{-13} M and a solid phase concentration of 4 g/L with ionic strength I = 0.1 M ($NaClO_4$). The sorption of Th(IV) in contact with kaolinite is strongly influenced by the pH. The sorption edge can be observed at pH ≈ 1 (Figure 67). This can be explained by the formation of strong thorium/surface site complexes. The sorption increases with increasing pH up to 85

% at pH 2.5 and 95 % at pH 7. The sorption of Th(IV) onto kaolinite in the presence and absence of CO_2 has also been investigated. No significant difference was found (Figure 68).

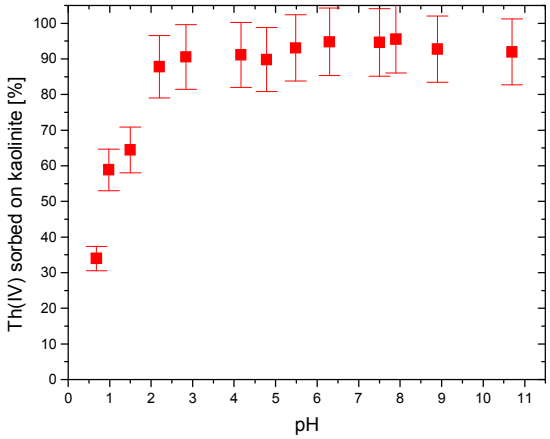

Figure 67: Sorption of Th(IV) onto kaolinite as a function of pH; [Th(IV)] = 6.13E-13 M , $pCO_2 = 10^{-3.5}$ atm, [KGa-1b] = 4 g/L, contact time = 72 h, measured by γ-spectroscopy.

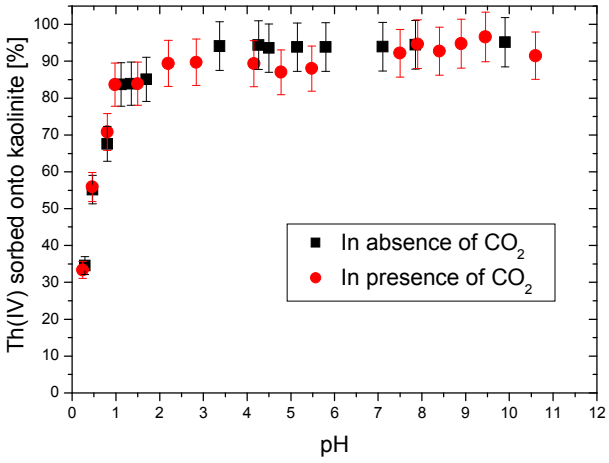

Figure 68: Sorption of Th(IV) onto kaolinite as a function of pH in the presence and absence of CO_2 ; [Th(IV)] = 6.6E-13M, ionic strength 0.1 M ($NaClO_4$), room temperature, measured by liquid scintillation counting (LSC).

As can be seen from the captions of Figure 67-68, two different detection methods (LSC and γ-spectroscopy) have been applied to determine the activity of ^{234}Th in the solution. The

measuring time for LSC was shorter than for γ-spectroscopy. The measured data shows consistence between the two techniques except for the lowest pH values (Figure 69).

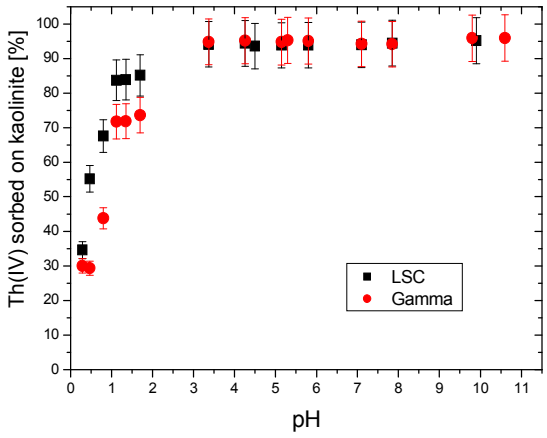

Figure 69: Comparison of two detection methods (LSC and γ-spectroscopy) for Th(IV) for the sorption of Th(IV) onto kaolinite as a function of pH and in the presence of CO_2; [Th(IV)] = 6.13E-13M, ionic strength 0.1 M ($NaClO_4$), room temperature.

4.4.2.3 Comparison of the sorption behavior of Pu(IV) and Th(IV)

For the two tetravalent actinides Th(IV) and Pu(IV), a similar sorption behavior was found as a function of pH (Figure 70). The sorption edges of Pu(IV) and Th(IV) for kaolinite are both at pH ≈ 1.

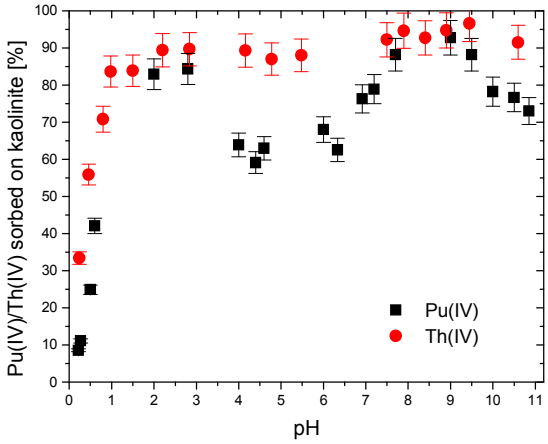

Figure 70: Comparison of the sorption of tetravalent actinides (Pu, Th) onto kaolinite as a function of pH; pCO2 = $10^{-3.5}$ atm, [KGa-1b] = 4 g/L, contact time = 120 h.

It is supposed that at pH > 8.5 tetravalent Pu carbonate species are responsible for the decrease in sorption where as no significant decreases found for Th(IV). At intermediate pH ranges (4 - 6), approx. 55 % - 65 % of the plutonium has been sorbed onto the kaolinite, whereas in the case of thorium, 80 - 90 % has been sorbed. As discussed earlier, at pH 4 - 6, the lower sorption for Pu(IV) may occur as a result of the (partial) oxidation of Pu(IV) in the liquid phase to Pu(V). Pu(V) exhibits a lower sorption than Pu(IV). Thorium exists in aqueous solution only as Th(IV) and hence no decrease in the sorption at pH 4-6 should occur. Thus, the Th(IV) data correlate the above interpretation.

4.4.3 Comparison of the sorption behavior of Pu(IV), Th(IV), Am(III), Pu(III), and other actinides

The effect of pH on the sorption of tri- and tetravalent actinides (Pu(III), Am(III) and Pu(IV), Th(IV)) onto kaolinite has been investigated. The study of the trivalent actinides Pu(III) and Am(III) was performed by Buda [Buda 2006]. As can be seen from Figure 71, a sorption edge at pH 5.2 was found for both trivalent actinides (Am, Pu). No significant effect was found in the presence of carbonate species in the solution, i.e., a decrease of the sorption of trivalent actinides onto kaolinite at pH > 8 was not observed.

In comparison to the sorption of trivalent actinides onto kalonite, a strong sorption of tetravalent actinides onto kaolinite at lower pH values was found due to their strong tendency to hydrolyze [Knop 99].

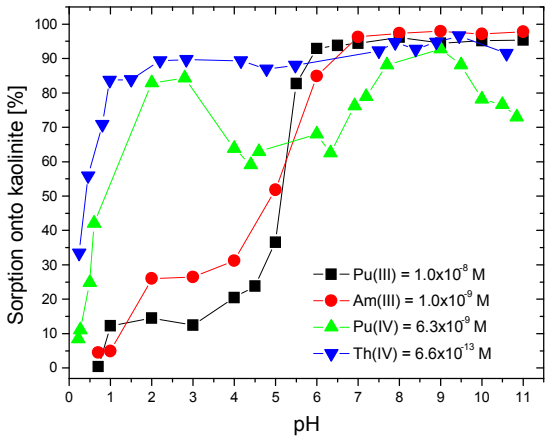

Figure 71: Sorption of trivalent (Pu, Am) and tetravalent (Pu, Th) actinides onto kaolinite as a function of pH; pCO2 = $10^{-3.5}$ atm, [KGa-1b] = 4 g/L, contact time = 120 h (Pu(III) and Am(III) data have taken from R. Buda [Buda 2006].

The sorption behavior of the relevant actinides in the environment is shown in Figure 72. Krepelova et al. [Krep 2006] reported the sorption behavior of U(VI) onto kaolinite as a function of concentration, pH, ionic strength, and CO_2. The investigation on the sorption of actinides onto kaolinite and other mineral surfaces shows that the sorption depends on the type of the metal ions (their oxidation state), pH, ionic strength I, temperature T, aerobic or anaerobic conditions, and the various mineral surface [Zava 2005, Yama 2004, Atun 2003, Reil 2005]. Sorption studies of plutonium and other tetravalent actinides onto mineral surfaces [Reil 2002, Sanc 85], e.g., goethite [Sanc 85], calcite [Zava 2005], or other soils [Tana 2002], were carried out. The sorption of tri-, tetra-, and pentavalent actinides (Am, Th, Np) on silica was also investigated [Righ 91].

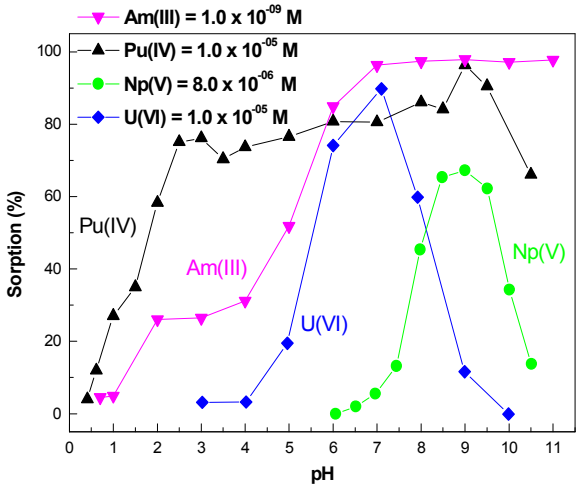

Figure 72: Comparison of the sorption of tri-, tetra, penta, hexavalent (Am, Pu, Np, U) actinides onto kaolinite as a function of pH; $pCO_2 = 10^{-3.5}$ atm, [KGa-1b] = 4 g/L, contact time = 120 h (Am from Buda and U, Np data from Amayri et al.) [Buda 2006, Amay 2006].

From Figure 72, the following sorption edges can be evaluated: at pH ≈ 1 for Pu(IV), pH ≈ 5.2 for Am(III), pH ≈ 6 for U(VI), and pH ≈ 8.0 for Np(V). These sorption edges can be shifted for different minerals due to their varying point of zero charge (PZC). The sorption of Am(III), Th(IV), Np(V) onto alumina is presented in Figure 73 [Bido 89].

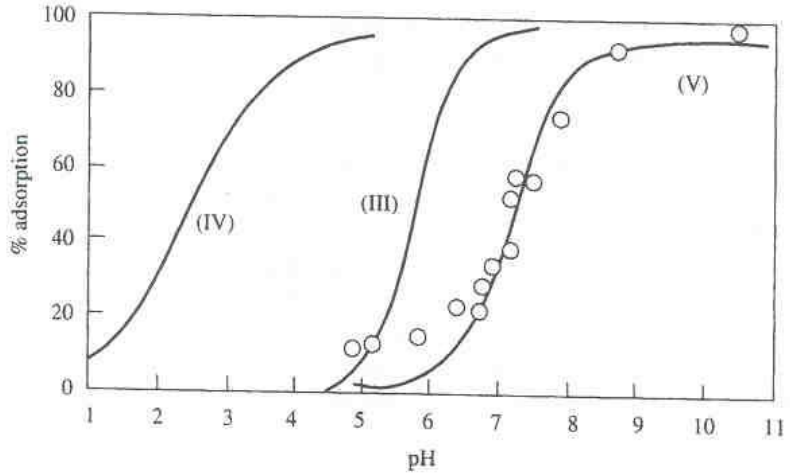

Figure 73: Sorption of actinide ions of different oxidation states onto alumina. The solid lines refer to the amount of sorption of Am(III), Th(IV), Np(V) onto alumina [Bido 89].

4.4.4 XAFS study of the sorption of plutonium onto kaolinite

XAFS spectroscopy is an important tool for the speciation of metal ions in solids and solution. XAFS provides information on the oxidation states, local structure and coordination number of the metal ions. XAFS structural parameters for Pu(IV) colloids and hydrolysis products have been reported in the literature [Roth 2004, Conr 2004]. K. Schmeide et al. [Schm 2005] studied the complexation of Np(IV) with humic substances at acidic pH by XAFS. So far, the interaction of plutonium with clay minerals like kaolinite by XAFS has not yet been studied.

Pu L_{III}-edge XAFS measurements have been performed to study the speciation of plutonium(IV) onto kaolinite as a function of pH. For the XAFS measurements at the INE beamline at ANKA, three ^{244}Pu(IV) samples were prepared as wet pastes with 1.0×10^{-5} M total Pu(IV) concentration, 4 g/L kaolnite in 0.1 M $NaClO_4$. These samples were prepared at pH 1, 4, and 9 in an air-equilibrated system (Table 38).

Table 38: Pu(IV) samples used for XAFS measurements

Sample name	pH	Sample description
A	1.0	94 ppm Pu(IV) , air
B	4.0	370 ppm Pu(IV), air
C	9.0	412 ppm Pu(IV), air

In the XANES spectrum the L_{III} absorption edge of plutonium occurs at about 18050 eV. It arises from allowed optical transitions between the $2p_{3/2}$ core state to the unoccupied $6d_{3/2}$ states and/or to the continuum. The Pu L_{III}-edge XANES spectra indicated that Pu in all samples is sorbed on the kaolinite surface in form of Pu(IV). Figure 74 shows the Pu L_{III}-edge XANES spectra of the Pu(IV) samples at different pH values.

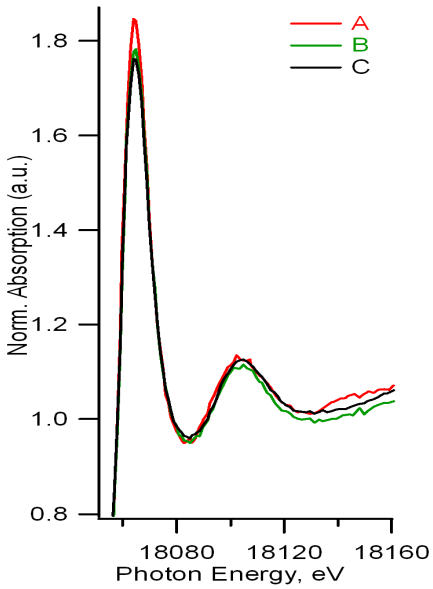

Figure 74: The Pu L_{III} edge X-ray Absorption Near Edge Structure (XANES) of Pu(IV) at different pH 1, 4, 9 (A = pH 1, B = pH 4, C = pH 9).

The Pu L_{III}-edge k^3-weighted EXAFS spectra are dominated by a low-frequency oscillation from eight oxygen atoms coordinated to Pu(IV) at an average distance of 2.3 Å. Table 39 shows the distance of plutonium neighbor atoms in the EXAFS measurements. A Pu-Pu interaction at ~3.7 Å with two Pu atoms is observed in all spectra indicating the formation of polynuclear Pu(IV) species at the surface. The Pu L_{III}-edge k^3-weighted EXAFS spectra and the corresponding Fourier transforms (FT) of Pu(IV) sample are shown in Figure 75.

Table 39: Distance to plutonium neighbor atoms in the EXAFS data

Pu(IV) sample name	**8 x O_1 [Å]**	**2 x Al/Si [Å]**	**2 x Pu [Å]**
A (pH = 1)	2.34	3.66	3.70
B (pH = 4)	2.28	3.62	3.69
C (pH =9)	2.27	3.62	3.68

In addition to Pu-O and Pu-Pu coordination shells, a third shell at an intermediate distance had to be included in all fits. The best fit to the data of the samples was obtained with a Pu-Al/Si coordination shell at 3.62 – 3.66 Å. This result can be explained by an inner-sphere sorption of polynuclear Pu(IV) species formed in solution to the kaolinite surface. Similar Pu-O distances were observed in Pu(IV) colloids [Conr 98].

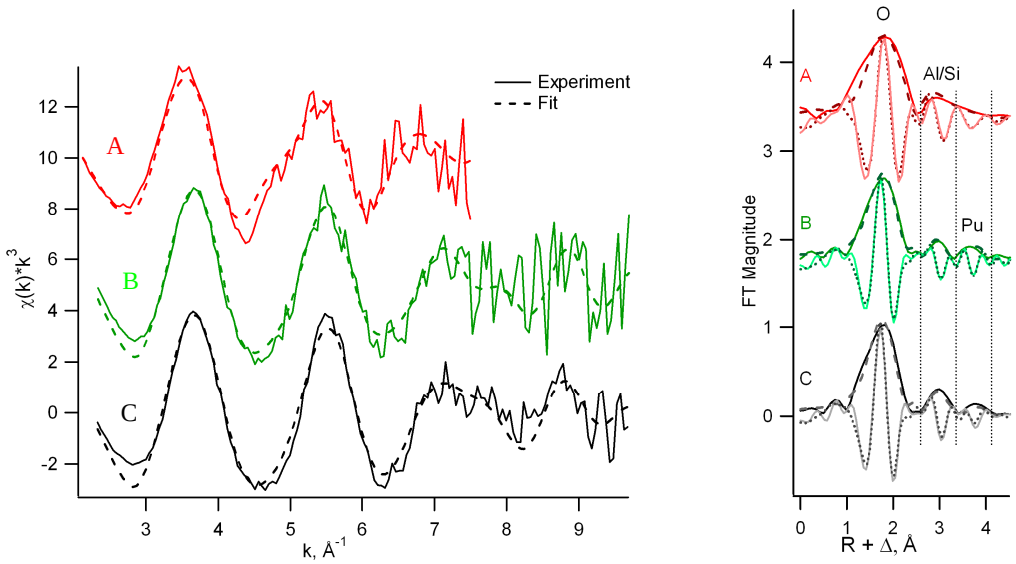

Figure 75: Plutonium L_{III} edge k^3-weighted EXAFS spectra (left) and corresponding Fourier Transforms (right) taken over k = 2.5-9.5 A^{-1} of (100-300) ppm Pu(IV) sorbed onto kaolinite at pH 1 (Sample A), pH 4 (Sample B), pH 9 (Sample C) , Experimental data: solid line, Fitted data: dotted line.

4.5 Sorption of Humic Substances onto Kaolinite

HA forms a precipitate at pH below 3 whereas FA is not precipitated over the whole pH range. For sorption experiments, Aldrich HA with concentrations 20-150 mg/L at pH 3.0, 5.0, 12 and Gorleben FA with concentrations 10-150 mg/L at pH 1.0, 5.0, and 8.0 have been used. The experimental parameters and conditions for the sorption experiments of humic and fulvic acid onto kaolinite are summarized in Table 40.

Table 40: Experimental parameters and operating conditions for the sorption of humic substances (HA, FA) onto kaolinite

Parameter	Conditions
Kaolinite, [KGa-1b]	4 g/L
[HA, FA]	10-150 mg/L
Ionic strength	0.1 M ($NaClO_4$)
pH	1-9
Preconditioning time	48 h
Contact time of kaolinite with HS	3, 5 days
pCO_2	$10^{-3.5}$ atm
Phase separation (centrifugation)	1 h (~ 2500 rpm)
Detection	UV-Vis spectroscopy (at 320 nm)

Sorption of Aldrich humic acid onto kaolinite

First, kinetic experiments have been performed to evaluate the time required for humic acid sorption equilibrium. The percentage of humic acid sorption onto kaolinite was determined as a function of time (20 h and 120 h) at pH 5 with varying concentrations of humic acid (20-100 mg/L). From Figure 76, it becomes evident that the sorption equilibrium is reached quite fast, i.e., no strong effect of the contact time on the sorption equilibrium was found.

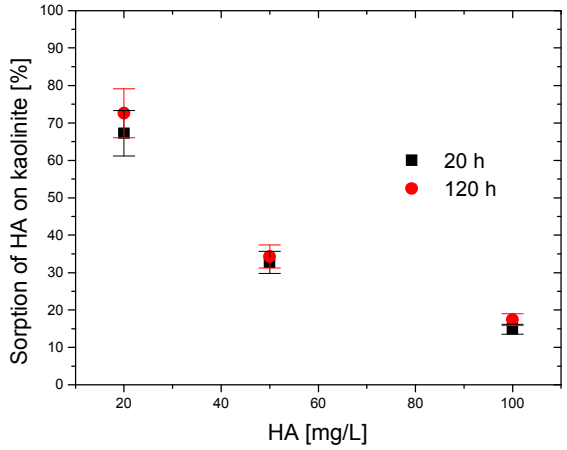

Figure 76: Sorption of Aldrich humic acid (HA) onto kaolinite as a function of humic acid (HA) concentrations for different contact times (20 h, 120 h) at pH 5.0; [KGa-1b] = 4 g/L, ionic strength 0.1 M $NaClO_4$.

In Figure 77 the sorption of HA onto kaolinite as a function of pH at initial HA concentrations of 20, 50, and 100 mg/L is presented. HA is strongly sorbed onto the kaolinite surface at low

pH values. At 20 mg/L HA about 90 % are sorbed onto kaolinite. The sorption of HA decreases with increasing pH value and with the initial concentration of HA. These results are in a good agreement with literature data [Sama 2000, Krep 2006, Taka 99, Niit 97].

The decrease of the HA sorption with increasing HA concentration is due to a saturation of the kaolinite binding sites, the decrease in sorption with increasing pH is regarded as a result of the electrostatic repulsion between the functional groups of HA and the binding sites of kaolinite [Krep 2006].

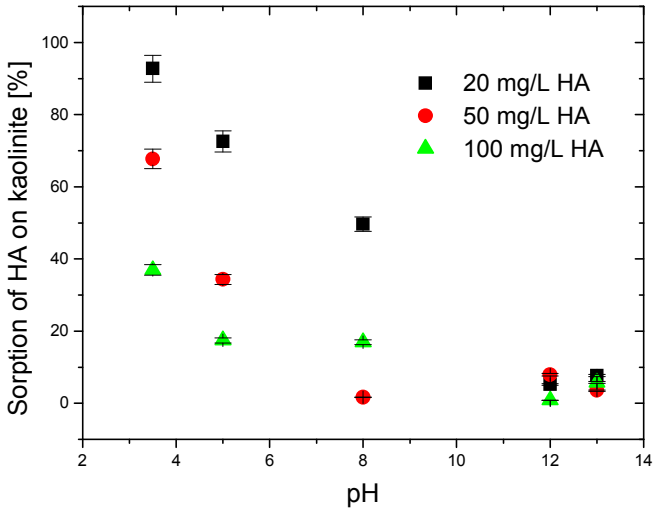

Figure 77: Sorption of Aldrich humic acid (HA) onto kaolinite as a function of pH for different humic acid (HA) concentrations; [KGa-1b] = 4 g/L, contact time = 120 h and ionic strength 0.1 M $NaClO_4$.

Carboxylic groups of HA are deprotonated at pH > 3 and give a negative charge of the HA. Kaolinite is expected to feature a negative surface charge for pH = 6 because of its point of zero charge. In the literature, the point of zero charge (PZC) and point of zero net charge (PZNCP) of kaolinite are reported to be 6.0 [Redd 98], 5.1 [Suth 99] and 4.9 [Schr 97], respectively.

The sorption mechanism of HA onto a mineral surface is not yet fully understood. There are two sorption mechanisms discussed in the literature: ligand exchange and or surface complexation reactions between the hydrolyzed groups of kaolinite and the anionic groups of HA. Murphy et al. [Murp 92] proposed that the HA ligand exchange sorption reaction can be explained by 1) protonation of surface hydrolyzed groups, 2) outer sphere complexation of the carboxylate groups and protonated hydroxyl groups, and 3) formation of an inner sphere

complex by its ligand exchange. The possible reaction mechanisms can be written as follows [Krep 2006]:

$$-SOH + H^+ \leftrightarrow SOH_2^+ \quad \text{(protonation)} \qquad (37)$$

$$SOH_2^+ + HACOO^- \leftrightarrow SOH_2^+ - {}^-OOCHA \quad \text{(outer sphere complex)} \qquad (38)$$

$$SOH_2^+ - {}^-OOCHA \leftrightarrow SOOCHA + H_2O \quad \text{(inner sphere complex)} \qquad (39)$$

Niitshu et al. [Niit 97] suggested that the interaction of colloidal HA species with mineral surface could be explained by the DLVO (Derjaguin-Landau-Verwey-Overbeek) theory for colloids in consideration of van der Waals interaction and electrical double layer repulsion. They proposed the following reaction between HA and mineral surfaces:

$$-x(-SOH_2^+) - yA^- = -(SOH_2A)_x A^{x-y}{}_{y-x} \qquad (40)$$

At pH 3, about 90 % of HA has been sorbed onto the kaolinite for a HA concentration of 20 mg/L, whereas only 8 % of the HA has been sorbed at a higher concentration of 150 mg/L.

Recent Krepelova et al. [Krep 2006] investigated the sorption of synthetic HA (M 42) onto kaolinite as a function of pH at varying HA concentrations and ionic strengths and found that the sorption decreases with increasing pH and concentration of the synthetic HA (Figure 78). Compared to Aldrich, the synthetic HA has more phenolic OH groups. It has also been concluded that the sorption of HA is dependent on the ionic strength of the solution due to a changing conformation of HA.

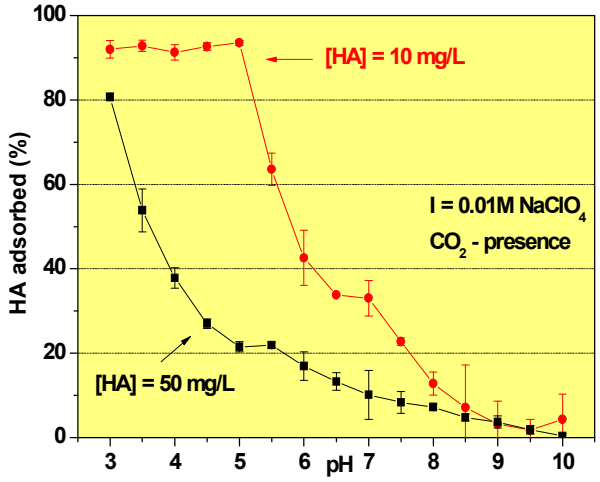

Figure 78: Sorption of synthetic humic acid (M 42) onto kaolinite as a function of pH for different synthetic humic acid (M 42- HA) concentrations; [KGa-1b] = 4 g/L and ionic strength 0.01 M $NaClO_4$ [Krep 2006].

An increase of HA sorption onto kaolnite with increasing ionic strength has also been reported in the literature. The data of Samadfam et al. [Sama 2000] for the sorption of Aldrich HA onto kaolinite as a function of pH are shown in a Figure 79.

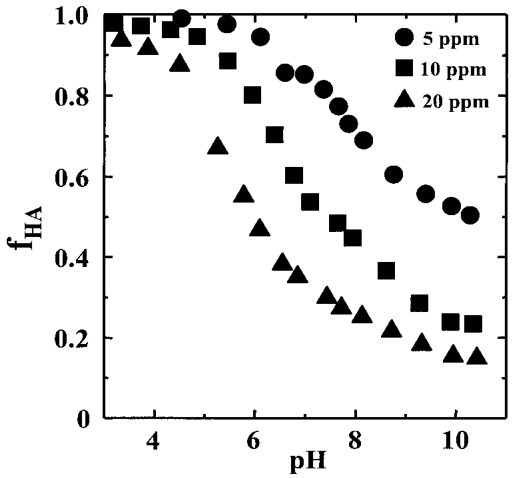

Figure 79: Sorption of Aldrich humic acid (HA) onto kaolinite as a function of pH and Aldrich humic acid (HA) concentration = 5, 10, 20 ppm; [KGa-1b] = 10 g/L and ionic strength 0.1 M $NaClO_4$ [Sama 2000].

Sorption of Gorleben fulvic acid onto kaolinite

The time dependence of Gorleben fulvic acid (FA) sorption was investigated with contact times between 20 h and 120. The experimental parameters and conditions are summarized in Table 40. Figure 80 shows the time dependence of FA sorption onto kaolinite as a function of pH. Only a little difference for the sorption in dependence of the contact time (20 h and 120 h) is observed. For the sorption experiments of FA onto kaolinite, 120 h contact time was chosen.

The sorption of Gorleben fulvic acid on kaolinite was determined by UV-Vis spectroscopy. Figure 81 shows the percentage of sorption as a function of pH with fulvic acid concentrations of 10, 20, 50, and 150 mg/L. The sorption of FA decreases with increasing pH values for all FA concentrations. The sorption depends strongly on the concentration ratio of fulvic acid and kaolinite. A similar sorption behavior was already found for humic acid.

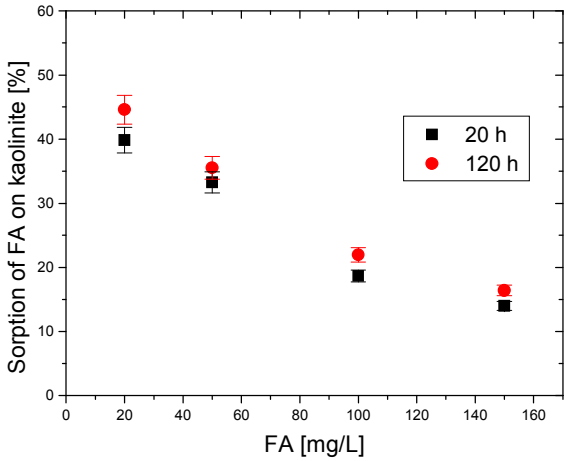

Figure 80: Sorption of Gorleben fulvic acid (GoHy-573) onto kaolinite as a function of fulvic acid (FA) concentrations for different contact times (20 h, 120 h) at pH 1.0; [KGa-1b] = 4 g/L, ionic strength 0.1 M $NaClO_4$.

At pH 1, about 50 % of FA are sorbed onto kaolinite at a FA concentration of 10 mg/L, whereas only 15 % of the FA are sorbed at a concentration of 150 mg/L. Sorption of FA decreases with increasing pH values similarly for all FA concentration

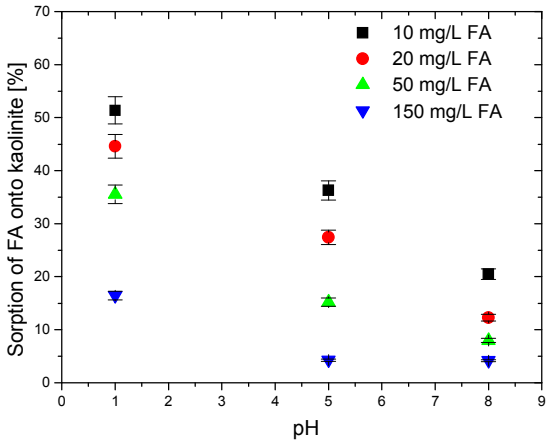

Figure 81: Sorption of Gorleben fulvic acid (GoHy-573) onto kaolinite as a function of pH for different fulvic acid (FA) concentrations; [KGa-1b] = 4 g/L, contact time = 120 h and ionic strength 0.1 M $NaClO_4$.

The decreased sorption of FA with increasing pH might be explained by the repulsion between the negatively charged kaolinite surface and the negatively charged fulvic acid

molecules. The point of zero charge of kaolinite is reported to be at pH ≈ 4 - 5. Thus, the surface charge of kaolinite at pH > 5 is negative. The negative charge density of kaolinite increases with increasing pH. Furthermore, at higher pH values, the dissociation of functional groups of FA is greater, which results in an increase in the negative charge density of the fulvic acid. The electrostatic interaction between both negatively charged surfaces repells the FA from the kaolinite surface and thus leads to a decrease in the sorbed fraction of FA at higher pH. Figure 82 displays the percentage sorption of HA/FA onto kaolinite at pH 5 for the concentrations 20, 50, and 100 mg/L.

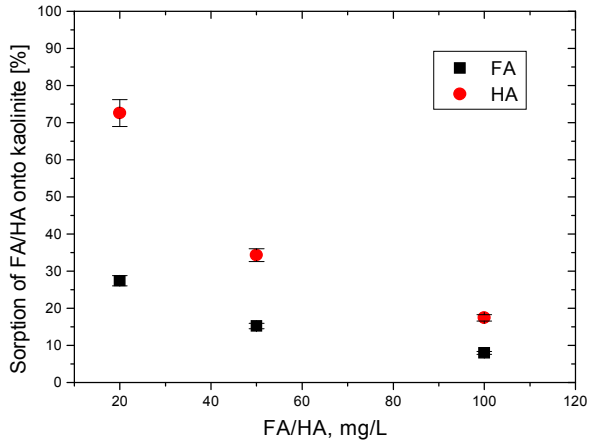

Figure 82: Sorption of Aldrich humic acid (HA) and Gorleben fulvic acid (FA) onto kaolinite as a function of FA/HA concentration; [KGa-1b] = 4 g/L, contact time = 120 h, pH = 5 and ionic strength 0.1 M $NaClO_4$.

The sorption of fulvic acid onto kaolinite is lower in comparison to humic acid. That might be explained by the lower molecular size of FA compared to HA and its less hydrophobic character.

4.6 Sorption of Tetravalent Plutonium and Thorium onto Kaolinite in the Presence of Humic Substances

The influence of humic substances on the sorption of Pu(IV) and Th(IV) onto kaoilnite was investigated. Here Th(IV) is considered as an oxidation analogue of tetravalent actinides (U, Np, Pu) and the results should be compared with data obtained for Pu(IV).

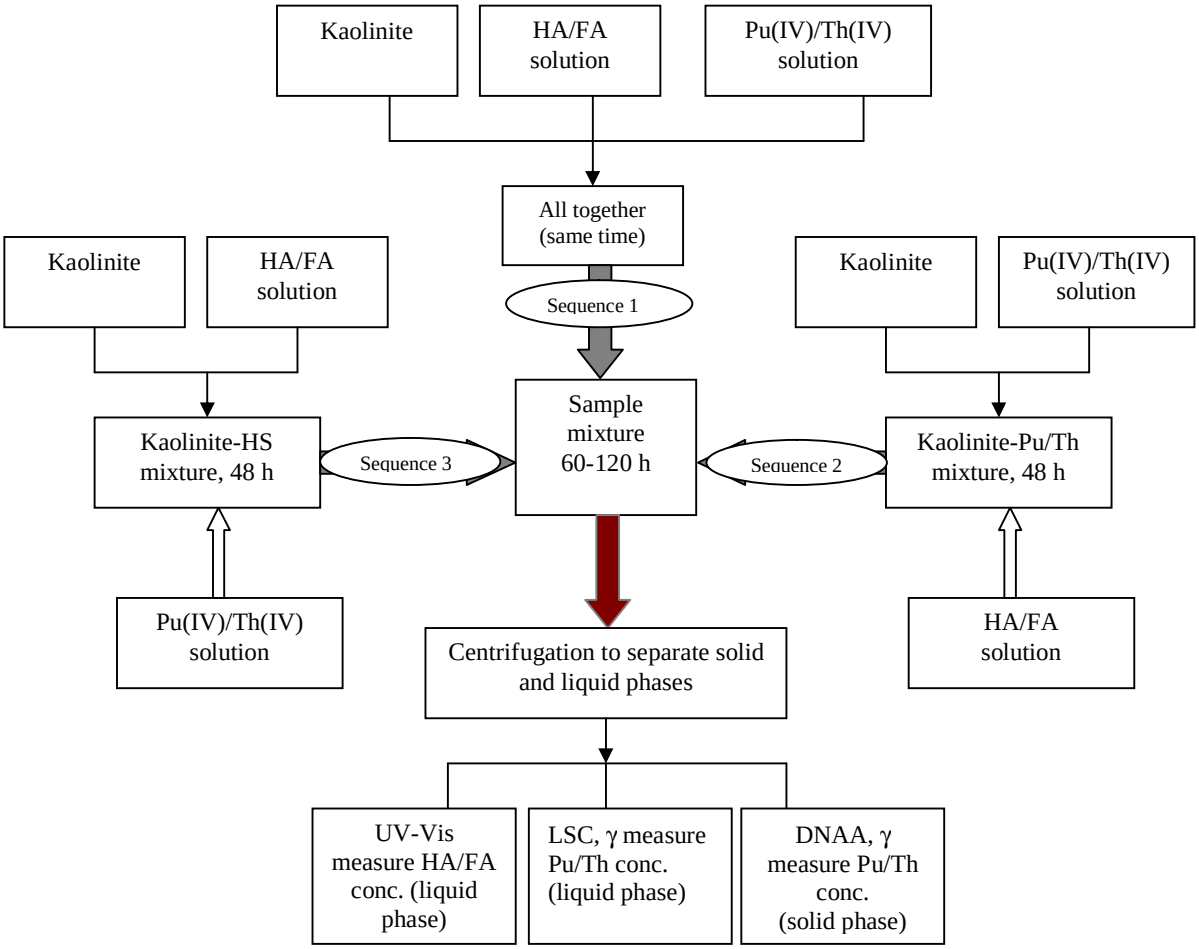

Figure 83: Scheme for the sorption experiments: Sequence 1 (all reactants are mixed together at the same time; (Pu(IV)/Th(IV), HS, kaolinite), sequence 2 mixing of reactants (Pu(IV)/Th(IV and kaolinite first, then added HS), sequence 3 mixing of reactants (HS and kaolinite, then added Pu(IV)/Th(IV)).

The ternary experiments were performed by three sequences described in Figure 83. The reason for performing three different adding sequences of the reactants (Th/Pu, HS, kaolinite) was to understand the influence of adding the components in the system (kaolinite-HS-Pu(IV)/Th(IV)). There are four possibilities with the three reactants. In this work only three

possibilities have been investigated (Figure 83). Sequence 1 where all of reactants are mixed at the same time; in sequence 2, a pre-equilibrium of metal ion and kaolinite was achieved and then the HS solution was added; and in sequence 3, a pre-equilibrium of kaolinite and HS was achieved; then the metal ion (Th(IV), Pu(IV)) solution was added.

4.6.1 Sorption of Pu(IV) onto kaolinite in presence and absence of fulvic acid

Influence of contact time

Figure 84 shows the results of the kinetic experiments for the ternary systems (Pu(IV), FA, kaolinite). They indicate that the systems reach a sorption equilibrium within a few hours after addition of Pu(IV) and FA to the pre-equilibrated kaolinite suspension. Comparing the different adding sequences of the reactants, no significant difference in the Pu(IV) sorption behavior was found.

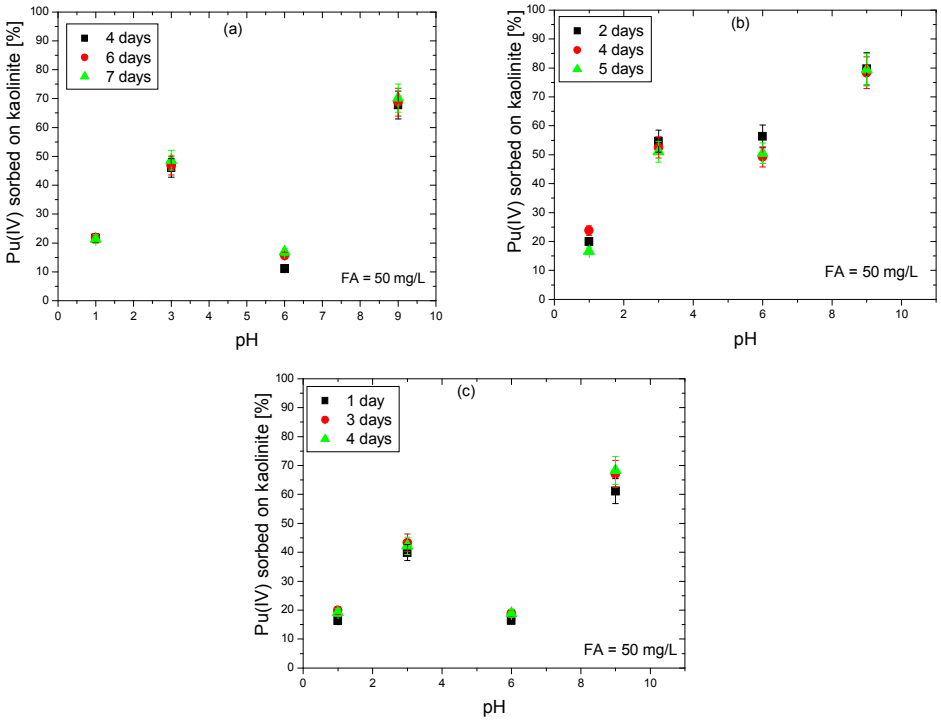

Figure 84: Sorption of Pu(IV) onto kaolinite in presence of FA (50 mg/L) as a function of pH at varying contact time (Pu(IV), FA, kaolinite); [Pu(IV)] = 7.1E-08 M, I= 0.1 M $NaClO_4$; a) adding sequence 1, b) adding sequence 2, c) adding sequence 3.

Reiler et al. [Reil 2005b] studied the influences of addition sequences and contact time on the Th(IV) retention on hematite in the presence of HA. Here, the Th(IV) retention was hindered when the HA and hematite were first equilibrated for 24 hours. When HA was added to the

Th(IV)-hematite system after a 24 h equilibration time , Th(IV) was barely desorbed from the hematite surface. In varying contact times between the reactants (Th, HA, hematite) of the ternary systems, a slight variation of Th(IV) sorption was found.

Influence of pH

The presence of FA influences significantly the sorption of Pu(IV) onto kaolinite. This was studied at the pH 1, 3, 6, and 9. Figure 85 describes the pH dependence of sorption onto kaolinite in varying adding sequences (1, 2, 3) at a FA concentration range of 10-100 mg/L. While the sorption behavior of Pu(IV) is comparable between pH 3 and 6 and the Pu(IV) sorption decreases at pH 1 in all adding sequences.

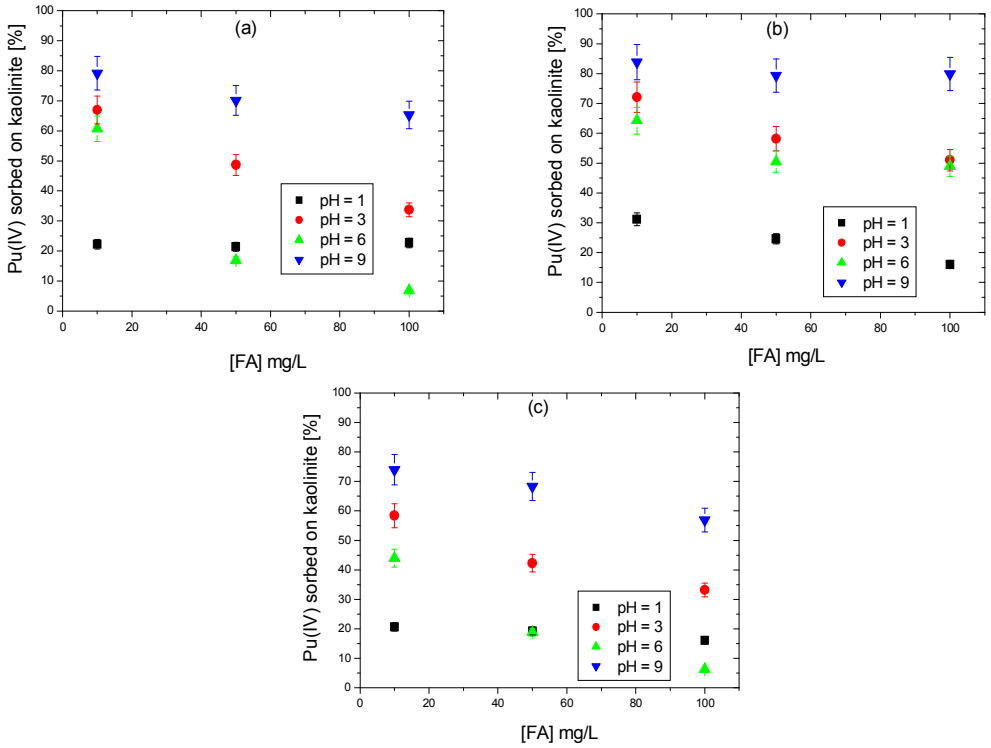

Figure 85: Sorption of Pu(IV) onto kaolinite as a function of FA concentration and pH; [Pu(IV)] = 7.1E-08 M, I= 0.1 M $NaClO_4$, contact time = 5 days; a) adding sequence 1, b) adding sequence 2, c) adding sequence 3.

At pH 9, the Pu(IV) sorption is increased; this might be due to competition reactions between the surface sites of kaolinite and FA solution [Reil 2002]. At pH values above neutral, Pu(IV) is in its tertahydroxo form (see Figure 61). Pu(IV) is complexed by kaolinite surface sites in its tertahydroxo form in this pH range ($\equiv SOPu(OH)_{n-1}^{4-n}$). A similar behavior has been found

for the sorption of Th(IV) onto hematite [Reiler 2002] and goethite [Hunt 88, Lafl 87] in the presence of HA..

Influence of FA concentration

Sorption experiments have been conducted at constant pH values (pH = 1, 3, 6, 9) and ionic strength (I = 0.1 M $NaClO_4$) as a function of FA concentration 10-100 mg/L.

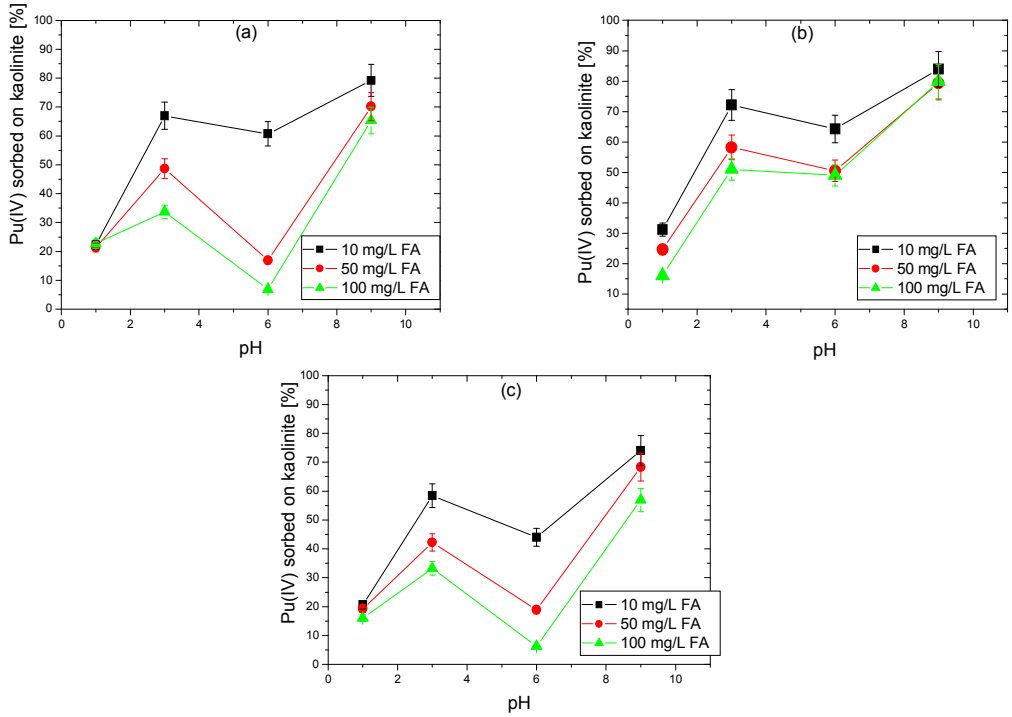

Figure 86: Pu(IV) sorption onto kaolinite as a function of pH and FA for the different adding sequences of the reactants (Pu(IV), FA, kaolinite); [Pu(IV)] = 7.1E-08 M, I= 0.1 M $NaClO_4$, contact time = 5 days; a) adding sequence 1, b) adding sequence 2, c) adding sequence 3.

Figure 86 represents the sorption of Pu(IV) for different pH values as a function of the FA concentration at varying adding sequences (1-3) of the reactants. In general, Pu sorption onto kaolinite decreases when FA concentration increases regardless of the pH and adding sequence of the reactants. This can be explained by the increased number of binding sites with increasing FA concentration in the solution.

Influence of the adding sequence

For the sorption of Pu(IV) onto kaolinite in the presence of FA a slight effect was observed on the adding sequences of the reactants (Pu(IV), kaolinite, FA) (Figure 87). The results obtained when Pu(IV) is pre-equilibrated with kaolinite before addition of FA (sequence 2) and when

Pu(IV) is added to the pre-equilibration of kaolinite and FA (sequence 3) are not so different. The Pu(IV) sorption is a little bit hindered when FA and kaolnite are equilibrated (sequence 3). The fact that a lower sorption of Pu(IV) was found could be explained by the interaction between fulvic acid and kaolinite surface sites, where less free sites are available to interact with plutonium metal ions.

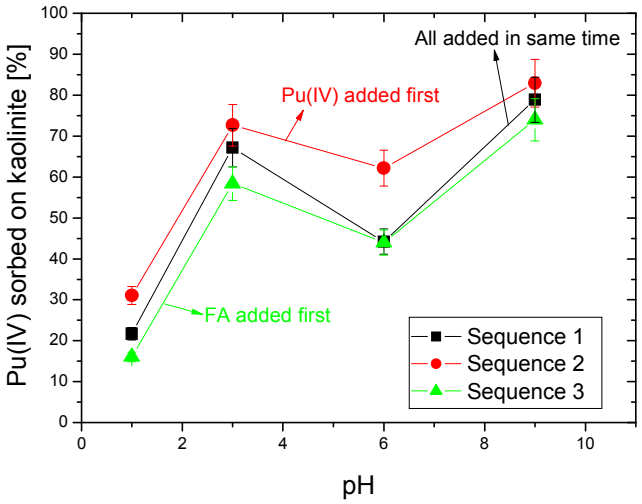

Figure 87: Pu(IV) sorption onto kaolinite as a function of pH and adding sequences of the reactants (Pu(IV), FA, kaolinite); [Pu(IV)] = 7.1E-08 M, I= 0.1 M $NaClO_4$, contact time = 5 days; [FA] = 10 mg/L.

Sorption of Pu(IV) onto kaolinite in presence and absence of FA

Figure 88 shows the effect of FA on the sorption of Pu(IV) onto kaolinite for a FA concentrations of 0, 10, 50, and 100 mg/L as a function of pH for varying adding sequences of the reactants. The sorption of Pu(IV) onto kaolinite is lower in the presence of FA compared to the free system of FA. This effect has been observed as a function of FA concentration (Figure 88) due to the competition reactions between kaolinite, sorbed fulvic acid sites, free fulvic acid, and plutonium ions.

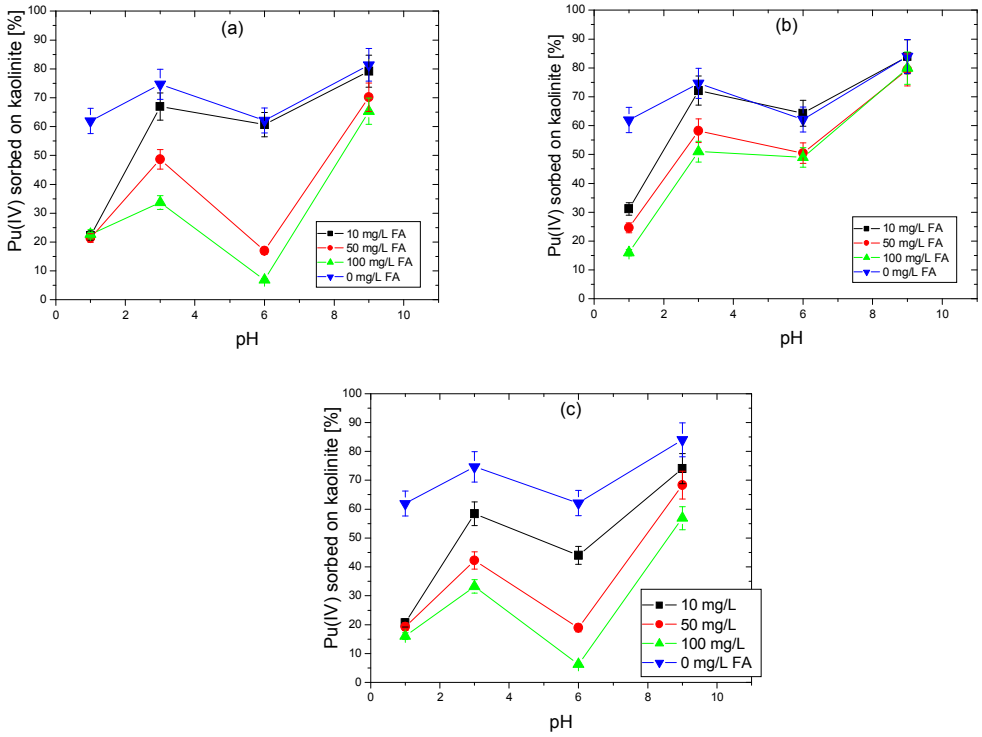

Figure 88: Influence of FA on the sorption of Pu(IV) onto kaolinite as a function of pH; [Pu(IV)] = 7.1E-08 M, I= 0.1 M $NaClO_4$, contact time = 5 days; a) adding sequence 1, b) adding sequence 2, c) adding sequence 3.

4.6.2 Sorption of Pu(IV) onto kaolinite in presence and absence of humic acid

In an earlier chapter, it was mentioned that HA precipitates at pH < 3, therefore, the experiments with HA in the ternary systems have been done at pH ≥ 3 to avoid an addition effect. It could be shown that the system Pu(IV), HA, kaolinite reaches sorption equilibrium within a few hours after addition of Pu(IV) and HA to the pre-equilibrated kaolinite suspension and no time dependence was found. Also no time dependence of Pu(IV) sorption in varying addition sequences of reactants was observed. Three days of equilibration time were chosen in the following experiments.

Sorption experiments were studied at constant pH (pH = 3, 6, 9) and ionic strength (I = 0.1 M $NaClO_4$) as a function of the HA concentration 10-100 mg/L. Figure 89 represents the sorption of Pu(IV) for different pH values as a function of HA concentration for two adding sequences (1-2) of the reactants. In a general manner, Pu sorption onto kaolinite decreases when HA concentration increases whatever the pH of the solution and adding sequence of the reactants are.

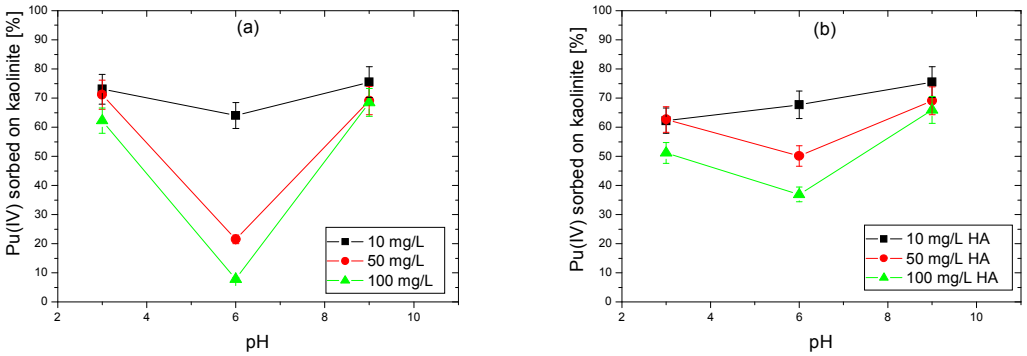

Figure 89: Pu(IV) sorption onto kaolinite as a function of pH and HA concentration (10, 50, 100 mg/L); [Pu(IV)] = 7.1E-08 M, I= 0.1 M $NaClO_4$, contact time = 3 days; a) adding sequence 1, b) adding sequence 2.

The effect of HA on the sorption of Pu(IV) onto kaolinite with varying HA concentration (0, 10, 50, and 100 mg/L) is presented in Figure 90. As expected, sorption of Pu(IV) onto kaolinite decreases with increasing HA concentration. A lower sorption of Pu(IV) was found in the presence of HA compared to the absence of HA in the system.

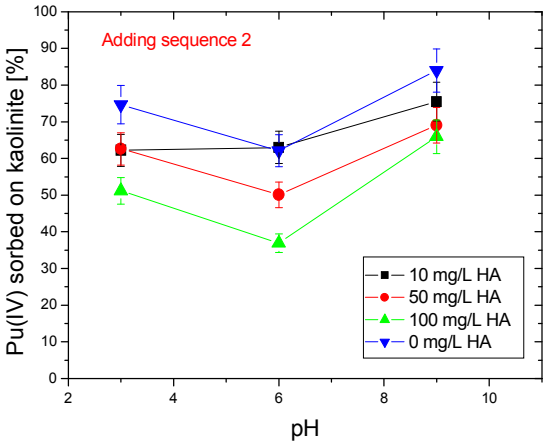

Figure 90: Influences of HA on the sorption of Pu(IV) onto kaolinite as a function of pH; [Pu(IV)] = 7.1E-08 M, I= 0.1 M $NaClO_4$, contact time = 3 days; adding sequence 2.

From Figure 90, one can see that in the presence of HA the sorption of Pu(IV) in all pH ranges is hindered compared to the system without HA due to the formation of dissolved plutonium humate complexes in the solution. A similar behavior was observed for the FA on the sorption of Pu(IV) in the ternary systems (chapter 4.6.1).

Sach et al. [Sach 2006] reported recently a slightly lower sorption of Np(V) (see Figure 91) and U(VI) [Krep 2006] onto kaolinite in the presence of HA compared to the HA- free system. Kautenburger et al. [Kaut 2006] showed a similar phenomenon for the sorption of Eu(III) and Gd(III) onto kaolinite in the presence of HA compared with the system without HA at alkaline pH range.

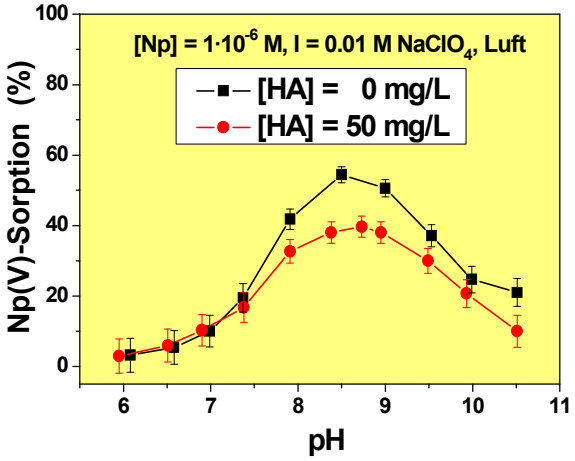

Figure 91: Influence of HA on the sorption of Np(V) onto kaolinite as a function of pH [Sach 2006].

Figure 92 shows the influences of FA and HA on the sorption of Pu(IV) onto kaolinite. A lower sorption of Pu(IV) has been observed in the presence of FA or HA compared to the absence of FA or HA. At acidic pH range, a significant lower sorption of Pu(IV) has been found in presence of FA in comparison to the presence of HA onto kaolinite. it might be explained by their different characteristic interactions between FA and HA with plutonium ion at acidic pH range. Murphy et al. [Murp 92] reported a slightly lower sorption of U(VI) onto hematite in the presence of HA compared to the HA-free system in the alkaline pH range. Payne et al. [Payn 96] observed a similar phenomenon for the sorption of U(VI) onto ferrihydrite and Schmeide et al. [Schm2004] reported a lower sorption of U(VI) onto Phyllite in the presence of HA.

Samadfam et al. observed a lower sorption of Am(III) and Cm(III) onto kaolinite in the presence of HA at pH above 5.5 [Sama 2000] and Niitshu et al. [Niit 97] also observed a similar behavior in the case of Np(V) sorption onto kaolinite in the presence of HA.

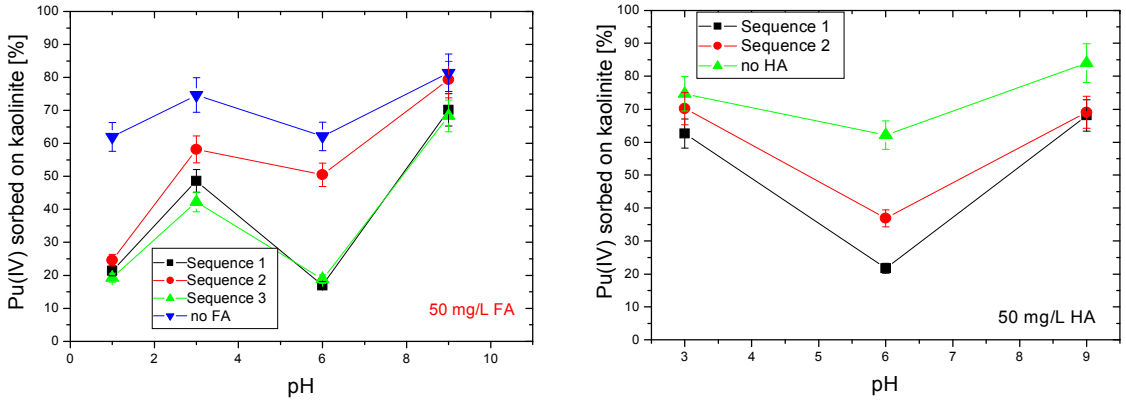

Figure 92: Influence of FA and HA on the sorption of Pu(IV) onto kaolinite as a function of pH; [Pu(IV)] = 7.1E-08 M, I= 0.1 M $NaClO_4$, contact time = 5 days.

4.6.3 Sorption of Th(IV) onto kaolinite in presence and absence of fulvic acid

The influence of fulvic acid (FA) on the sorption of Th(IV) onto kaolinite was also investigated. The effect of contact time, pH, concentration of FA, and adding sequences of the reactants on the sorption of Th(IV) onto kaolinite was studied.

The kinetics experiments were performed at different contact times (24 to 120 h). No significant time dependence was observed. It was found that the system reaches sorption equilibrium within a few hours after addition of Th(IV) and FA to the pre-equilibrated kaolinite suspension. Comparing the different modes of adding sequences of the reactants, no significant difference in the Th(IV) sorption behavior have been observed.

Influence of FA concentration

The Th(IV) sorption isotherm onto kaolinite in the presence of FA (10-100 mg/L) at pH 1, 3, 6, and 7 and with two different adding sequences is presented in Figure 93. The sorption of Th(IV) onto kaolinite decreases with increasing FA concentration. A similar behavior was also observed for the Th(IV) sorption onto hematite [Reil 2002] and Zr(IV) onto kaolinite [Taka 99]. In the presence of FA, a strong impact on the sorption in the slightly basic media occurs due to the formation of soluble organic thorium complexes. Figure 93 shows the experiments of adding sequences 1 where all the reactants were mixed at the same time. A similar effect of the FA concentration on the sorption of Th(IV) onto kaolinite for adding sequences 2 was observed.

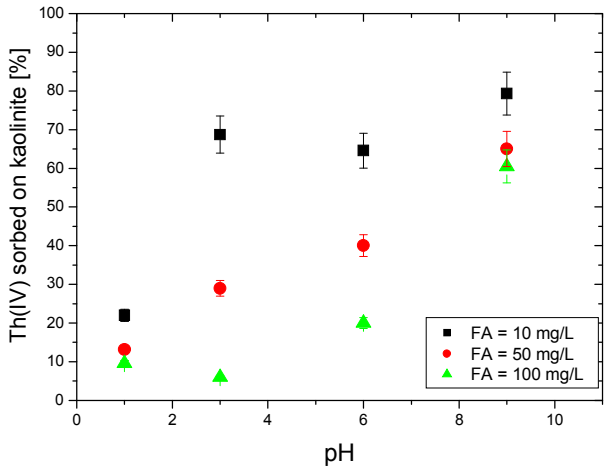

Figure 93: Th(IV) sorption onto kaolinite as a function of pH and FA (10, 50, 100 mg/L); [Th(IV)] = 5.6E-13 M, I= 0.1 M $NaClO_4$, contact time = 5 days, adding sequence 1.

Influence of adding sequence

The influence of the adding sequences in the system (kaolinite-fulvic acid-Th(IV)) was investigated in two sequences (sequence 1 and sequence 2) of the reactants (kaolinite, FA, Th(IV)) at pH 1-9 with ionic strength 0.1 M $NaClO_4$

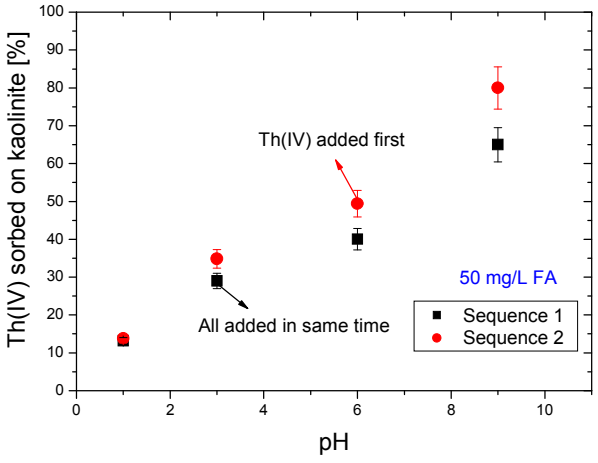

Figure 94: Th(IV) sorption onto kaolinite as a function of pH and the different adding sequences of reactants (Th(IV), FA, kaolinite); [Th(IV)] = 6.5E-13 M, I= 0.1 M $NaClO_4$, contact time = 3 days, [FA] = 50 mg/L.

Figure 94 shows a slight effect of different adding sequences on the sorption of Th(IV) onto kaolinite. Adding sequence 2 shows a slightly increased effect on the sorption compared to sequence 1 (where all of reactants are mixed at the same time).

Sorption of Th(IV) onto kaolinite in presence and absence of FA

Sorption of Th(IV) onto kaolinite was studied at pH range from 1 to 9 and a fulvic acid concentrations of 0 to 100 mg/L and an ionic strength of 0.1 M $NaClO_4$ (Figure 95).

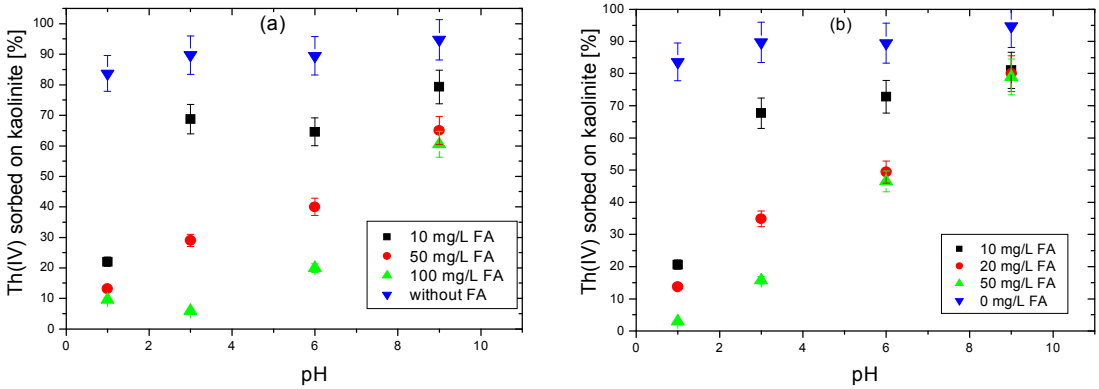

Figure 95: Influence of FA on the sorption of Th(IV) onto kaolinite as a function of pH; [Th(IV)] = 5.6E-13 M, I= 0.1 M $NaClO_4$, contact time = 5 days; a) adding sequence 1, b) adding sequence 2.

A slight difference of the sorption behavior was found for the varying adding sequences of the reactants in the ternary systems. In the absence of FA, the sorption of Th(IV) increases with increasing pH values but introducing of FA into the reaction mixture, the sorption of Th(IV) decreases with increasing FA concentration. The metal-fulvate complexes, whether in solution or on a mineral surface, might be the main factor leading to the decrease of the sorption of Th(IV) in the presence of FA.

5.0 Conclusions and Outlook

The knowledge of the physical and chemical processes responsible for the speciation of plutonium in a geogenic system enables to predict the migration of plutonium and thus advances the long term safety assessments of nuclear waste repositories or facilitates the development of new remediation strategies for contaminated sites. A dominant contribution to the radiotoxicity over storage times of up to one million years is delivered by plutonium; however, its migration behavior in the environment is not well understood at present. For the speciation of tetravalent plutonium in aqueous systems, its (I) redox reactions, (II) complexation, and (III) sorption behavior under environmental conditions have been studied in this work.

I) Redox Speciation of Plutonium

Ubiquitous humic substances (HS) play an essential role in the migration of plutonium due to their complexation and reducing abilities. The redox speciation of Pu(VI) in contact with Aldrich humic acid (HA) and Gorleben fulvic acid (FA) has been investigated by online coupling of capillary electrophoresis to inductively coupled plasma mass spectrometry (CE-ICP-MS) and UV-Vis spectroscopy. A reduction of Pu(VI) by Aldrich humic acid (HA) and Gorleben fulvic acid (FA) to Pu(IV) and Pu(III) occurs within a couple of days or weeks, a short time on the scale of nuclear waste disposal in a deep geological formation. Similar reduction behavior has been found for humic rich Gorleben ground water [Kuzc 2003]. The reduction of Pu(VI) with FA occurs faster with increasing pH compared to HA. The enhanced reduction of Pu(VI) with increasing pH can be explained by the increasing fraction of dissociated groups of the HS. The performed studies show that the reduction of Pu(VI) to Pu(V) is fast compared to the reduction of Pu(V) to Pu(IV) and Pu(III). In aqueous systems under environmental conditions, plutonium in contact with humic substances is present mainly in the tri- and tetravalent state.

A further investigation should be the redox behavior of U(VI) and Np(V) in contact with Aldrich humic acid and Gorleben fulvic acid taking into account varying parameters such as pH, Eh, ionic strength of the solution. The obtained redox kinetics results for U(VI) and Np(V) should be compared with the data already obtained for Pu(VI).

Since the speciation of plutonium oxidation states is necessary to understand the plutonium solution chemistry, a sensitive and reliable technique needs to be explored. Capillary

electrophoresis (CE) coupled online to ICP-MS has been developed as a method for the speciation of plutonium oxidation states. The detection limit is 20 ppb (10^{-6}-10^{-7} mol/L) for one oxidation state. To improve the sensitivity further, the coupling of CE to resonance ionization mass spectrometry (RIMS) has been developed. The offline CE-RIMS has been introduced as a new sensitive, speciation technique for the determination of plutonium oxidation states at the ultratrace level. The detection limit of CE-RIMS enables the concentration of plutonium to be decreased 2 to 3 orders of magnitude compared to CE-ICP-MS. The speciation of the oxidation states of plutonium at ultra trace levels of 10^{-9} to 10^{-10} mol/L appears to be possible.

(II) Complexation of Tetravalent Plutonium

The time dependence of the plutonium complexation with HA has been investigated and the complexation constants of Pu(IV) at various pH values were determined. Different concentrations of plutonium (6.6×10^{-6} to 6.6×10^{-8} M for Pu(IV) and HA (0.01 to 25 mg/l) have been used. The experiments show that a period of about one week is necessary to reach equilibrium for the complexation of Pu(IV) with HA. The complexation constants ($\log ß_{LC}$) were determined by means of ultrafiltration. For the loading capacity (LC) values of 3.3% at pH 1.8, 4.5% at pH 2.5, and 9.2% at pH 3 for Pu(IV) have been found. Using these LC data, $\log ß_{LC}$ values between 6.4 - 8.4 for Pu(IV) have been calculated. The scattering of the $\log ß_{LC}$ values for Pu(IV) might be influenced by the precipitation of humic acid at low pH and colloid formation of plutonium. Further experiments are necessary to test a new reliable method for the determination of $\log ß_{LC}$ values for Pu(IV). The CE-ICP-MS-DAD system can be used as a suitable method for the determination of $\log ß_{LC}$ values for Pu(IV). The complexation of tetravalent Np with HS will further be investigated by a spectroscopic method.

(III) Sorption of Tetravalent Plutonium in Aqueous Systems

The sorption of tetravalent plutonium onto kaolinite, a model clay mineral, has been investigated as a function of pH. The sorption studies have been performed by batch experiments under aerobic and anaerobic conditions, at pH values of 0 – 11, Pu(IV) concentrations of 3.6×10^{-7} – 6.9×10^{-9} M and a solid phase concentration of 4 g/L kaolinite were used. The sorption experiments have been conducted with different contact times (2 - 7 days), but no significant dependence on the contact time was observed. A sorption edge at pH ≈ 1 and a maximum of the sorption at pH ≈ 8 for Pu(IV) have been found. In the presence of

CO_2 at pH > 8.5, the sorption of plutonium is decreased due to the formation of soluble plutonium carbonato complexes.

To compare the sorption behavior of Pu(IV), the sorption of the redox stable Th(IV) onto kaolinite has been investigated. In the case of Pu(IV), for intermediate pH = 4 - 6, a decrease in the sorption can be observed. For Th(IV), no decrease in the sorption at pH values of 4 - 6 has been found. To investigate possible reasons for this minimum, the oxidation state of plutonium in solution (after sorption of Pu(IV) onto kaolinite) has been determined by liquid-liquid extraction and it has been found that Pu(V) is the dominant species in the solution at pH = 4. Thus, initially added Pu(IV) in contact with kaolinite at pH = 4 - 6 has been oxidized in solution partially to Pu(V), and the sorption of Pu(V) onto kaolinite is weaker than Pu(IV) for that pH value. The sorption behavior of tetravalent Pu and Th are comparable. Moreover, the speciation of the sorbed Pu(IV) (pH = 1, 4, 9) onto kaolinite has been studied by extended x-ray absorption and fluorescence spectroscopy (EXAFS). The results show that Pu(IV) is the sorbed species.

The sorption behavior of Aldrich humic acid (HA) and Gorleben fulvic acid (FA), onto kaolinite has also been investigated and the results are compared with literature data. The sorption of both HA and FA onto kaolinite decreases with increasing pH for all studied concentrations of HA and FA, which might be explained by electrostatic repulsion. More humic acid has been sorbed than fulvic acid.

Strong sorption of tetravalent plutonium in the aqueous systems has been found. Three different chemical processes (redox reactions, complexation, and sorption) of tetravalent plutonium in the aqueous system have been investigated. So far, the binary systems Pu(IV)-HS, Pu(IV)-kaolinite, and HS-kaolinite have been studied and the data have been compared with the data of the binary system of Th(IV)/kaolinite. Further detailed EXAFS studies will be needed to understand the molecular level information on the interaction of Pu(IV) with kaolinite.

The influence of humic substances on the sorption of tetravalent plutonium and thorium onto kaolinite have been investigated at varying experimental parameters as pH of the solution, HS concentration, contact time, and adding sequences of the reactants. HS has an effect on the sorption of tetravalent actinides onto kaolinite surface, even in the pH range of ground water ($pH \geq 6$). A decrease of tetravalent plutonium and thorium sorption onto kaolinite is observed due to the formation of humate complexes in the solution. The adding sequence of the

reactants in the ternary systems has only little influence on the sorption of Pu(IV)and Th(IV) onto kaolinite.

Further studies will be focused on the sorption of tetravalent plutonium and thorium in the presence of HS in the kaolinite system with varying parameters such as ionic strength of the solution, and concentration of metal ions. The EXAFS technique will also be applied to obtain molecular level information on the interaction of Pu(IV)/Th(IV) with HS and the kaolinite system

Finally, the obtained results of the binary and ternary systems (plutonium-kaolinite-humic substance) will be used to model the speciation of plutonium in the aquifer close to a radioactive waste repository.

6.0 Literature

[Aike 85] Aiken. G. R, McKnight. D. M, Wershaw. R. L, MacCarthy. P. M. (1985) Humic Substances in Soils, Sediments and Water, Willey, New York.

[Albi 2002] Albinsson. Y, Ekberg. C, Holgersson. S, Jakobsson. A.-M, Lendgren. A, Skarnemark. G. (2002) A Method for Preparation and Purification of ^{234}Th, Applied Radiation and Isotopes, **56**, 681-684.

[Alfa 2004] Alfasssi. Z. B. (2004) On the Precipitation of Salts/Complexes of Trivalent Cations with Humic Acid, Journal of Radioanalytical and Nuclear Chemistry, **262**, 77-81.

[Alfa 2002] Alfasssi. Z. B. (2002) On the Complex of Humic-Am^{3+}, Journal of Radioanalytical and Nuclear Chemistry, **251**, 307-309.

[Alla 82] Allard. B, Rydberg. J. (1982) Behavior of Plutonium in Natural Waters, Plutonium Chemistry, Plutonium Chemistry; Kansas City, Mo; U.S.A, pp. 275-295 .

[Altm 2005] Altmaier. M, Neck. V, Müller. R, Fanghänel. T. (2005) Solubility of $ThO_2.xH_2O$(am) in Carbonate Solution and the Formation of Ternary Th(IV) Hydroxide-Carbonate Complexes, Radiochimica Acta, **93**, 83-92.

[Amba 2005] Ambard. C, Delorme. A, Baglan. N, Aupiais. J, Pointurier. F, Madic. C. (2005) Interfacing Capillary Electrophoresis with Inductively Coupled Plasma Mass Spectrometry for Redox Speciation of Plutonium, Radiochimica Acta , **93**, 665-673.

[Amay 2006] Amayri. S. (2006) Workshop zum Forschungsvorhaben „ Migration von Actiniden im System Ton, Huminstoff, Aquifer“, 28.-29.03. Mainz, Germany

[Andr 2000] Andre. C, Choppin. G. R. (2000) Reduction of Pu(V) by Humic Acid, Radiochimica Acta, **88**, 613-616.

[Annu 98] Annunziata. M. F. (1998) Handbook of Radioactivity Analysis, Academic Press, UK.

[Arti 2000] Artinger. R, Marquardt. C. M, Kim. J. I, Seibert. A, Trautmann. N, Kratz. J. V. (2000) Humic Colloid-borne Np Migration: Influences of the Oxidation State, Radiochemica Acta, **88**, 609.

[Atun 2003] Atun. G, Bascetin. E. (2003) Adsorption of Barium on Kaolinite, Illite and Montmorillonite at Various Ionic Strengths, Radiochimica Acta, **91**, 223-228.

[Bajo 2003] Bajo. S, Eikenberg. J. (2003) Preparation of a Stable Tracer Solution of Plutonioum(IV), Radiochimica Acta, **91**, 495-497.

[Beck 2002a] Becker. J. S. (2002) State-of-the-art and Progress in Precise and Accurate Isotope Ratio Measurements by ICP-MS and LA-ICP-MS Plenary Lecture**,** Journal of Analytical Atomic Spectrometry, **17**, 1172.

[Beck 2002b] Becker. J. S. (2002) ICP-MS: Determination of Long-lived Radionuclide, Spectroscopy Europe, **14**/6.

[Beck 2004] Beckmerhagen. J. A. (2004) Recent Waste Management Related Developments in Germany, Journal of Nuclear Science and Technology, **41**, 393-398.

[Bert 81] Bertrand. P. A, Choppin. G. R. (1981) Separation of Actinides in Different by Solvent Extraction, Radiochimica Acta, **31**,135-137.

[Berz 1839] Berzelius. J. J. (1839) Lehrbuch der Chemie, Wöhler, Dresden and Leipzig.

[Bido 89] Bidoglio. et. al. (1989) Interaction and Transport of Plutonium-Humic Acid Participles in Groundwater Environments, Mat. Res. Soc. Symp. Proc. **127**, 823-830.

[Bite 2003] Bitea. C, Müller. R, Neck. V, Walther. C, Kim. J. I. (2003) Study of the Generation and Stability of Thorium(IV) Colloids by LIBD Combined with Ultrafiltration, Journal of Colloids and Surfaces A, **217**, 63-79.

[Bite 2002] Bitea. C, Kim. J. I, Kratz. J. V, Marquardt. C, V. Neck, Seibert. A, Walther. C, Yun. J. I. (2002) A Study of Colloid Generation and Disproportionation of Pu(IV) in Aquatic Solutions by LIBD and LPAS, Institute für Kernchemie, Universität Mainz, Mainz, Germany, Annual Report, C4.

[Bond 76] Bondietti. E. A, Reynolds. S. A, Shanks. M. H. (1976) Interaction of Pu with Complexing Substances in Soils and Natural Waters, In Transuranium Nuclides in the Environment, IAEA, Vienna, 273.

[Buda 2006] Buda. R. A. (2006) Speciation of Pu(III) in the Environmental System Humic Substances-Groundwater-Kaolinite, Doctoral Thesis, Institut für Kernchemie, Universität Mainz, Mainz, Germany.

[Buff 77] Buffle. J, Greter. F, Haerdi. W. (1977) Measurements of Complextation Properties of Humic and Fulvic Acids in Natural Waters with Lead and Copper ion-Selective Electrodes, Analytical Chemistry, **49**, 216-222.

[Bürg 2005a] Bürger. S, Banik. N. L, Buda. R. A, Kratz. J. V, Kuczewski. B, Trautmann. N. (2005) Speciation of the Oxidation States of Plutonium in Aqueous Solutions by CE-ICP-MS and CE-RIMS, Radiochimica Acta (submitted)

[Bürg 2005b] Bürger. S. (2005) Spurenanalyse von Uran und Plutonium sowie Speziationsuntersuchungen an Plutonium mit massenspektrometrischen und kapillarelectrophoretischen Methoden, Doctoral Thesis, Institut für Kernchemie, Universität Mainz, Mainz, Germany.

[Carl 89] Carlsen. L. (1989) The Role of Organics on the Migration of Radionuclides in the Geosphere, Final Report, Contact EC N^0 FI1W/0066, Task 4 (Mirage 2) Euro 12024 en.

[Cho 2006] Cho. H. R. (2006) Chemistry of Tetravalent Plutonium and Zirconium: Hydrolysis, Solubility, Colloid Formation and Redox Reactions, Doctoral Thesis, University of Heidelberg, Heidelberg, Germany.

[Cho 2006a] Cho. H. R, Marquardt. C. M, Neck. V, Seibert. A, Walther. C, Yun. J. I, Fanghänel. T. (2006) Redox Behavior of Plutonium(IV) in Acidic Solutions, Proceedings of the Int. Conf. "Actinides 2005", Recent Advances in Actinide Science, RSC Publishing, p. 602.

[Chop 2004] Choppin. G. R. (2004) Actinide Chemistry: From Weapons to Remendation to Stewardship, Radiochimica Acta, **92**, 519-523.

[Chop 2003] Choppin. G. R. (2003) Actinide Speciation in the Environment, Radiochimica Acta, **91**, 645-649.

[Chop 2001] Choppin. G. R, Morgenstern. A. (2001) Distribution and Movement of Environmental Plutonium, in Plutonium in the Environment, A. Kudo, Edition, p.91.

[Chop 2000] Choppin. G. R, Morgenstern. A. (2000) Radionuclide Separations in Radioactive Waste Disposal, Journal of Radioanalytical and Nuclear Chemistry, **243**, 43-48.

[Chop 99] Choppin. G. R. (1999) Utility of Oxidation States Analogs in the Study of Plutonium Behavior, Radiochimica Acta, **89**, 89-95.

[Chop 98] Choppin. G. R, Wong. P. J. (1998) The Chemistry of Actinides Behavior in Marine Systems, Aquatic Geochemistry, **4**, 77-101.

[Chop 97a] Choppin. G. R, Wall. N. L. (1997) Comparison of Two Models for Metal-Humic Interactions, Journal of Radioanalytical and Nuclear Chemistry, **221**, 67-71.

[Chop 97b] Choppin. G. R, Bond. A. H, Hromadka. P. M. (1997) Redox Speciation of Plutonium, Journal of Radioanalytical and Nuclear Chemistry, **221**, 203-210.

[Chop 91] Choppin. G. R. (1991) Redox Speciation of Plutonium in Natural Water, Journal of radioanalytical Nuclear Chemsitry, **147**, 109.

[Chop 88] Choppin. G. R. (1988) Humics and Radionuclide Migration, Radiochimica Acta, **44/45**, 23-28.

[Chop 81] Choppin. G. R, Nash. K. L. (1981) Dissociation Kinetics of Thorium and Humic Acid, Journal of Inorganic & Nuclear Chemistry, **43**, 357-359.

[Chop 78] Choppin. G. R, Kullberg. L. (1978) Protonation Thermodynamics of Humic Acid, Journal of Inorganic and Nuclear Chemistry, **40**, 651-655.

[Clar 2000] Clark. D. L. (2000) The Chemical Complexities of the Plutonium, Los Alamos Science, **26**, 368.

[Clev 79] Cleveland. J. M. (1979) The Chemistry of Plutonium, American Nuclear Society.

[Cohe 61a] Cohen. D. (1961) Electrochemical Studies of Plutonium Ions in Perchloric Acid Solutions, Journal of Inorganic and Nuclear Chemistry, **18**, 207-210.

[Cohe 61b] Cohen, D. (1961) The Absorption Spectra of Plutonium Ion in Perchloric Acid Solutions, Journal of Inorganic Nuclear Chemistry, **18**, 211.

[Conr 2004] Conradson. S. D et. al. (2004) Higher Order Speciation Effects on Plutonium L_3 X-ray Absorption Near Edge Spectra, Journal of Inorganic Chemistry, **43**, 116-125.

[Conr 98] Conradson . S. D. (1998) Application of XAFS to Materials and Environmental Science, Applied Spectroscopy, **52**, 252A

[Crom 98] Cromieres. L, Moulin. V, Fourest. B, Giffaut. E. (1998) Sorption of Thorium onto Hematite Colloids, Radiochimica Acta, **82**, 249-256.

[Czer 97] Czerwinski. K, Kim. J. I. (1997) Complexation of Transuranic Ions by Humic Substances: Application of Laboratory Results to the Natural Systems, Mat. Res. Soc. Symp. Proc. **465**, 743.

[Czer 96] Czerwinski. K. R, Kim. J. I, Rhee. D. S, Buckau. G. (1996) Complexation of Trivalent Actinide Ions (Am^{3+}, Cm^{3+}) with Humic Acid: The Effect of Ionic Strength Radiochimica Acta, **72**, 179-187.

[Czer 94] Czerwinski. K. R, Buckau. G, Scherbaum. F, Kim. J. I. (1994) Complexation of the Uranyl Ion with Aquatic Humic Acid, Radiochimica Acta, **65**, 111-119.

[Davi 84] Davis. J. A. (1984) Complexation of Trace Metals by Adsorbed Natural Organic Matter, Geochim. Cosmochim. Acta, **48**, 679-683.

[Dela 90] Delany. J. M, Lindeen. S. R. (1990) The LLNL Thermochemical Database, Lawrence Livermore National Laboratory Report UCRL-21658, P.150.

[Dupl 77] Duplessis. J, Guillaumont. R. (1977) Hydrolyse du Neptunium Tetravalent, Radiochem. Radioanalytical Letters. **31**, 293 .

[Ekbe 2000] Ekberg. C, Albinssion. Y, Comarmound. M. J, Brown. P. L (2000) Studies on the Complexation Behavior Thorium(IV). 1. Hydrolysis Equilibria, Journal of Solution Chemistry, **29**, 63-71.

[Erdm 97] Erdmann. N. (1997) Doctoral Thesis, Institut für Kernchemie, Universität Mainz, Mainz, Germany.

[Erik 93] Eriksson. T. E, Ndalamba. P, Cui. D, Bruno. J, Caceci. M, Saphiu. K. (1993) Solubility of the Redox-Sensitive Radionuclides ^{99}Tc and ^{237}Np under Reducing Conditions in Neutral to Alkaline Solutions. Effect of Carbonate, Swedish Nuclear Fuel and Waste Management Co. Report SKB TR 93-18, Stockholm.

[Ewin 99] Ewing. R. C. (1999) Nuclear Waste Forms for Actinides, Proc. Natl. Acad. Sci., **96**, 3432-3437.

[Farr 2000] Farr. J. D, Schulze. R. K, Honeymann. B. D. (2000) Aqueous Pu(IV) Sorption on Brucite, Radiochimica Acta, **88**, 675-679.

[Flur 2003] Flury. M, Harsh. J. B. (2003) Fate and Transport of Plutonium and Americium in the Subsurface of OU 7-13/14, Department of Crop and Soil Sciences, Center for Multiphase Environmental Research, Washington State University, Pullman, Washington.

[Fowl 86] Fowler. M. M, Daniels. W. R, Gunten. H. R. V, Gäggeler. H, Hoffman. D. C, Lee. D, Gergorich. K, Moody. K. J, Lerch. M, Herrmann. G, Trautmann. N. (1986) Radiochemical Separation of Actinides from Copper and Gold Catcher Foils from Heavy Ion Reactions with Targets, Radiochimica Acta, **40**, 75-79.

[Fuku 2003] Fukuda. K. et. al (2003) IAEA Overview Global Spent Fuel Storage, IAEA-CN-102/60, Int. Conf. on Storage of Spent Fuel from Power Reactors, Vienna, 2-6 June.

[Gehm 86] Gehmecker. H, Trautmann. N, Herrmann. G. (1986) Separation of Plutonium Oxidation States by Ion Exchange Chromatography, Radiochimica Acta, **40**, 81-88.

[Ghab 2004] Ghabbour. E. A, Davies. G, Goodwillie. M. E, O'Donaughy. K, Smith. T. L. (2004) Thermodynamics of Peats-, Plants-, and Soil-Derived Humic Acid Sorption on Kaolinite, Journal of Environmental Science & Technology, **38**, 3338-3342.

[Guil 92] Guillaumont. R, Adolff. J. P. (1992) Behavior of Environmental Plutonium at Very Low Concentration, Radiochimica Acta, **58/59**, 53-60.

[Hahn 39] Hahn. O, Strassmann. F. (1939) Concerning the Existence of Alkaline Earth Metals Resulting from Neutron Irradiation of Uranium, Die Naturwissenschaften 27, p. 11-15.

[Haye 78] Hayes. M. H. B, Swift. R. S. (1978) The Chemistry of Soil Constituents, Willey, Chichester, p.p 179-320.

[Heig 92] Heiger. R, David. N. (1992) "High Performance Capillary Electrophoresis: An Introduction" France, Hewlet-Packard Company,

[Ho 85] Ho. C. H, Miller. N. H. (1985) Effect of Humic Acid on Uranium Uptake by Hematite Particles, Journal of Colloid and Interface Science, **106**, 281-288.

[Holm 95] Holm. E. (1995) Plutonium in the Baltic Sea, Applied Radiation and Isotopes, **46**, 1125-1229.

[Huer 98] Huertas. F. J, Chou. L, Wollast. R. (1998) Mechanism of Kaolinite Dissolution at Room Temperature and Pressure: Part 1. Surface Speciation, Geochimica et Cosmochimica Acta, **62**, 417-431.

[Hunt 88] Hunter. K. A, Hawke. D. J, Kwee. C. L. (1988) Equilibrium Adsorption of Thorium by Metal Oxides in Marine Electrolytes, Geochim. Cosmochim. Acta, **52**, 627.

[IAEA 98] International Atomic Energy Agency (IAEA) (1998) Safe Handling and Storage of Plutonium, Safety Series No. 9, IAEA, Vienna.

[IAEA 89] International Atomic Energy Agency (IAEA) (1989) Principles for the Exemption of Radiation Sources and Practice from Regulatory Control, Safety Series No 89, Vienna.

[Ibar 77] Ibarra. J. V, Osacar. J, Gavilain. G. M. (1977) Ann. Quim, 77, 224-229.

[Jano 2003] Janos. P. (2003) Separation Methods in the Chemistry of Humic Substances, Journal of Chromatography A, **983**, 01-18.

[Jian 93] Jianxin. T, Yaozhong. C, Zhangji. L. (1993) A Kinetic Study of the Reduction of Plutonium with Humic Acid, Radiochimica Acta, **61**, 73-75.

[Kenn 2002] Kannamkumarath. S. S, Wrobel. K, Wrobel. K, Hymer. C, Caruso. J. A. (2002) Capillary Electrophoresis- Inductively Coupled Plasma-Mass Spectrometry: an Attractive Complementary, Journal of Chromatography A, **975**, 245-266.

[Kaut 2006] Kautenburger. R, Nowotka. K, Beck. H. P. (2006) Workshop zum Forschungsvorhaben „Migration von Actiniden im System Ton, Huminstoff, Aquifer“, 28.03-29.03, Mainz, Germany.

[Katz 86] Katz, Seaborg and Morss. (1986) The Chemistry of the Actinides Elements, Vol.1 and 2, Second Edition, Chapmann and Hall.

[Keen 85] Kenney-Kennicutt. W. L, Morse. J. W. (1985) The Redox Chemistry of PuO_2^+ Interaction with Common Mineral Surfaces in Dilution Solutions and Seawater, Geochim. Cosmochim. Acta, **49**, 2577-2588

[Kohl 99] Kohler. M, Honeyman, B. D, Leckie, J.O. (1999) Neptunium(V) Sorption to Hematite (α-Fe_2O_3) in Aqueous Suspension: The effect of CO_2, Radiochimica Acta, **85**, 33.

[Kim 2000] Kim. J. I. (2000) Aquatic Chemistry of Actinides: is a Thermodynamic Approach to Describe Natural Dynamics System?, American Institute of Physics, Proceedings—July 7,Vol. 532, Issue 1, pp. 45-46.

[Kim 96] Kim. J. I, Czerwinski. K. R. (1996) Complexation of Metal Ions with Humic Acid: Metal Ion Charge Neutralization Model, Radiochimica Acta, **73**, 05-10.

[Kim 93] Kim. J. I, Rhee. D. S, Wimmer. H, Buckau. G, Klenze. R. (1993) Complexation of Trivalent Actinide Ions (Am^{3+}, Cm^{3+}) with Humic Acid: A Comparison of Different Experimental Methods, Radiochimica Acta, **62**, 35-43.

[Kim 91a] Kim. J. I. (1991) Actinide Colloid Generation in Groundwater, Radiochimica Acta, **52/53**, 71-81.

[Kim 91b] Kim. J. I, Rhee. D. S, Buckau. G. (1991) Complexation of Am(III) with Humic Acids of Different Origin, Radiochimica Acta, **52/53**, 49-55.

[Kim 90] Kim. J. I, Buckau. G, Li. G. H, Duschner. Psarros. H. N. (1990) Characterization of Humic Acid and Fulvic Acids from Gorleben Groundwater, Fresenius Journal of Analytical Chemistry, **338**, 245-252.

[Kim 89] Kim. J. I, Kanellakopulos. B. (1989) Solubility Products of Plutonium(IV) Oxide and Hydroxide, Radiochimica Acta, **48**, 145-150.

[Kim 88] Kim, J. I, Buckau, G. (1988) Report RCM 02188, Institut für Radiochemie der TU München, Germany.

[Kim 86] Kim. J. I. (1986) Handbook on the Physics and Chemistry of the Actinides, eds. A. J. Freeman and C. Keller, Elsevier, New York.

[Knop 99] Knopp. R, Neck. V, Kim. J. I. (1999) Solubility Hydrolysis and Colloid Formation of Plutonium(IV), Radiochimica Acta, **86**, 101-108.

[Koop 2001] Koopal. L. K, Riemsdijk. W. H, Kinniburgh. D. G (2001) Humic Matter and Contaminant General Aspects and Modeling Metal Ion Binding, Journal of Pure Applied Chemistry, **73**, 2005-2016.

[Krep 2006] Křepelová. A, Sachs. S, Bernhard. G. (2006) Uranium(VI) Sorption onto Kaolinite in the Presence and Absence of Humic Acid, Radiochimica Acta, in press.

[Kucz 2003] Kuczewski. B, Marquardt. C. M, Seibert. A, Gecckeis. H, Kratz. J. V, Trautmann. N. (2003) Separation of Plutonium and Neptunium Species by Capillary Electrophoresis- Inductively Coupled, Journal of Analytical Chemistry, **75**, 6769-6774.

[Kucz 2004] Kuczewski. B. (2003) Trennung der Oxidationsstufen des Plutonium mit CE-ICP-MS und Untersuchung des Redoxverhaltens von Plutonium im Grundwasser, Doctoral Thesis, Institut für Kernchemie, Universität Mainz, Mainz, Germany.

[Kudo 2001] Kudo. A. (2001) Plutonium in the Environment, Elsevier.

[Kuja 2002] Kujawinski. E. B, Hatcher. P. G, Freitas. M. A, Zang. X. (2002) The Application of Electrospray Ionization Mass Spectrometry to the Structural Characterization of Natural Organic Matter, Anlaytical Chemistry, **33**, 171-180.

[Labo 97] Labonne-Wall. N, Moulin. V, Vilarem. J. P. (1997) Retention Properties of Humic Substances onto Amorphous Silica: Consequences for the Sorption of Cations, Radiochimica Acta, **79**, 37.

[Lafl 87] Laflamme. B. D, Murray. J. W. (1987) Solid/Solution Interaction: the Effect of Carbonate Alkalinity on Adsorbed Thorium, Geochim. Cosmochim. Acta, **51**, 243.

[Land 97] Landers. J. P. (1997) Handbook of Capillary Electrophoresis, 2nd Edition, CRC Press.

[Law 91] Law No. 91-1381 of December 30, IAEA (1991) Radioactive Waste Management Research, Annex I: Country specific examples of radwaste management and disposal

[Li 80] Li. W. C, Victor. D. M. Chakrabarti. C. L. (1980) Effect of pH and Uranium Concentration on Interaction of Uranium(VI) and Uranium(IV) with Organic Ligands in Aqueous Solutions, Analytical Chemistry, **52**, 520-523

[Lies 91] Lieser. K. H, Hill. R, Mühlenweg. U, Singh. R. N, Shu-de. T, Steinkopff. T. (1991) Actinides in the Environment, Journal of Radioanalytical and Nuclear Chemsitry, **147**, 117-131.

[Lipp 2005] Lippold. H, Müller. N, Kupsch. H. (2005) Effect of Humic Acid on the pH-Dependent Adsorption of Terbium (III) onto Geological Materials, Applied Geochemistry, **20**, 1209-1217.

[Liu 99] Liu. A, Gonzalez. R. D. (1999) Adsorption/Desorption in a System Consisting of Humic Acid, Heavy Metals, and Clay Minerals, Journal of Colloid and Interface Science, **267**, 225-232.

[Lloy 78] Lloyed. M. H, Haire. R. G (1978) The Chemistry of Sol-Gel Processes, Radiochimica Acta, **25**, 139.

[Lu 2003a] Lu. N, Reimus. P. W, Parker. G. R, Conca. J. L, Triay. I. R. (2003) Sorption Kinetic and Impact Temperature, Ionic Strength and Colloid Concentration on the Adsorption of Plutonium-239 by Inorganic Colloids, Radiochimica Acta, **91**, 713-720.

[Marq 2004] Marquardt. C. M, Seibert. A, Artinger. R, Denecke. M. A, Kuczewski. B, Schild. D, Fanghänel. T. (2004) The Redox Behavior of Plutonium in Humic Rich Groundwater, Radiochimica Acta, **92**, 617-623.

[Marq 2001] Marquardt. C. M, Pirlet. V, Kim. J. I. (2001) Complexation of Tetravalent Neptunium with Fulvic Acid. In: Abstract of the International Conference Actinides, Hayama, Japan, p.140.

[Marq 2000] Marquardt. C. M. (2000) Annual Report, FZK, Karlsruhe.

[Marq 98] Marquardt. C, Kim. J. I. (1998) Complexation of Np(V) with Humic Acid: Intercomparison of Results from Differential Laboratories, Radiochimica Acta, **88**, 129-137.

[Marq 96] Marquardt. C, Herrmann. G, Trautmann. N. (1996) Complexation of Np(V) with Humic Acid at very Low Concentration, Radiochimica Acta, **73**, 119-125.

[Meie 99] Meier. M, Namjesni. K, Maurice. P. A, Chin. Y, Aiken. G. R. (1999) Fractionation of Aquatic Natural Matter Upon Sorption to Goethite and Kaolinite, Chemical Geology, **157**, 275-284.

[Mitc 95] Mitchell. P. I, Battle. J. V, Downes. A. B, Condren. O. M, Vintro. L. L, Sanchez-Cabeza. J. A. (1995) Recent Observations on the Physico-Chemical Speciation of Plutonium in the Irish Sea and Western Mediterranean, Applies Radiation Isotopes, **46**, 1175-1190.

[Mors 91] Morse. J, Choppin. G. R. (1991) The Chemistry of Transuranic Elements in the Natural Waters, Review in Aquatic Sciences, **4(1)**, 01-22.

[Moul 2005] Moulin. V, Ansoborlo. E, Bion. L, Doiz. D, Moulin. C, Cote. G, Madic. C, Lee. J. V. (2005) Speciation Needs in Relation with Environmental and Biological Purposes, Radioprotection, Suppl. 1. **40**, S11-S18.

[Moul 2001] Moulin. V, Moulin. C. (2001) Radionuclide Speciation in the Environment: a Review, Radiochimica Acta, **89**, 773-778.

[Moul 92] Moulin. V, Tits. J. (1992) Complexation Behavior of Humic Substances towards Actinides and Lanthanides Studied by Time-Resolved Laser-Induced Spectrofluorometry, Radiochimica Acta, **58/59**, 121-128.

[Moul 89] Moulin.V, Stammose. D. (1989) Chemical Processes at the Mineral Oxide-Water Interface: System Al_2O_3-Organic Matter-Am(III), TM IN: Water-Rock Interaction, WRI-6. Proceedings of the 6th International Symposium on Water-Rock Interaction, Malvern, 3-8 August, A. A. Balkema, Rotterdam, The Netherlands. 1989. p 505-509.

[Murp 92] Murphy. E. M, Zachara. J. M, Smith. S. C, Phillips, J. L. (1992) The Sorption of Humic Acids to Mineral Surfaces and their Role in Contaminant Binding, Science and Total Environment, **117/118**, 413.

[Naga 97] Nagasaki. S, Tanaka. S, Suzuki. A. (1997) Affinity of Finely Dispersed Montmorillonite Colloidal Particles for Americium and Lanthanides, Journal of Nuclear Materials, **244**, 29-35.

[Nash 81] Nash. K, Fried. S, Friedman. A. M, Sulllvan. J. C. (1981) Redox Behavior, Complexing and Adsorption of Hexavalent Actinides by Humic Acid and Selected Clays, Journal of Environmental Science and Technology, **15**, 835-839.

[Nash 80] Nash. K. L, Choppin. G. R. (1980) Interaction of Humic and Fulvic Acids with Th(IV), Journal of Inorganic and Nuclear Chemistry, **42**, 1045-1050.

[Neck 2006] Neck. V. Altmaier. M, Fanghänel. T. (2006) Solubility and redox reactions of PuO2.xH2O(s), Oral Presentation, Institut für Kernchemie, Universität Mainz, Germany.

[Neck 2003] Neck. V, Altmaier. M, Müller. R, Bauer. A, Fanghänel. T, Kim. J. I. (2003) Solubility of Crystalline Thorium Dioxide, Radiochemica Acta, **91**, 253.

[Neck 2001a] Neck. V, Kim. J. I. (2001) Solubility and Hydrolysis of Tetravalent Actinides, Radiochimica Acta, **88**, 1-16.

[Neck 2001b] Neck. V, Kim. J. I, Seidel. B. S, Marquardt. C. M, Dardenne. K, Jensen. M. P, Hauser W. (2001) A Spectroscopic Study of the Hydrolysis, Colloids Formation and Solubility of Np(IV), Radiochimica Acta, **89**, 439-446.

[Neck 99] Neck. V, Kim. J. I. (1999) Solubility and Hydrolysis of Tetravalent Actinides , Wissenschaftliche Berichte, FZKKA-6350, p. 37, Forchungszentrum Karlsruhe, Karlsruhe, Germany.

[Niit 97] Niitsu. Y, Sato. S, Ohashi. H, Sakamoto. Y, Naga. S, Ohnuki. T, Muraoka. S. (1997) Effects of Humic Acid on the Sorption of Neptunium(V) on Kaolinite, Journal of Nuclear Materials, **248**, 328-332.

[Nits 94] Nitsche. H, Roberts. K, Xi. R. H, Prussin. T, Becraft. K, Silber. H. B, Carpenter. S. A, Gatti. R. C, Novak. C. F. (1994) Long Term Plutonium Solubility and Speciation Studies in a Synthetic Brine. Radiochimica Acta **66/67**, 03.

[Nits 88] Nitsche. H, Lee. S. C, Gatti. R. C. (1988) Determination of Plutonium Oxidation States at Trace Levels Pertinent to Nuclear Waste Disposal, Journal of Radioanalytical and Nuclear Chemistry **124**, 171-185.

[Nunn 98] Nunnemann. M, Erdmann. N, Hasse. H. U, Huber. G, Kratz. J. V, Kunz. P, Mansel. A, Passler. G, Trautmann. N, Waldek. A. (1998) Trace Analysis of Plutonium in Environmental Samples by Resonance Ionization Mass Spectroscopy (RIMS), Journal of Alloys and Compounds, **271**, 45-48.

[Park 99] Parkhurst. D. L, Appelo. C. A. J. (1999) User's Guide to PHREEQC--A Computer Program for Speciation, Batch-Reaction, One-Dimensional Transport, and Inverse Geochemical Calculations, U.S. Department of the Interior, U.S. Geological Survey Water-Resources Investigations, Report 99-4259 .

[Payn 2004] Payne. T. E, Davis. J. A, Lumpkin. G. R, Chisari. R, Waite. T. D. (2004) Surface Complexation Model of Uranyl Sorption on Georgia Kaolinite. Applied Clay Science, **26**, 151.

[Payn 96] Payne. T. E, Davis. J. A. Waite. T. D. (1996) Uranium Adsorption on Ferrihydrite-Effects of Phosphate and Humic Acid, Radiochimica Acta, **74**, 239.

[Pena 2005] Pena-Mendez. E. M, Havel. J, Patocka. J. (2005) Humic Substances-Compounds of Still Unknown Structure: Application in Agriculture, Industry, Environment, and Biomedicine, J. Appl. Biomed, **03**, 13-24.

[Pirl 2003a] Pirlet. V. (2003) The Investigation of the Neptunium Complexes Formed upon Interaction of High level Waste Glass and Boom Clay Medium, Doctoral Thesis, University of Liege, Belgium.

[Pirl 2003b] Pirlet. V, Van. I. P. (2003) Neptunium Speciation in Humic Acid-rich Clay Water upon Interaction with Radioactive Waste Glass Samples, Materials Research Society, Symp. Proceedings, **757**, 117.

[Prue 93] Pruett. R. J, Webb. H. L. (1993) Sampling and Analysis of KGa-1B Well-Crystallized Kaolin Source Clay. Clay and Clays Minerals, **41**, 514.

[Rai 95] Rai. D, Felmy. A. R, Moore. D. A, Mason. M. J. (1995) The Solubility of Th(IV) and U(IV) Hydroxide in Concentrated $NaHCO_3$ and Na_2CO_3 Solution, Materials Research Society Symposium Proceedings, **353**, 1143-1150.

[Rao 95] Rao. L, Choppin. G. R. (1995) Thermodynamic Study of the Complexation of Neptunium(V) with Humic Acids, Radiochimica Acta, **80**, 87-95.

[Redd 98] Redden. G. D, Jinhe. L, Leckie. J. (1998) Adsorption of U(VI) and Citric Acid on Goethite, Gibbsite, and Kaolinite. Comparing Results for Binary and Ternary Systems, In: Adsorption of Metals by Geomedia. Variables, Mechanism and Model Applicatios, Academic Press, San Diego.

[Reil 2005a] Reiller. P. (2005) Prognosticating the Humic Complexation for Redox Sensitive Actinides Through Analogy Using the Charge Neutralization Model, Radiochimica Acta, **93**, 43-55.

[Reil 2005b] Reiller. P, Casanova. F. (2005) Influence of Addition Order and Contact Time on Thorium(IV) Retention by Hematite in the Presence of Humic Acids, Journal of Environmental Science and Technology, **39**, 1641-1648.

[Reil 2002] Reiller. P, Moulin. V, Casanova. F, Dautel. C. (2002) Retention Behavior of Humic Substances onto Mineral Surfaces and Consequences Upon Thorium(IV) Mobility: case of Iron Oxides, Journal of Applied Geochemistry, **17**, 1551-1562.

[Righ 91] Righetto. L, Bidogilo. G, Bellobono. I. R. (1991) Competitative Actinide Interactions in Colloidal Humic Acid-Mineral Oxide Systems, Journal of Environmental Science and Technology, **25**, 1913-1917.

[Roth 2004] Rothe. J, Walther. C, Denecke. M. A, Fanghänel. T. (2004) XAFS and LIBD Investigation of the Formation and Structure of Colloidal Pu(IV) Hydrolysis Products, Inorganic Chemistry, **43**, 4708-4718.

[Rose 2002] Rosenqvist. J (2002) Surface Chemistry of Al and Si (Hydroxides, with Emphasis on Nano-Sized Gibbsite (α-$Al(OH)_3$), Doctoral Thesis, Department of Chemistry, Umea University, Umea, Sweden.

[Rudo 77] Rudolph. W, Kratz. K. L., Herrmann. G. (1977) Half-lives, Fission Yields and Neutron Emission Probabilities of Neutron-rich Antimony Isotopes, Journal of Inorganic Nuclear Chemistry, **39**, 753.

[Rund 2000] Runde. W. (2000) Spectroscopic for Environmental Studies of Actinides Species, Los Alamos Science, **26**, 412.

[Saku 2002] Sakuragi. T, Tokuyama. A, Sato. S, Kozaki. T, Mitsugashira. T, Hara. M, Suzuki. Y. (2002) Effect of Calcium Ions on the Sorption of Am(III) and Eu(III) onto Kaolinite in the Presence of Humic Acid, Journal of Nulcear Science & Technology, **3**, 520.

[Sanc 85] Sanchez. A. L, Murray. J. W, Sibley. T. H. (1985) The Adsorption of Plutonium IV and V on Goethite, Geochimica et Cosmochimica Acta, **49**, 2297-2307.

[Sach 2006] Sachs. S, Křepelová. A, Schmeide. K, Mibus. J, Brendler. V, Bernhard. G. (2006) Workshop zum Forschungsvorhaben „Migration von Actiniden im System Ton, Huminstoff, Aquifer“, 28.-29.03. Mainz, Germany

[Sait 2004] Saito. T, Nagasaki. S, Tanaka. S, Koopal. L. K. (2004) Application of the NICA-Donnan Model for Proton, Copper and Uranyl Binding to Humic Acid, Radiochimica Acta, **92**, 567-574.

[Sama 2000] Samadfam. M, Jintoki. T, Sato. S, Ohashi. H, Mitugashira. T, Hara. M, Suzuki.Y. (2000) Effects of Humic Acid on the Sorption of Am(III) and Cm(III) on Kaolinite, Radiochimica Acta, **88**, 717-721.

[Schul 93] Schulten. H. R, Schintzer. M. (1993) A State-of-the-Art Structural Concept for Humic Substances, Naturwissenschaften, **80**, 29-30.

[Schm 2005] Schmeide. K, Reich. T, Sachs. S, Brendler. V, Heise. K. H, Bernhard. G. (2005) Neptunium(IV) Complexation by Humic Substances Studied by X-ray Absorption Fine Structure Spectroscopy, Radiochimica Acta, **93**, 87-196.

[Schm 2000] Schmeide. K, Brendler. V, Pompe. S, Bubner. M, Heise. K. H, Bernhard. G. (2000) Kinetic Studies of the Uranium(VI) and Humic Acid Sorption onto Phyllite, Ferrihydrite and Muscovite, In: FZKA-6524, Wissenschaftliche Berichte, Forschungszentrum Karlsruhe GmbH, Karlsruhe 2004, p. 149.

[Scha 99] Schaumlöffel. D, Prange. A. (1999) A New Interface for Combining Capillary Electrophoresis with Inductively Coupled Plasma-mass Spectrometry, Fresenius Journal of Analytical Chemistry, **364**, 452-45.

[Schn 72] Schnitzer. M, Khan. S. U. (1972) Humic Substances in the Environment, Marcel Decker Inc. New York

[Schi 2000] Schild. D, Marquardt. C. M. (2000) Analysis of Th(IV)-Humate by XPS, Radiochimica Acta, **88**, 587-591.

[Schr 97] Schroth. B. K, Sposito. G. (1997) Surface Charge Properties of Kaolinite, Clays and Clay Mineral, **45**, 85.

[Seab 46] Seaborg. G. T, Mcmillan. E. M, Kennedy. J. W, Wahl. A. C. (1946) Radioactive Element 94 from Deuterons on Uranium, Physical Review, **69**, 366–367.

[Seab 45] Seaborg. G. T. (1945) The Chemical and Radioactive Properties of the Heavy Elements, Chem. Eng. News, **23**, 2190.

[Seah 98] Seah. M. P, Gilmore. I. S, Beamson. G. (1998) "XPS: Binding Energy Calibration of Electron Spectrometers 5 – Re-evaluation of the Reference Energies", Surf. Interface Anal. **26**, 642-649.

[Seib 2001] Seibert. A, Mansel. A, Marquardt. C. M, Keller. H, Kratz. J. V, Trautmann. N. (2001) Complexation Behavior of Neptunium with Humic Acid, Radiochimica Acta, **89**, 505-510.

[Seib 99] Seibert. A. (1999) Wechselwirkung von Neptunium mit Huminstoffen unter naturnahen Bedingungen, Doctoral Thesis, Institut für Kernchemie, Universität Mainz, Germany.

[Selt 2005] Seltborg. P. (2005) Source Efficiency and High-Energy Neutronics in Accelerator Driven Systems, Doctoral Thesis, KTH, Sweden.

[Shan 76] Shannon. R. D. (1976) Revised Effective Ionic Radii and Systematic Studies of Interatomic Distances in Halides and Chalcogenides, Acta Cryst, **32**, 751.

[Silv 95] Silver. G. L, Nitsche. H. (1995) Actinide Environment Chemistry, Radiochimica Acta, **70/71**, 377.

[Spos 80] Sposito. G, Mattigod. S. V. (1980) A Computer Program for the Calculation of Chemical Equlibria in Soil Solutions and Other Natural Water Systems, Doctoral Thesis, Department of Soil Science, University of California, USA.

[Suth 99] Sutheimer. S. H, Maurice. P. A, Zhou. Q. (1999) Dissolution of Well and Poorly Crystallized Kaolinites, Al Speciation and Effects of Surface Charcteristics, American Minerology, **84**, 620.

[Sten 2003] Stenson. A. C, Marshall. A. G, Copper. W. T. (2003) Exact Masses and Chemical Formula of Individual Suwanne River Fulvic Acids from Ultrahigh Resolution ESI FT-ICR Mass Spectroscopy, Analytical Chemistry, **75**, 1275-1284.

[Stev 82] Stevenson, F. J. (1982) Humus Chemistry Genesis, Composition, Reactions, Willey Inter science, New York

[Stum 84] Stumpe. R, Kim. J. I, Schrepp. W, Walther. H. (1984) Speciation of Actinide Ions in Aqueous Solution by Laser-Induced Pulsed Photoacoustic Spectroscopy, Applied Physics, B **34**, 203-206.

[Tabl 96] Table of Isotopes (1986.) R. B. Firestone, V. S. Shirly (Editors), 8th edition, Wiley, New York.

[Taka 99] Takahashi. Y, Minai. Y, Ambe. S, Makide. Y, Ambe. F. (1999) Comparison of Adsorption Behavior of Multiple Inorganic Ions on Kaolinite and Silica in the Presence of Humic Acid Using Multitracer Technique, Geochimica et Cosmochimica Acta, **63**, 815- 836.

[Tana 2002] Tanaka. T, Nagao. S, Sakamoto.Y, Ogawa. H. (2002) Sorption Behavior of Plutonium(IV) onto Soils in the Presence of Humic Acid, supplement **3**, 524-527.

[Tayl 95] Taylor. D. M. (1995) Environmental Plutonium in Humans, Journal of Applied Radiation and Isotopes, **46**, 1245-1252.

[Tipp 93] Tipping. E. (1993) Modelling the Binding of Europium and the Actinides by Humic Substances, Radiochimica Acta, **62**, 141-152.

[Tipp 92] Tipping. E. Hurley. M. A. (1992) Modelling the Binding of Europium and the Actinides by Humic Substances, Geochimica and Cosmochimica Acta, **56**, 3627-3641.

[Tors 88] Torstenfel. B, Rundberg. R. S, Mitchell. A. J. (1988) Actinide Sorption on Granites and Minerals as a Function of pH and Colloids/Pseudocolloids, Radiochimica Acta, **44/45**, 111-117.

[Trau 2004] Trautmann. N, Passler. G, Wendt. K. D. A. (2004) Ultratrace Analysis and Isotope Ratio Measurements of Long Lived Radioisotopes by Resonance Ionization Mass Spectrometry (RIMS), Journal of Analytical and Bio analytical Chemistry, **378**, 348-355.

[Watt 83] Watters. R. L, Hakonson. T. E, Lane. L. J. (1983) The Behavior of Actinides in the Environment, Radiochemica Acta, **72**, 209-215.

[Wils 2005] Wilson. R. E, Hu. Y. J, Nitsche. H. (2005) Detection and Quantification of Pu(III; IV, V, and VI) Using a 1.0-meter Liquid Core Wavelength, Radiochimica Acta, **93**, 203-206.

[Wolf 2004] Wolf. M, Buckau. G, Geyer. S. (2004) Isolation and Characterization of New Batches of Gohy-573 humic and fulvic acids, personally collected.

[Xian 2001] Xiangke. W, Wenming. D, Yingchun. G, Changhui. W, Zuyi. T. (2001) Sorption Characteristics of Radioeuropium on Bentonite and Kaolinite, Journal of Radioanalytical and Nuclear Chemistry, **250**, 267-270.

[Xian 2000] Xiangke. W, Wenming. D, Xiongxin. D, Aixia. W, Jinzhou. D, Zuyi. T. (2000) Sorption and Desorption of Eu and Yb on Alumina: Mechanism and Effect of Fulvic Acid, Applied Radiation & Isotopes, **52**, 165-173.

[Yama 2004] Yamaguchi. T, Nakayama. S, Yoshida. T. (2004) Interactions Between Anionic Complex Species of Actinides and Negatively Charged Mineral Surface. Radiochimica Acta , **92,** 678.

[Zach 94] Zachara. J. M, Resch. C. T, Smith. S. C. (1994) Influences of Humic Substances on Co^{2+} Sorption by Subsurface Mineral Separate and its Mineralogic Components, Geochim. Cosmochim. Acta, **58**, 553.

[Zava 2005] Zavarin. M, Roberts. S, Hakem. N, Sawvel. A. M, Kersting. A. B. (2005) Eu(III), Sm(III), Np(V), Pu(V), and Pu(IV) Sorption to Calcite. Radiochimica Acta, **93,** 93.

[Zeh 99a] Zeh. P, Kim. J. I, Marquardt. C. M, Artinger. R. (1999) The Reduction of Np(V) in Groundwater Rich in Humic Substances, Radiochimica Acta, **87**, 23-26.

[Zeh 99b] Zeh. P, Kim. J. I, Marquardt. C. M, Artinger. R. (1999) The Reduction of Np(V) Ground Water Rich Humic Substances, Radiochemica Acta, **88**, 609.

[Zhij 2005] Zhijun. G, Lijun. N, Zuyl. T. (2005) Sorption of Th(IV) Ions onto TiO_2: Effects of Contact Time, Ionic Strength, Thorium Concentration and Phosphate, Journal of Radioanalytical and Nuclear Chemistry, **266**, 333-338.

[Zuyi 94] Zuyi. T, Huanxiic. G. (1994) Use of the Ion Exchange Method for the Determination of Stability Constants of Thorium with Humic and Fulvic Acids, Radiochimica Acta, **65**, 121-123.

7.0 Appendix

7.1 Complexation constants of La(III) with humic acid by centrifugation

In the charge neutralization model [Kim 96], the binding for each cation is assumed to be associated with a number of carboxylic groups equal to the cationic charge, i.e., the cation can not react with all anionic sites in the humate molecule [Kim 96, Alaf 2004]. This fraction is dependent on the pH of the solution. Alfassi investigated the soluble and precipitated complex of trivalent ions (Am^{3+}) in contact with humic acid at pH 4.2 and determined the loading capacity of HA by the centrifugation method [Alfa 2002].

Alfassi et al. [Alfa 2002] proposed a new concept for determining the loading capacity for the soluble and precipitated complex of trivalent metal ion in the solution:

$$La^{3+} + HA(z) \rightarrow LaHA(III)_{soluble} \Leftrightarrow LaHA(III)_{precipitate} \tag{37}$$

The Loading Capacity can be written as

$$LC = \frac{z}{(PEC)(M_{La})(ppt-ratio)} \tag{38}$$

PEC = Proton exchange capacity of humic acid, eq/l

M_{La}= Molecular mass of lanthanide, g/mol

z = Charge of the La, eq/mol

ppt-ratio = $[HA]_{ppt}/ [La^{3+}]_{ppt}$

To check this, different concentrations of the lanthanide ion were brought in contact with humic acid. The humic acid concentration was kept constant and the metal ion concentration was varied. At high lanthanide ion concentrations, more precipitate was formed. The soluble and the precipitated complexes were separated by centrifugation. The activity of the lanthanide was measured by gamma spectroscopy and the concentration of HA by UV-Vis spectroscopy. Using the derived equation (38) the loading capacity of HA was determined at varying concentration of the metal ion. Table I shows the calculated loading capacity for the complexation of ^{140}La(III) with humic acid at pH 4.2.

Table I: Determination of loading capacity for ^{140}La(III) with humic acid at pH 4.2

$[HA]_{ppt}/ [La^{3+}]_{ppt}$	Decay correction	Loading capacity (LC)	Average LC	Error
9.400262	14.705774	0.273		
9.5545166	14.947090	0.268	0.284	0.015
8.7459720	13.682202	0.293		
8.5535505	13.381177	0.300		

Table II: Loading capacity of Gohy-573 humic acid for the complexation with metal ions at different pH values

Metal ion	pH value and method	Loading capacity (LC)	Literature
La(III)	4.2 (Centrifugation)	0.22±0.02	[Alfa 2004]
Eu(III)	4.2 (Centrifugation)	0.29±0.02	[Alfa 2004]
An(III)	4.0 (Ultrafiltration)	0.23±0.01	[Czer 96]
Am(III)	4.0 (Spectroscopy)	0.25±0.04	[Kim 93]

The loading capacity of Gohy humic acid for the complexation with trivalent actinides and lanthanides at different pH are reported in the literature (Table II). However, the experimental conditions and methods were not same; therefore, small differences between the LC for trivalent actinides and lanthanides have been found. The obtained results show with lanthanide a consistent agreement with the literature data.

7.2 List of Figures

7.3 List of Tables

7.4 List of Abbreviations

AAS *Atomic absorption spectrometry*

AES *Atomic emission spectrometry*

AHA *Aldrich humic acid*

ANKA *Angströmquelle Karlsruhe*

CE *Capillary electrophoresis*

CEC *Cation exchange capacity*

CMS *Clay mineral society*

DAD	*Diode array detector*
EXAFS	*Extended X-ray absorption fine structure spectroscopy*
EOF	*Electrosmotic flow*
ES-MS	*Electrospray mass spectrometry*
FA	*Fulvic acid*
HA	*Humic acid*
HS	*Humic substances*
HLW	*High level waste*
HPLC	*High performance liquid chromatography*
IAEA	*International atomic energy agency*
ICP-MS	*Inductively coupled plasma mass spectrometry*
LL	*Long lived*
LLW	*Low level waste*
LILW	*Low and intermediate level waste*
INE	*Institute für nuklear entsorgunng*
LCW	*Liquid core wave length*
LC	*Loading capacity*
LIBD	*Laser induced breakdown detection*
LPAS	*Laser induced photoacoustic spectroscopy*
LSC	*Liquid scintillation counting*
NOM	*Natural organic matter*
PEC	*Proton exchange capacity*
PTFE	*Polytertafluorethylen*
SL	*Short lived*
STM	*Scanning and transmission microscopy*
TLS	*Thermal lensing spectroscopy*
TRLIF	*Time resolved laser induced fluorescence*
TRIGA	*Training research isotopes general atomics*
RIMS	*Resonance ionization mass spectrometry*
VLLW	*Very low level waste*
XAFS	*X-ray absorption fine structure spectroscopy*

XANES *X-ray absorption near-edge structure spectroscopy*

XPS *X-ray photoelectron spectroscopy*